

# Soft Actuators for Small-Scale Robotics

Lindsey Hines, Kirstin Petersen, Guo Zhan Lum, and Metin Sitti\*

This review comprises a detailed survey of ongoing methodologies for soft actuators, highlighting approaches suitable for nanometer- to centimeter-scale robotic applications. Soft robots present a special design challenge in that their actuation and sensing mechanisms are often highly integrated with the robot body and overall functionality. When less than a centimeter, they belong to an even more special subcategory of robots or devices, in that they often lack on-board power, sensing, computation, and control. Soft, active materials are particularly well suited for this task, with a wide range of stimulants and a number of impressive examples, demonstrating large deformations, high motion complexities, and varied multifunctionality. Recent research includes both the development of new materials and composites, as well as novel implementations leveraging the unique properties of soft materials.

## 1. Introduction

As indicated by the continued and growing rate of related publications, research into small-scale soft actuators and stimuli-responsive materials is flourishing. These materials have the potential to revolutionize healthcare, wearable devices, manufacturing, and robotics. In contrast to their rigid counterparts, soft systems may easily deform and adapt to changing environments and dynamic task settings, be resilient to high loads,<sup>[1,2]</sup> be compliant and safe around humans,<sup>[3]</sup> and allow inexpensive mass production.<sup>[4]</sup> As soft actuators decrease in size, they become important to the development of artificial muscles,<sup>[5]</sup> cell scaffolds,<sup>[6]</sup> micromanipulators,<sup>[7,8]</sup> microrobots,<sup>[9]</sup> microlenses,<sup>[10]</sup> and smart transforming sheets,<sup>[11,12]</sup> while adding diverse multifunctionality including drug delivery,<sup>[13]</sup> sensing,<sup>[14–16]</sup> biodegradability and biocompatibility,<sup>[17,18]</sup> and color change.<sup>[19,20]</sup>

While a number of comprehensive reviews that focus on individual soft materials or specific applications exist, a review

of soft actuators for small-scale systems is still absent. This review comprises a detailed survey of ongoing methodologies for such actuators, highlighting approaches suitable for nanometer- to centimeter-scale robotic applications. Soft robots present a special design challenge in that their actuation and sensing mechanisms often are highly integrated with the robot body and overall functionality.<sup>[3]</sup> Soft robots measuring less than a centimeter are an even more special subcategory of robots, in that they often lack on-board power, sensing, computation, and control.<sup>[21–24]</sup>

In an effort not to overwhelm the reader, the scope of the paper is limited in several ways. The focus is on artificial materials; for reviews on biomolecular, biohybrid muscle cells, or microorganism-driven systems, the reader may refer to reviews that include the work of Carlsen et al., Shimizu et al., and Sung et al.<sup>[25–27]</sup> Furthermore, the focus here is primarily on methods that enable intrinsically soft actuators; therefore, options such as compliant, flexure-based ceramics will also be excluded from this review.

In the Section 2, we outline the field of soft miniature actuators, define key terminologies and give a high-level introduction to the major classes of materials used. Next, we give a detailed overview of the different stimuli (thermal, light, pressure, chemical, and electric or magnetic fields) and materials (polymers, gels, paper, carbon, and fluids) that pertain to these actuators (Figure 1). For clarity this wealth of topics is divided first by the type of stimuli required for the actuator to work, then according to material. We close with a broader perspective recommending future research directions and applications.

## 2. Overview of Methods and Materials for Soft Actuators

Here, we define soft actuators as highly deformable materials or composites that can be activated by external stimuli to generate desired motions and forces/torques. To facilitate easy deformation, many of these actuators are constructed from either materials that have low elastic moduli or those that incorporate fluids. Depending on their geometrical configurations, stiff materials with high elastic moduli can also be used in soft actuators; this pertains to some structures of mesh, foam, springs, sheets, threads/wire, and can even apply to linkage systems. As previously mentioned, the scope here is limited, and we primarily focus on the former, intrinsically soft actuators, since they generally can have a greater ability to produce and

Dr. L. Hines, Dr. G. Z. Lum, Dr. M. Sitti  
Max Planck Institute for Intelligent Systems  
Heisenbergstraße 3, 70569 Stuttgart, Germany  
E-mail: sitti@is.mpg.de

Dr. K. Petersen  
Cornell University  
324 Rhodes Hall, Ithaca, NY 14853, USA

Dr. M. Sitti  
Max Planck ETH Center for Learning Systems  
Heisenbergstraße 3, 70569 Stuttgart, Germany

Dr. M. Sitti  
Carnegie Mellon University  
5000 Forbes Ave., Pittsburgh, PA 15213, USA

DOI: 10.1002/adma.201603483



withstand large strains, achieve motion with multiple degrees of freedom with complex functionalities, emulate biological systems, and match tissue characteristics.

In both the design and the selection of soft actuators, there are a number of key features that merit consideration. **Table 1** lists a number of factors that are both active areas of research and play an important role in choosing an appropriate actuator for a specific application. In the wide range of soft actuators that exist, one of the most significant distinguishing characteristics is their mechanism of operation, which has implications on their effective performance and ability to function at certain size scales. Although it is difficult to make direct comparisons, one can use scaling laws to make some general statements as to how a produced force scales according to a characteristic length,  $L$ . For most soft actuators, including those based on electrostatic forces, thermal expansion, magnetostriction, and pressure, the produced force scales with  $L^2$  and is proportional to the actuator cross-sectional area.<sup>[33–35]</sup> Two key exceptions are magnetic and surface-tension forces. The magnetic forces on a soft actuator scale with the actuator's volume,  $L^3$ ; thus, the produced forces will decrease exponentially as  $L$  shrinks. Indeed, a practical limit will be reached when the length scale of such actuators approaches  $\approx 1 \mu\text{m}$ .<sup>[22,36,37]</sup> At small scales, volume-based effects such as gravity, inertial forces, and buoyancy become comparable or almost negligible to perimeter and surface-area effects like viscous forces, friction, and adhesion. Therefore, attractive actuation alternatives include surface tension and capillary forces, which scale with  $L$  and are proportional to the wetted contact perimeter.<sup>[34]</sup> Though they are not without their shortcomings, miniature actuators utilizing surface tension and capillary effects are a quickly growing area of research.

The selection of stimulant is critical for the soft actuators. Signals such as light, electric and magnetic fields are easy to accurately and rapidly modulate with respect to magnitude, phase, and frequency. These stimuli can also be applied remotely, which enables miniaturization down to the micrometer scale with no tether. Electric fields can be generated with compact setups, and many controllers are commercially available. Magnetic fields penetrate most materials; furthermore, forces and torques acting on the material can be separately controlled over small areas to allow a greater range of motion. Light can be applied with high intensity to concentrated regions. For biomedical applications, thermal triggers can be safer than solvent or UV light, but they may also be slower and less efficient than is desired for many applications. Pressure-driven fluidic actuators can produce high force and have the potential to be lightweight; however, they typically require connection to a relatively large external pump or compressor. Actuators driven by changes in chemical composition, humidity, or pH levels must operate in fluids, precisely controlled environments, or be sealed. Response time is also typically slow and diffusion based. A number of soft robotic systems using each stimulus have been demonstrated in the literature, with several examples depicted in Figure 1.

There are several useful metrics commonly used to compare actuator performance. Among them are generated stress and strain, measured stiffness or Young's modulus, as well as their energy, work, power, and force density. For active materials, the



**Lindsey Hines** received her B.Sc. in mechanical engineering and her B.A. in mathematics from the University of St. Thomas, St. Paul, USA and her M.S. and Ph.D. in robotics from Carnegie Mellon University, Pittsburgh, PA, USA. She is currently a postdoctoral researcher with the Physical Intelligence Department at the Max Planck Institute for Intelligent Systems, Stuttgart, Germany. Her interests include miniature robotics and bioinspired systems.

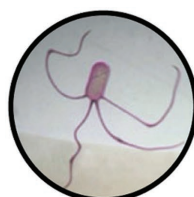


**Kirstin Petersen** received her B.Sc. in electro-technical engineering from the University of Southern Denmark, and her Ph.D. in computer science from Harvard University, USA. She did a two-year postdoc on novel soft-actuator mechanisms with the Physical Intelligence Department at the Max Planck Institute for Intelligent Systems, and is currently an assistant professor in the ECE department at Cornell University, Ithaca, NY, USA. Her interests involve collectives of physically intelligent robots able to interact with and manipulate their environment.



**Metin Sitti** is the director of the Physical Intelligence Department at the Max-Planck Institute for Intelligent Systems, Stuttgart, Germany and a professor at Carnegie Mellon University, Pittsburgh, USA. His research interests include physical intelligence, small-scale mobile robots, bioinspired and soft micro/nanomaterials and robots, and programmable self-assembly.

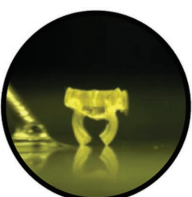
elastic energy density is typically used, which is a function of the potential mechanical energy stored and dependent upon the material's elastic modulus.<sup>[38,39]</sup> Performance of mammalian skeleton muscle is a common benchmark, with a number of active materials matching or outperforming it. Mammalian muscle typically produces around 20% strain and 100 kPa stress, with a work density of  $8 \text{ kJ m}^{-3}$  and power to mass ratio of  $50 \text{ W kg}^{-1}$ . At its highest performance, its strain can reach above 40%, stress above 0.35 MPa, work density above  $40 \text{ kJ m}^{-3}$  and power to mass ratio above  $284 \text{ W kg}^{-1}$ .<sup>[5,40]</sup>



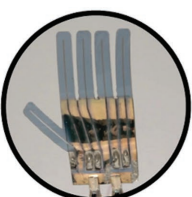
Electrically Responsive



Magnetically Responsive



Chemically Responsive



Thermally Responsive

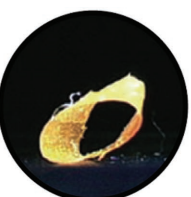


Photo Responsive



Pressure Driven

**Figure 1.** Examples of small soft robotic systems actuated with various stimuli. Systems include swimmers, jumpers, rollers, and manipulators. Electrically responsive: adapted with permission.<sup>[9]</sup> Copyright 2008, John Wiley & Sons Inc. Magnetically responsive: adapted with permission.<sup>[28]</sup> Copyright 2009, IOP Publishing. Chemically responsive: Adapted with permission.<sup>[29]</sup> Copyright 2010, The Royal Society of Chemistry. Thermally responsive: adapted with permission.<sup>[30]</sup> Copyright 2015, John Wiley & Sons Inc. Photoresponsive: adapted with permission.<sup>[31]</sup> Copyright 2008, John Wiley & Sons Inc. Pressure-driven: adapted with permission.<sup>[32]</sup> Copyright 2015, Publisher.

Previous material-performance comparisons have been listed in the work of Brochu et al., Freni et al., and Madden et al.,<sup>[40–42]</sup> newly reported values are included in their respective sections here, where available.

The following sections give a general introduction to the major categories of soft, stimuli-responsive materials, along with their composition and characteristics. **Figure 2** gives a rough overview of the Young's modulus or Young's modulus approximation of different materials. It is interesting to notice that, although carbon nanotubes (CNTs) are at the stiffest end of the spectrum, they are extensively used in composites to create soft stimuli-responsive materials. **Table 2** gives a broad overview of what type of materials have previously been used with which type of stimulus, a more comprehensive version of which can be found at the end of this work.

## 2.1. Polymers and Gels

We will discuss a range of soft actuators that are constructed by polymers and gels. This will include synthetic polymers such as silicone rubbers and polyurethanes, as well as some brief mentions of natural polymers, such as DNA or proteins. Similarly, we will also discuss a range of actuators that are created by gels, e.g., hydrogels, oil-based gels, and aerogels. These actuators can use extremely diverse stimuli for actuation – often several at the same time. Another attractive feature for these actuators is that their mechanical properties can be easily programmed

through the addition of fillers and the creation of composites during the synthesis process. Because they also have the potential to be lightweight, biocompatible, biodegradable, and easily manufactured,<sup>[49,50]</sup> a wide range of polymer- and gel-based soft actuators have been developed.

There are two specific classes of polymeric materials that are widely used and designed to respond to many different stimuli, so they deserve special attention and a brief overview here. The first is liquid-crystal (LC) polymeric materials and the second shape-memory polymers (SMPs). Liquid-crystal molecules, also called mesogens, are typically polar, relatively stiff rod-like molecules that can be easily reoriented in electric fields. When attached to polymeric backbones, they can form liquid-crystal polymers (LCPs), liquid-crystal elastomers (LCEs), and liquid-crystal polymer networks (LCNs), depicted in **Figure 3**.<sup>[44]</sup> LCEs and LCNs are most widely studied for use in actuators due to their material properties. LCEs are lightly crosslinked materials, are capable of large deflections, and display behavior similar to a traditional rubber; glassy LCNs are moderately to densely crosslinked and fail at lower strains, but are capable of greater mesogen alignment.<sup>[44,51]</sup>

The organization of the mesogens in these materials define the material's phase, with two important examples being nematic and smectic. In the nematic phase, the mean orientation of the mesogens is uniform. In the smectic phase, the mesogens are organized, additionally, in separate layers.<sup>[53]</sup> The LC phase has implications on both the type of actuation method that can be used, as well as the produced motion. When nematic-phase LC materials are heated, they can transition to an isotropic phase, where the mesogens are randomly aligned and bundled, producing reversible and repeatable contraction, as depicted in Figure 3A.3.<sup>[53]</sup> Actuation without an isotropic phase transition is also possible, such as the case of smectic ferroelectric LCE films actuated by electric fields.<sup>[54]</sup>

Shape-memory polymers are materials that are able to “remember” one or more shapes. A deformed temporary shape can be fixed under certain conditions – commonly polymer crystallization or vitrification (the transition into a “glassy”-like state) – and then recovered under various stimuli including heat, light, and solvent.<sup>[49,55]</sup> This transition results in an effective tunable stiffness that varies by several orders of magnitude, which is also used in smart, reconfigurable surfaces.<sup>[45,56,57]</sup>

**Table 1.** Summary of important factors to take into consideration when choosing a soft actuator.

• Actuation strain and force production	• Operating environment (in solution, air, etc.)
• Size scale	• Remote or tethered power source
• Resistance to other stimuli	• Yield stress
• Power consumption	• Durability and fatigue resistance
• Actuation speed and response time	• Self-healing properties
• Biocompatibility	• Hysteresis (and material viscoelasticity)
• Biodegradability	• Anisotropy
• Multifunctionality	

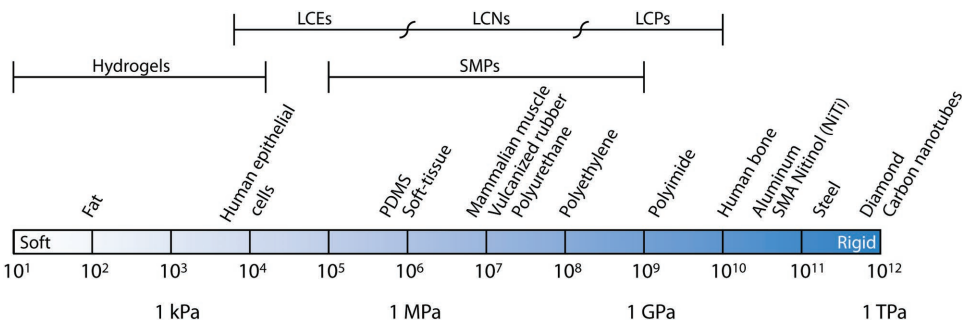


**Figure 2.** Comparison of Young's modulus for different materials. Values are approximate. Inspired from refs. [3,43]; additional data sources include refs. [5,44–48].

Material recovery to its initial state typically produces large strains but low forces, dependent upon the elasticity of the polymer network.

There is a wide range of polymers that exhibit the shape-memory effect, to a greater or lesser degree. Crosslinked polymers behave elastically above a glass-transition temperature  $T_g$  if amorphous or a melting-transition temperature  $T_m$  if crystalline.<sup>[45]</sup> The material can be strained easily if at a temperature  $T > T_g$  or  $T_m$  and that strain stored if  $T$  is then lowered below this value.<sup>[45]</sup> Increasing  $T$  again will release this stored strain and recover the original shape. A simple example of this thermomechanical cycle is depicted Figure 3B. More than a single

temporary shape is also possible, with up to a quintuple SMP demonstrated.<sup>[58]</sup> Reversible SMPs are subject to current research and vary in type. Normally, manual deformation is necessary to reset the material; alternatively, an SMP can be operated under constant load. There are a few examples of reversible bidirectional SMPs where an external stress is not required,<sup>[59,60]</sup> but they are uncommon. Some papers discuss the repeatable phase shift of LC materials as a reversible shape-memory effect.<sup>[45,61]</sup>

There are a number of recent reviews on specific polymer- and gel-based applications and materials for those interested in further reading. Liu et al. has compiled a review on film folding, which includes a number of approaches involving soft

**Table 2.** A selection of soft materials and their demonstrated actuation stimuli.

	Electric field	Magnetic field	Pressure differential	Heat (electro-, photothermal, etc.)	Light	Chemical (solvent, water, pH, etc.)
Polymers and gels	×	×	×	×	×	×
• Conductive polymers	×					
• Liquid-crystal polymers (LCPs), polymer networks (LCNs), elastomers (LCEs)	×			×	×	×
• Ionic-polymer–metal composites (IPMCs)	×					
• Dielectric elastomer actuators (DEAs)	×					
• Shape-memory polymers				×	×	×
• Hygromorphic polymers				×		×
• Ferrogels and ferroelastomers		×				
• Hydrogels	×	×	×	×	×	×
Fluids	×	×	×	×	×	×
• Electrorheological fluid (ERFs)	×					
• Magnetorheological fluids (MRFs)		×				
• Ferrofluids		×				
• Dielectric fluids (electroconjugate fluids (ECFs))	×					
• Liquid metals	×	×		×	×	×
• Liquid marbles	×	×			×	×
Paper (cellulose)	×	×		×		
Carbon	×		×	×		
• Carbon nanotube (CNT) sheets, yarn	×		×	×		
• CNT aerogel	×					

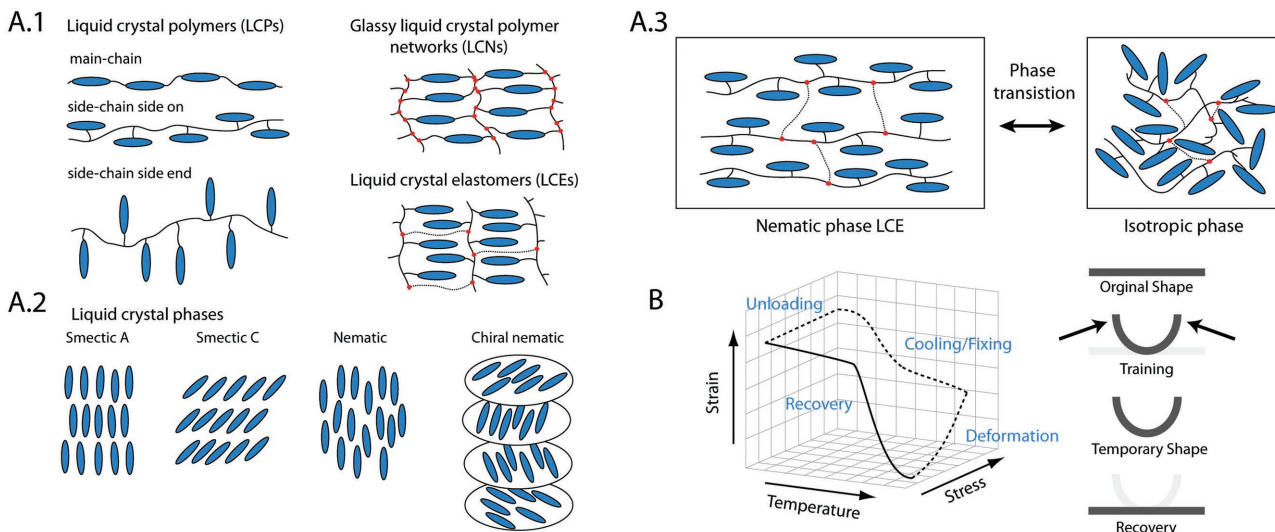


**Figure 3.** A) Liquid-crystal polymeric materials A.1) Depiction of liquid-crystal polymers, polymer networks, and elastomers, which vary in mesogen attachment to the polymer backbone and crosslink density. A.2) Several important LC material phases; in the smectic phase, mesogens are both aligned and ordered in layers; nematic phases have no layered order. A.3) LCE phase transition between nematic and a disordered, isotropic phase. The black lines represent polymer chains, the blue ovals represent mesogens, and the red circles represent crosslinks. The diagrams are inspired by work in refs. [44,52] B) Example thermomechanical cycle for a one-way shape-memory polymer. The dotted line represents SMP training/fixing for the creation of a temporary shape.

actuators.<sup>[62]</sup> Reviews on LC materials include the work of White et al., Collyer et al., and Broer et al.<sup>[44,63,64]</sup> Microscale LCEs are reviewed by Yang et al.,<sup>[65]</sup> LCEs for actuators and sensors by Ohm et al.,<sup>[52]</sup> and LCEs for artificial muscles by Li et al.<sup>[53]</sup> A few recent SMP reviews include those by Hager et al.,<sup>[49]</sup> Meng et al.,<sup>[61]</sup> Hu et al.,<sup>[66]</sup> Sun et al.,<sup>[67]</sup> and Behl et al.<sup>[68]</sup>

## 2.2. Fluids

Here, we will discuss principles behind and examples of fluid-based soft actuators. In general, these actuators can be activated by an increase of pressure, modification of viscosity, and/or selective surface-tension control of the liquid interface. The possibility for fluid manipulation at high speeds and the favorable scaling of surface-tension forces at small sizes make fluid actuators an attractive alternative for some applications. However, in general, fluids have a number of disadvantages compared to solid-material actuators. For example, fluid-based actuators may not be repeatable as they can be subject to leakage. When pushing an object with a droplet there is a risk of passing, surrounding, or capturing it, which can complicate reliable transportation and deposition. Fluid flows can experience complex dynamics when operating near solid structures and may mix in undesirable ways when operating with or within other fluids. Furthermore, many fluids are also highly dependent on environmental conditions and in small quantities can easily and quickly evaporate. Although these shortcomings can be significant, many can be addressed by encapsulating the fluid in elastic chambers, films, or gels.

Alternatively, liquid droplets can be coated with hydrophobic particles, making them nonwetting. This novel composite was introduced in 2006 by Aussillous et al. and termed liquid marbles.<sup>[69]</sup> Being encapsulated microreservoirs of fluid, liquid

marbles avoid some of the disadvantages of working with fluids, while adding extra functionality.<sup>[69]</sup> While the use of hydrophobic particles may seem counterintuitive, McHale et al. has shown that the surface free energy of a droplet is always less when replacing a droplet's liquid–vapor interface with the liquid–solid interface between spherical particles, regardless of surface chemistry.<sup>[70]</sup> Because of their hydrophobicity, the particles do not mix within the liquid, and instead remain on the surface to coat the droplet. This prevents fluid contact with other substrates, completely coating the liquid marble, leaving it nonwetting, not only on solid surfaces, but on liquid interfaces as well.<sup>[69,71]</sup> Comprehensive recent overviews of active droplets have been compiled by Lach et al.<sup>[71]</sup> and liquid marbles by McHale et al.,<sup>[72]</sup> Ooi et al.,<sup>[73]</sup> and Bormashenko et al.<sup>[74]</sup>

## 2.3. Paper

Paper is ubiquitous in our society. While it has a long history of use in printing, packing, and cleaning, it is only relatively recently that it has formed the basis of actuators as a new smart material. Paper is composed of a porous network of cellulose fibers<sup>[75]</sup> and is typically classified in terms of weight per area. As it is biodegradable, cheap, abundant, and lightweight, and it has great potential in applications ranging from cheap miniature diagnostic tools to mass manufacturing of small-scale printable robots.<sup>[76–79]</sup>

## 2.4. Carbon

Despite the high Young's moduli of carbon nanotubes (CNTs) (>1000 GPa when axially loaded<sup>[80]</sup>), they, along with carbon particles and graphene, have been frequently incorporated

into soft actuators because of their high electrical and thermal conductivity, as well as their light-absorbent characteristics. CNTs can exist in a number of different forms, but among the most common are single-walled (SWCNT) and multiwalled (MWCNT) CNTs. SWCNTs have a diameter close to 1 nm, but their length can be many millions of times longer. MWCNTs are composed of a series of nested tubes, with an overall diameter that can be greater than ten times their single-walled counterparts. The rolling angle and radius of the tube determines its properties, e.g., whether it is a metal or semiconductor. The tubes are electrically and thermally conductive along their length, but good insulators laterally to the tube axis.

Although CNTs are not easily stretchable, they can also function independently as foldable soft actuators when they are made into sheets, termed bucky paper,<sup>[81]</sup> or yarns.<sup>[82]</sup> CNT actuators were first proposed by Baughman et al. in 1996 and demonstrated in 1999.<sup>[83,84]</sup> The produced strain remains relatively low compared to other materials, with 0.7% demonstrated for SWNTs and 0.5% for MWNT yarn.<sup>[82,85]</sup> The price of these materials has dropped remarkably over the last decade, and a gram of SWCNTs is now typically around US\$ 2, making them more viable for commercial products. A comprehensive review of CNT sensors and actuators was published in 2008 by Li et al.<sup>[86]</sup>

### 3. Electrically Responsive Soft Actuators

Soft, flexible materials able to convert electrical energy to mechanical energy are plentiful, and include polymers, gels, fluids, paper, and even stand-alone CNTs. Driving actuators by electronic signals allows the easy modulation of magnitude, phase, and frequency. Furthermore, as these actuators are compatible with conventional electronics and batteries, it is easy to integrate them with electrical drivers and power sources. The applications are endless; some of the biggest research thrusts are seen in artificial muscles,<sup>[87–90]</sup> small-scale robots,<sup>[9,91–93]</sup> manipulation of microscale objects,<sup>[94,95]</sup> and microfluidic systems.<sup>[96,97]</sup>

#### 3.1. Electrically Responsive Polymers

Electroactive polymers (EAPs) are polymers that change size or shape upon electrical stimulation. They can exhibit sizable strains and/or stresses, have high mechanical flexibility, simple material composition, high fracture toughness, and inherent vibration damping, produce low noise, and are lightweight, easy to fabricate, and in many cases low cost.<sup>[98]</sup> Here, we discuss the most common electroactive materials, including: i) non-ionic EAPs driven by electric fields or Coulomb forces, such as dielectric elastomers, ferroelectric polymers, electrostrictive polymers, and LCEs, and ii) ionic EAPs driven by mobility and diffusion of ions and their conjugated substances such as ionic conducting polymers and ionic polymer–metal composites (IPMCs).

Whereas ions play a major role in the electrical actuation of ionic EAPs, non-ionic EAPs are dependent on a Faradic transduction mechanism. Non-ionic EAPs generally show rapid

response, large strain, high mechanical energy density, and the ability to hold their induced displacement under a DC voltage. However, they require high activation fields ( $>10\text{ V }\mu\text{m}^{-1}$ ) that are often close to the electrical breakdown of the materials.<sup>[50]</sup> In contrast, ionic polymers are ideal for biomimetic devices and require only few volts to operate, but tend to have slow response times, low electromechanical coupling, and must be immersed in an electrolyte or encapsulated for operation in air.

##### 3.1.1. Dielectric Elastomers

The operating principle behind dielectric-elastomer actuators (DEAs) is based on the Coulomb force attracting two flexible electrodes of different potential on either side of a compressible membrane. These actuators are compliant, exhibit large strains, high energy density, and self-sensing properties, are well modeled,<sup>[99]</sup> and have been compared in usefulness to biological muscles,<sup>[89]</sup> especially when combined antagonistically.<sup>[100]</sup> Overall performance is highly dependent upon the elastomer stiffness, dielectric constant, and breakdown voltage. The downside to DEAs include leakage currents and the need for driving voltages on the order of kilovolts, which increases the risk of electrical breakdown.<sup>[41,38]</sup> The latter can be caused by an electromechanical instability, the so-called pull-in effect, where the induced stress grows faster than the resisting elastic stress, leading to a drop in material thickness and an eventual short across the membrane. Finally, the viscoelastic properties of DEAs are known to strongly affect their dynamic performance; Hong discusses this phenomenon in detail and presents a reliable model for general load conditions.<sup>[101]</sup>

Typical membrane materials include acrylic elastomers, silicones, polyurethanes, and rubber, with varying performance characteristics. Acrylic elastomers such as the commonly used VHB4910, can produce very large deformations, but are very viscoelastic, which can limit actuator bandwidth. Silicone- and polyurethane-based elastomers exhibit much faster response times and can be cast in any shape and softness, but generated strain is considerably less. Silicones also generally have lower dielectric constants, requiring higher activation voltages than polyurethanes and acrylic elastomers.<sup>[39]</sup> Active research to improve the performance of DEAs focuses on increased membrane permittivity using elastomers with embedded microparticles<sup>[41,102]</sup> or completely organic membranes.<sup>[103]</sup> It is well known that prestraining DEA membrane improves the frequency and actuation response of many elastomer films; however, it may also cause membrane relaxation over time, it may reduce the actuator shelf life because of fatigue, and it typically requires a bulky support frame on which to suspend the elastomer.<sup>[41]</sup>

DEA electrodes need to be compliant and robust, and offer low resistance.<sup>[104]</sup> Carbon grease is an especially popular choice because of its ability to adhere to most surfaces and comply to very high strains without changing the elasticity of the membrane. For electrodes that do not smear, crosslinked hydrogel polymers have been shown capable of up to 167% strain.<sup>[105]</sup> For lower strain electrodes (175% and less) that can be micropatterned, researchers have used CNTs, stamps of carbon powder, carbon-based ink, and metal-ion-implanted

electrodes.<sup>[8,106]</sup> Researchers have also reported self-clearing electrodes, in which the electrical breakdown of the dielectric medium causes local evaporation of the electrode, thereby supporting continued function.<sup>[107]</sup>

DEAs can be planar in form, as well as stacked, folded, framed, inflated, and rolled. They can bend, extend, and exhibit buckling. Kwangmok et al. demonstrated an annelid-like robot using modules of millimeter-scale actuators stacked along the length of the robot.<sup>[91]</sup> Shintake et al. showed versatile soft grippers using electroadhesion;<sup>[108]</sup> and in very recent work, Shian et al. showed controllable and reversible spatially nonuniform surface deformations in a thin sheet of a dielectric elastomer.<sup>[109]</sup> By combining the DEA with a buckling frame, it is possible to produce very large and sometimes faster deformations.<sup>[106,110,111]</sup> Another well-explored technique relies on sealed pressurized chambers covered by DEAs to produce extremely large deformations (e.g., 1165%<sup>[112]</sup> and 1692%<sup>[113]</sup>). Fluidically coupled membranes have been shown to be advantageous for making these deformations reversible, as well as creating safe-to-contact moveable surfaces.<sup>[114,115]</sup> To achieve stable configurations, the DEA stiffness can be modified through controlled heating about its glass-transition temperature,<sup>[116]</sup> composite DEAs with embedded low melt alloys can be stiffened through electric or thermal stimulation,<sup>[117]</sup> or the material nonlinearity can be leveraged to create stable inflated sizes.<sup>[114]</sup> The smallest DEA presented to date was used to perform stretching of individual cells on the nanoscale.<sup>[8]</sup>

### 3.1.2. Ferroelectric and Electrostrictive Polymers

Ferroelectric polymers are a class of crystalline polymers that are able to transition from polar to nonpolar states, producing lattice strain and dimensional change under electric fields.<sup>[118]</sup> Ferroelectric polymers are easily produced, cheap, and lightweight, and can be cast into any shape; however, they do exhibit large hysteresis when strained. One of the biggest challenges related to ferroelectric actuators, and non-ionic polymers in general, is how to significantly reduce the applied field required to drive the high strain and improve the elastic energy density.<sup>[119]</sup> Miehe and Rosato published an extensive study concerning modeling and numerical simulations of the electro-mechanical and dissipative response of ferroelectrics.<sup>[120]</sup>

The most popular choice of material for these actuators has been the piezoelectric material poly(vinylidene fluoride) (PVDF), commonly used in acoustic transducers. The same dipolar structure that enables piezoelectricity also causes pyroelectricity, i.e., the electrical response to a change in temperature.<sup>[121]</sup> Generally, PVDF films are popular for their stable thermal and chemical properties and are widely used in piping products, sheets, tubing, plates, insulators, and sensors.<sup>[122–124]</sup> Lehmann et al. presented ultrathin (<100 nm) ferroelectric LCEs exhibiting more 4% strain at just 1.5 MV m<sup>-1</sup>.<sup>[54]</sup> Later, Huang et al. reported a PVDF actuator with a strain up to 7% at around 150 MV m<sup>-1</sup>.<sup>[119]</sup>

The electrostrictive effect, present in all dielectric insulators, is a term used to denote a quadratic coupling between strain and electric polarization.<sup>[125]</sup> Typically, these materials are used with high voltages for DEAs; however, at more moderate

electric fields, the electroactive response of the materials is due to electrostriction. Under such moderate fields, the elastomer contracts perpendicularly to the electric field and independently of the field direction.<sup>[125]</sup> The reason for this effect has yet to be fully understood, but several hypotheses have been suggested, including that the observed strain is due to the relaxation of the polymer matrix under the electric field by induced crystallization, or that the strain is due to the presence of electric charges inside the material.<sup>[126]</sup> Richards et al. suggested a comprehensive model including the relationship between load, deformation, electric displacement, and the applied electric field.<sup>[127]</sup> The electromechanical response is strongly dependent on the thickness of the membranes, and thin films have been shown to achieve up to 7% strain at 16 MV m<sup>-1</sup>.<sup>[128]</sup>

The two effects mentioned above are often combined in hybrid materials.<sup>[129–131]</sup> Bauer et al., for example, has demonstrated a ferroelectric composite with high elastic modulus (>0.3 GPa) and electrostrictive strains (>7%).<sup>[130]</sup>

### 3.1.3. Electrically Responsive Liquid-Crystal Polymeric Materials

Under an electric field, LC mesogens will attempt to align themselves along the field lines. As they are attached to polymeric chains, this results in an overall deformation of the material. Demonstrated electrically responsive LC polymeric materials include the previously mentioned ferroelectric LCE films,<sup>[54]</sup> polydomain nematic LCEs with isotropic genesis,<sup>[132]</sup> and nematic gels.<sup>[20,133–135]</sup> In an LC gel swollen with LC solvents, actuated strain can be increased significantly, but subsequent relaxation can occur on the order of 10<sup>3</sup> s.<sup>[133]</sup> In a nematic LCN gel swollen with nematic solvents, Urayama et al. demonstrated strains of 20% at an electric field of ≈0.5 MV m<sup>-1</sup>.<sup>[134]</sup> Similar strains, along with a corresponding linear change in optical transmissibility, have been achieved with nematic solvent-swollen LCEs.<sup>[135]</sup> With a swollen chiral (helically oriented) LCE, strains of up to 32% have been demonstrated along with a change in color, with both quick contraction and relaxation.<sup>[20]</sup>

### 3.1.4. Ionic Conducting Polymers

Although polymers are commonly known for their excellent insulating properties, conjugated polymers can become highly electrically conductive when subjected to a structural process called “doping”.<sup>[136]</sup> The term “conjugated” refers to the alternating single and double bonds in the polymer chain that allow electrons to be shared among many atoms. The doping process detaches or adds electrons to the polymer backbone resulting in cations and anions that can move freely under the influence of electrical fields thus increasing conductivity.<sup>[137]</sup> These conducting polymers can exhibit large dimensional changes depending on their oxidation state, thereby converting electrical energy into mechanical work. The switching of a conducting polymer between the oxidized and the reduced states is a reversible process that can be driven electrochemically by small changes in voltage.<sup>[138]</sup> An anion-transporting conjugated polymer will expand during oxidation and contract during

reduction, while a cation-transporting polymer will demonstrate the opposite behavior.<sup>[139]</sup>

Conductive conjugated-polymer actuators feature low operation voltages and are typically lightweight, flexible, and biocompatible. They tend to have negligible self-discharge, no mechanical creep, high force-generation capabilities, high energy density per cycle, and are feasible to manufacture on the nano- and microscales.<sup>[83]</sup> Compared to ferroelectric polymers, these actuators are capable of generating an order of magnitude more stress. Polypyrrole and polyaniline are two of the most investigated conjugated polymers because of their good chemical stability and substantial strains.<sup>[139]</sup> Disadvantages include their limited cycle rate, limited cycle life, and high oxygen sensitivity;<sup>[83]</sup> many actuators are restricted to use in aqueous solutions, such as bodily fluids; however, some use lamination for dry operation.<sup>[138]</sup>

Early demonstrations in liquid electrolytes include uni-, bi-, and trilayer cantilever devices.<sup>[37,139,140]</sup> When low voltages (typically 1–3V) are applied to the conducting electrode layer, ions are exchanged with the electrolyte, making the polymer swell or shrink and subsequently causing bending motions of the entire laminated strip.<sup>[141]</sup> Smela et al. used this technique to

design microscopic hinges for automatic folding of microscale cubes.<sup>[142]</sup> Jager et al. showed microscale actuators for glass-bead manipulation<sup>[94]</sup> and cascading configurations for three-dimensional movements.<sup>[143]</sup> Conducting conjugated-polymer actuators have also been used to produce linear strain.<sup>[138]</sup> Dry air demonstrators typically rely on an active material coupled to a passive supporting electrode layer, such as trilayer benders,<sup>[144]</sup> cellulose-based cantilevers,<sup>[145]</sup> and McKibben style actuators with radial strain.<sup>[37]</sup> Must et al. carried out several studies of ionic EAPs, including characterization,<sup>[146]</sup> rolling robots,<sup>[147]</sup> and untethered walking robots (Figure 4B).<sup>[92]</sup>

Fabrication methods for microscale actuators typically rely on soft lithography, using injection molding in capillaries,<sup>[148]</sup> but photolithography, inkjet printing, and deposition via volume-controlled or pneumatic microsyringes have also been used.<sup>[37]</sup> Future improvements in this field are likely to focus on thinner electrodes for faster response times (i.e., decreasing the ion diffusion distances),<sup>[140]</sup> increasing ionic and electrical conductivities,<sup>[149]</sup> better lamination between polymers and electrodes, and more-intelligent control systems with feedback loops.<sup>[139]</sup> At much smaller scales, with a higher surface-to-volume ratio, isolated microscale actuators will also provide higher power densities.<sup>[83]</sup>

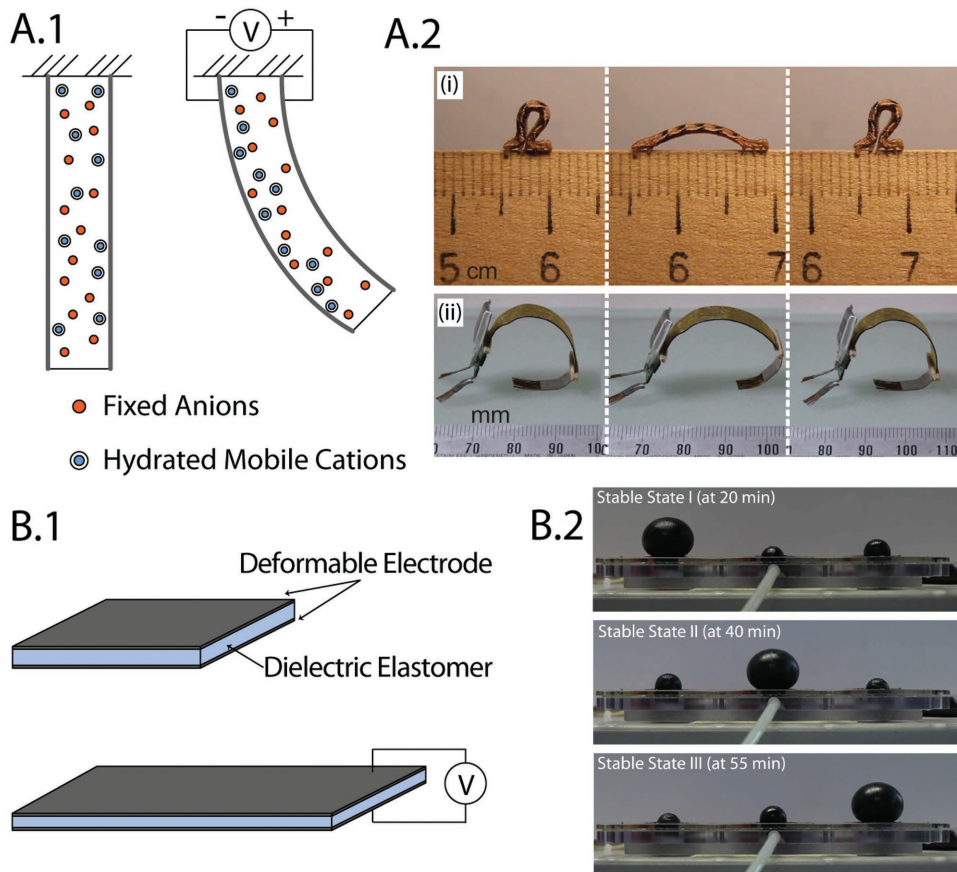


**Figure 4.** A,B) Ionic (A) and dielectric elastomer (B) actuators. A.1) Principle of operation for an IPMC. Upon application of an electric field, the hydrophilic positive ions will move toward the cathode, causing swelling and cantilever bending. A.2) Motion of an inchworm (i), and its artificial counterpart comprised of ionic polymer (ii). B.1) Diagram of operation of a dielectric elastomer. Upon activation, electrodes are pulled together by Coulomb forces, squeezing the membrane and causing planar expansion. B.2) Inflated dielectric elastomer with three fluidically connected membranes. Due to the elastomer membranes' nonlinearity, the deformation is large and stable. A) Reproduced with permission.<sup>[92]</sup> Copyright 2015, John Wiley & Sons Inc. B) Reproduced with permission.<sup>[114]</sup> Copyright 2016, John Wiley & Sons Inc.

### 3.1.5. Ionic Polymer–Metal Composites

IPMCs are also known as ionic polymer–conductor composites, ionic conducting polymer gel films, and ionic polymer transducers. They were developed as a response to the disadvantages found for polymeric hydrogels, including the need to operate in solvent baths.<sup>[150]</sup>

The classic IPMC actuator layout includes an ion-conducting polyelectrolyte membrane with thin flexible electrodes on both sides, which allows the application of electric fields along the membrane (Figure 4).<sup>[5]</sup> When hydrated, the positive ions in the membrane move freely, whereas the negative ions are fixed, bonded with carbon chains in the polymer. Upon the application of an electric field, the positively charged ions tend to accumulate near the cathode, which, in turn, exerts stress on the surrounding molecules due to the high concentration. This highly localized stress results in bending of the IPMC structure.<sup>[151]</sup> Several aspects play a role in actuator performance: the ion-exchange capacity, the ion conductivity, the electrode conductivity, the thickness, and the electrode–polymer interlocking. Good interlocking between the layers enhances the capacitance of the actuator by allowing a larger accumulation of ions at the electrode and thereby bigger deflection.<sup>[150]</sup>

IPMCs are well suited as actuators because of their low driving voltages, high actuation strains, light weight, flexibility, high degrees of freedom, and nano- and microscale manufacturing feasibility.<sup>[152]</sup> Typical work densities have been reported to be around  $5.5 \text{ kJ m}^{-3}$ .<sup>[153]</sup> Compared to shape-memory alloys IPMCs have faster response times, and exhibit lower stress and higher strain.<sup>[154]</sup> When a step-voltage is applied, the actuator displays a fast initial reaction followed by a slow relaxation, the direction of which is dependent on the polyelectrolyte used.<sup>[5]</sup> Researchers have proposed many actuator models and considered closed-loop control for handling this positional drift, but, as of yet, no appropriate internal sensing option has been found.<sup>[151,155]</sup> Due to the time it takes water and hydrated ions to dissipate through the surface electrodes, operating the actuator at lower frequencies leads to higher displacements.<sup>[156]</sup> Further improvement of these actuators is dependent on reducing or eliminating water leakage out of the surface electrode, so that water transport within the IPMC can be more effectively utilized for actuation. Liu et al. achieved significant improvements in the electromechanical performance by using CNTs to create continuous paths for fast ion conduction in the polyelectrolyte, minimal conduction resistance, and a tailored elastic modulus for enhanced actuation strain.<sup>[157]</sup>

IPMCs have been used for a multitude of robotic applications. Because of their ability to function in aqueous solutions, underwater fish,<sup>[154,158–164]</sup> ray,<sup>[165]</sup> jellyfish,<sup>[166]</sup> walking,<sup>[167,168]</sup> and catheter robots<sup>[93]</sup> have been extensively explored. Encapsulation can improve performance in dry air,<sup>[169]</sup> with demonstrations including distributed conveyor belts<sup>[170]</sup> and miniature grippers.<sup>[171]</sup>

Despite all of their advantages, IPMCs suffer from several significant drawbacks including low actuation bandwidth, relatively low durability in dry operation, environmental unfriendliness, and high costs.<sup>[172]</sup> This has prompted very recent work in high-performance polymer actuators composed of ionic liquid, soluble sulfonated polyimide polyelectrolytes, and ubiquitous

carbon materials.<sup>[172,173]</sup> These actuators are inexpensive, and they show favorable mechanical properties and good durability of more than 5000 cycles in dry air.<sup>[174]</sup>

### 3.2. Electrically Responsive Gels

Of all the solid-state materials, gels provide the biggest actuated change in volume;<sup>[175]</sup> EAP gels, capable of absorbing and releasing large amounts of fluid under electric fields,<sup>[176,177]</sup> will be discussed in the following sections.

#### 3.2.1. Ionic Gels

Applying an electric field to a gel submerged in an ionic solution will cause it to swell asymmetrically toward the cathode because of a difference in mobile-ion concentrations between the inside and outside of the gel.<sup>[37,178]</sup> Polyelectrolyte gels have shown the ability to absorb up to 2000 times the polymer weight of solution into the network.<sup>[179]</sup> The actuation relies on four competing forces acting on the ionic networks: rubber elasticity, polymer–solvent viscous interactions, counter-ion osmotic pressure, and electrophoretic interactions.<sup>[180,181]</sup> The first two typically counterbalance and leave the gel in a stable condition; the latter two are used to displace the equilibrium point of the gel.<sup>[182]</sup>

Ionic EAP gels require low driving voltages, use soft biocompatible materials, and promise many future applications, including manipulation of biological components in aqueous solutions, cell scaffolds, soft actuators, and replacement of biological tissues.<sup>[7,176,179]</sup> The biggest shortcomings of polyelectrolyte gels are that their electromechanical response is typically slow and strongly dependent on both temperature and humidity.<sup>[50]</sup> Other shortcomings involve inevitable heat and gas generation with electrolysis of the aqueous solution caused by leakage of the solvent in the gel,<sup>[183]</sup> and large leakage currents under strong electric fields. These effects typically lead to shortened material life span and low energy-conversion efficiencies.<sup>[10]</sup> Effort has been invested in closed-loop control to account for internal induced heating and viscoelastic creep.<sup>[184]</sup> Several accurate and/or computationally tractive analytical models have been developed to characterize the deformation dependent on electric-field strengths, gel dimensions, and mechanical factors such as resistance and capacitance.<sup>[177,181]</sup> Because the gel swells by imbibing solvent molecules, smaller actuators take less time to reach equilibrium and therefore have faster response times. When the gel actuator is smaller than the Debye length (a measure of how far the range of the electrostatic effect in a solution persists), however, the behavior may deviate from that of larger gels.<sup>[177]</sup>

Several types of small-scale ionic-gel-based robotic demonstrators exist. Osada et al. showed worm-like motion in one of the first robotic demonstrations of ionic gels.<sup>[185]</sup> Kwon et al. presented soft aquabots, including octopus, sperm, and walkers controlled by cyclical electric fields of varying strength and angle (Figure 5B).<sup>[9]</sup> Hong et al. showed inhomogeneous deformation by mixing soft and hard materials.<sup>[177]</sup> Palleau et al.

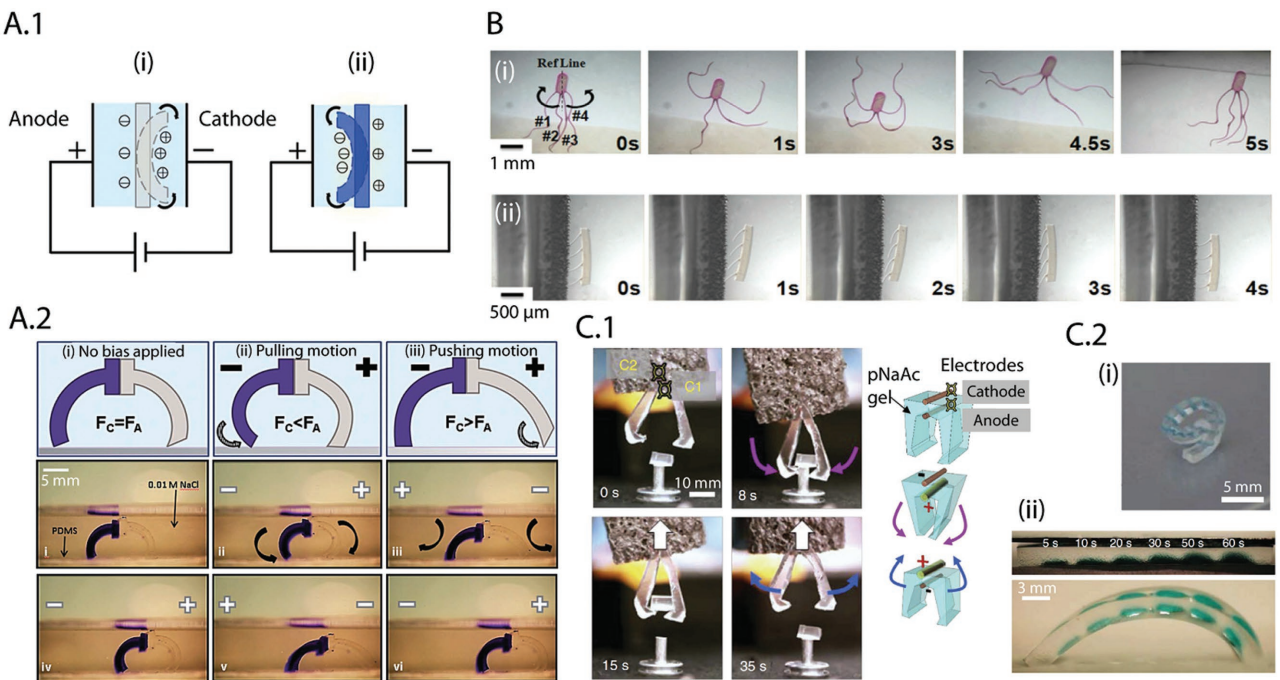


**Figure 5.** Ionic-gel actuators A.1) Basic diagram of mechanism: with an anionic (i) and cationic (ii) gel in the same solution, one can achieve opposite bending directions under the same applied field. A.2) Walker achieved using both an anionic and cationic gel. A field of  $5\text{ V cm}^{-1}$  is applied, with the electrode field directions listed on the images. B) Locomotion of an anionic gel octopus (i) and walker (ii) under an electric field in solution. The applied voltage signals were an alternating ( $+7\text{ V}/-15\text{ V}$ ) and ( $\pm 15\text{ V}$ ) respectively. C) Patterning of hydrogel using ionoprinting for directional embedding of ions. The imprinted-area size and location affect the degree of bending (C.2(ii)). A gel gripper is able to grasp and release items (C.1). A.1,A.2) Adapted with permission.<sup>[7]</sup> Copyright 2014, The Royal Society of Chemistry. B) Reproduced with permission.<sup>[9]</sup> Copyright 2008, John Wiley & Sons Inc. C) adapted with permission.<sup>[176]</sup> Copyright 2013, Macmillan Publishers Ltd.

introduced ionoprinting to rapidly and reversibly pattern ions in hydrogels in two- and three dimensions, and, among others, demonstrated a miniature gripper (Figure 5C).<sup>[176]</sup> Wu et al. devised an anisotropic gel by including special fiber-like regions that exhibit differential shrinkage and elastic modulus under electric fields.<sup>[186]</sup> Morales et al. combined two oppositely deforming polyelectrolyte hydrogels to create a walker (Figure 5A).<sup>[7]</sup> Furthermore, several researchers are working on nanoscale implementation of gel actuators.<sup>[180,187,188]</sup>

Finally, Bucky gel actuators are composed of an ionic-liquid-induced polyelectrolyte film encompassed by two compliant electrode layers, resulting in an ionic and capacitive trilayer structure able to operate in free air.<sup>[184]</sup> Due to relocation of cations and anions within the actuator upon application of a voltage, Bucky gel actuators exhibit fast bending followed by a small reverse motion, referred to as the back relaxation. Several types of electrodes have been explored for improved performance, including SWCNTs,<sup>[189]</sup> activated carbon nanofibers,<sup>[190]</sup> and blends of the two.<sup>[191]</sup>

### 3.2.2. Non-ionic Gels

Like ionic EAP gels, non-ionic EAP gels exhibit rapid response times, large strains, and high mechanical energy density at the cost of high operating voltages (100–1000 V).<sup>[50]</sup> Actuation with ionic EAP gels has been shown in two major categories of

materials, electrorheological fluid gels (ER fluid gels) and plasticized poly(vinyl chloride) (PVC) gel membranes.

The theory behind ER fluids is described in Section 3.3.1, and is basically characterized as an electric-field-driven rapid and reversible increase in apparent viscosity and yield stress.<sup>[192]</sup> These are typically suspensions of dielectric particles in an insulating fluid, and, while many variations exist, the most sensitive are typically hard to synthesize, highly complex, expensive, and environmentally unfriendly.<sup>[193]</sup> Furthermore, they suffer from coagulation of particles, which can give rise to an unstable response. To solve these problems, researchers have developed crosslinked gels containing dielectric particles, which exhibit higher reproducibility over long-term use, as well as operation in air.<sup>[194]</sup> As an example, Gao et al. prepared a gelatin/water composite system for an easily synthesized, inexpensive, and environmentally friendly ER gel.<sup>[193]</sup> Koyanagi et al.<sup>[195]</sup> demonstrated an ER-gel linear actuator where the surface shear stress increased several tenfold upon activation of the electrical field.

Driven by shortcomings in ionic EAP gels, researchers have recently started looking into soft materials made of plasticized PVC (Figure 6). PVC is a commercially available, inexpensive material with a low dielectric constant, which can become very flexible when plasticized and offers reasonably high surface tension.<sup>[183]</sup> These actuators consist of PVC gel sandwiched between conductive solid or meshed electrodes. The force generated when under an applied electric field stems from a creeping motion along the anode. This creep is believed to be

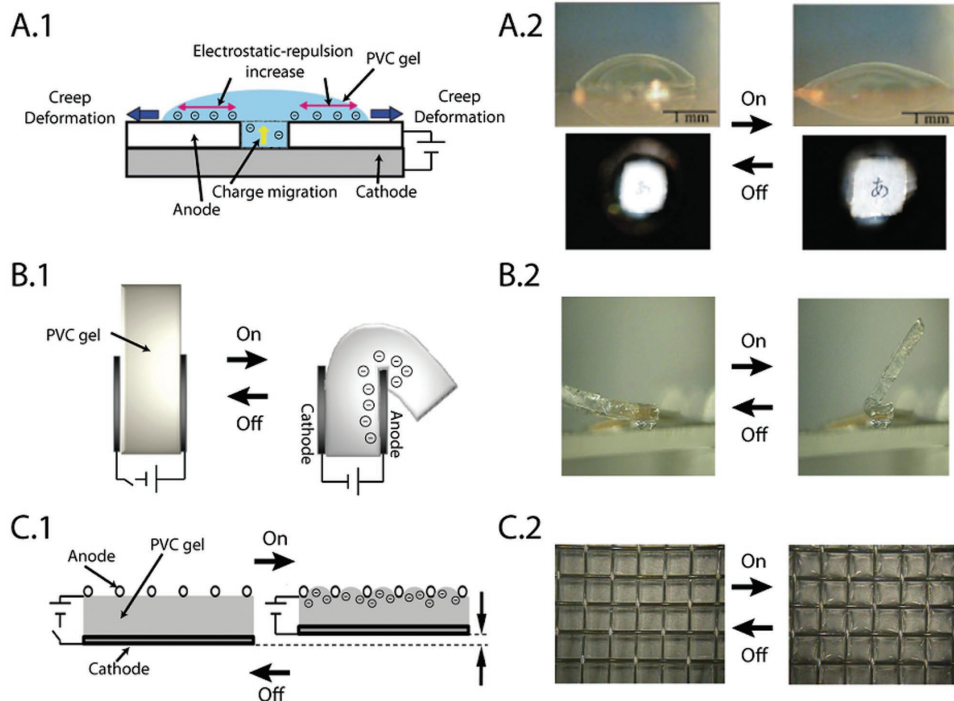


**Figure 6.** Various electrode arrangements for actuation of PVC gel, a type of non-ionic electric-field-responsive gel. A) Symmetric deformation of clear PVC gel allows the creation of an active lens. B) Significant bending motion can be achieved with an overhanging gel sandwiched between electrodes. C) Contraction in the thickness direction of a PVC gel film is achieved with mesh electrodes. Stacked layers amplify this motion. A.1,A.2) Adapted with permission.<sup>[10]</sup> Copyright 2009 John Wiley & Sons Inc. B.1) adapted with permission.<sup>[196]</sup> Copyright 2010, Elsevier. B.2,C.2) Adapted with permission.<sup>[87]</sup> Copyright 2008, IEEE. C.1) Adapted with permission.<sup>[88]</sup> Copyright 2009, IEEE.

due to the polarization of the accumulated charge density in the electric field, and depends on the Coulomb force between the two electrodes.<sup>[196]</sup> Uddin et al. examined the effect of different plasticizers, especially with respect to activation speed.<sup>[183]</sup> Several groups are researching artificial muscles by stacking of PVC gel actuators; the biggest response reported so far is a contraction of 14% with a response rate of 7 Hz and a force output of 4 kPa in a field of  $\approx 1.3$  MV m<sup>-1</sup>.<sup>[88]</sup> The authors showed that the characteristics of the actuator are strongly dependent on the electrode configuration and operation temperature, and that the stiffness of the actuator increases as the applied DC field increases. Yamano et al. showed a bending actuator curving more than 150° in 1 MV m<sup>-1</sup>, with immediate deformation recovery as the field was switched off.<sup>[87]</sup> Harai et al. demonstrated a tunable artificial pupil in air made from PVC gel, stable for about 100 times operation over two years at room temperature.<sup>[10]</sup> The authors reported leak currents in the nano-ampere level, which is negligible compared to that of ionic EAPs. PVC-gel actuators have also been examined with respect to their shape-memory effects.<sup>[197]</sup>

### 3.3. Electrically Responsive Fluids

Activation of fluids by electric fields falls into three main categories: viscosity modification of dielectric-liquid particle suspensions, pumping of dielectric liquids, and selective surface-tension control of liquid droplets on surfaces. The latter

methodology, when performed on a dielectric surface, can function with most liquids. Electroactivation of fluids typically requires high voltages, ranging from hundreds to thousands of volts.

#### 3.3.1. Electrorheological Fluids

ER fluids are a class of liquids with rheological properties that can be tuned under an applied electric field. They are typically heterogeneous fluids composed of suspensions of dielectric particles in an insulating oil.<sup>[198]</sup> When an electric field is applied, the difference between the dielectric constant of the liquid and particles leads to polarization and the formation of a dipole moment. The end result is particle aggregation in chains along the field direction and a subsequent increase in fluid viscosity (Figure 7A).<sup>[199]</sup> The transformation is fast (order of milliseconds) and the change in viscosity is significant, especially in the case of giant ER fluids (GERFs) where upwards of  $\approx 200$  kPa yield strengths have been observed under a field of 5 MV m<sup>-1</sup>.<sup>[200]</sup> In GERFs, molecular rather than induced dipoles are utilized,<sup>[198]</sup> resulting in an increase of the induced maximum yield stress by more than an order of magnitude over previous ER fluids.<sup>[200]</sup> This discovery has changed an interesting, but not terribly useful, effect into a mechanism that could be implemented in a range of applications including microfluidics, dampers, and transmissions.<sup>[199]</sup>

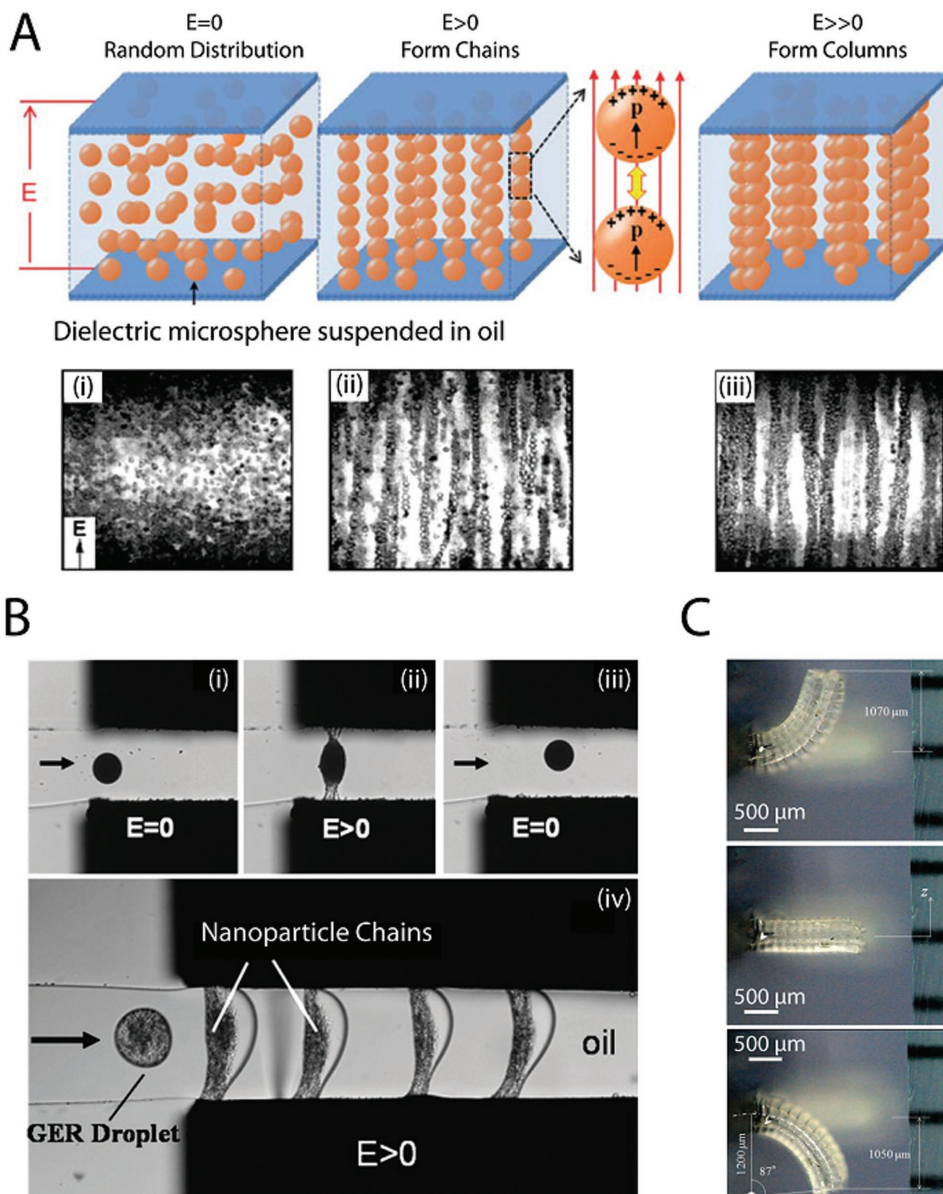


**Figure 7.** Electrorheological fluid demonstrations A) Activation of ERF and particle formation as electric field ( $E$ ) increases from (i)–(iii). B) ERF droplet in immiscible liquid stopping under an applied field (i)–(iii) and experiencing large deformations (iv). C) Bending cantilever that is deflected using fluid flow directed with ERF valves. A) (top) Adapted with permission.<sup>[199]</sup> Copyright 2012, The Royal Society of Chemistry. A) (bottom) Adapted with permission.<sup>[201]</sup> Copyright 2008, The Royal Society of Chemistry. B) Adapted with permission.<sup>[95]</sup> Copyright 2009, The Royal Society of Chemistry. C) Adapted with permission.<sup>[202]</sup> Copyright 2016, Elsevier.

ER fluids can be formed out of a variety of particles and carrying fluids.<sup>[203–205]</sup> These suspensions, however, do have a tendency for particle sedimentation or solidification, and can cause damage or clogging when used in microchannels. An alternative is homogeneous ER fluids, such as those based on liquid crystals. ER liquid-crystal molecules typically have length of 20 Å, making them suitable for microfluidic applications.<sup>[206]</sup> However, their time response and change in yield stress tend to be lower than for particulate ER fluids (demonstrated 3–50 kPa change, >5 s).<sup>[207–209]</sup> Liu et al. gave a comprehensive

comparison of yield stress and particle sizes between different ER fluid suspensions.<sup>[204]</sup>

The transition between liquid- and solid-like behavior, or the ability to withstand shear stress on demand, is useful in the indirect actuation of soft systems. While not actuators themselves, ER fluids can be used to modulate externally applied forces or fluid flow. To better categorize how they may be utilized in systems, three modes of operation have been defined: squeeze, shear, and flow.<sup>[210,211]</sup> In the squeeze mode, the ER fluid is compressed between two electrodes. In the shear mode,

the ER fluid is used to modulate the friction between two surfaces sliding against one another. In the flow mode, field-activated ER fluids act as microvalves, diverting flow. When the ER fluid is activated in a channel, the fluid flow through that channel can be slowed or even stopped.<sup>[212,213]</sup> For over two decades, ER fluids have been used as the basis for tactile displays, operating under one or more of these modes in combination with elastic membranes to create surfaces with various shapes and stiffnesses.<sup>[214–216]</sup> With the pressure differentials created using ER fluids as microvalves, a controllable, flexible miniature platform,<sup>[217]</sup> along with deformable bending cantilevers have also been demonstrated (Figure 7C).<sup>[202]</sup>

Smart GERC droplets, alternatively, have interesting potentials for microscale manipulation in microfluidic systems. Droplets of GERCs can be placed in a flowing fluid that is immiscible with its own composition. While typically a spherical shape carried by the flow, under an electric field it will deform, elongate, and change in velocity, possibly stopping completely. GERC droplets are also capable of creating pressure differentials and, if bracketing another inactive droplet or object, can be used for sorting (Figure 7B).<sup>[95,199]</sup>

### 3.3.2. Electro-Conjugate Fluids

In electro-hydrodynamic pumping, a dielectric fluid interacts with an electric field, generating a fluid flow. The electric body force, primarily the Coulomb force, is the source of this motion. Depending upon the particular fluid and electrode configuration chosen, four main pumping mechanisms have been shown to dominate: ion-drag, conduction, induction pumping, and flow generated by Maxwell pressure gradients.<sup>[96,218]</sup>

Ion-drag pumping involves the direct injection of free charges into the fluid. These charges flow along the electric-field lines from the source electrode to the collector electrode, pulling fluid along with them, resulting in an overall generated flow.<sup>[218]</sup> Conduction pumping relies similarly on the flow of free charges, though their generation is significantly different and is primarily due to the dissociation of the dielectric molecules or polar impurities.<sup>[96,218]</sup> Maxwell pressure-gradient flow occurs when an electric pressure gradient is produced by an applied non-uniform field. Induction pumping is a specific case of this mechanism, where flow is based on fluid charges occurring because of gradients in the electric conductivity. These can be produced with an interface of two materials with different electrical properties (such as the fluid and an insulating channel wall) or with a temperature-induced difference of electrical properties, thereby allowing electrodes to be placed outside of the liquid channel or bath.<sup>[96]</sup>

Historically, the majority of work has been focused on applications such as microfluidic systems including cooling, pumps, valves, reactors, and separators.<sup>[96]</sup> More recently researchers have used the electro-hydrodynamic jetting phenomenon to produce miniature pumps specifically for soft devices. With certain dielectric fluids (termed electro-conjugate-fluids (ECF)) and special electrodes (Figure 8A) the ion-drag phenomena will contribute to produce strong jets under a DC field, allowing high fluid pressures to be created by a compact device.<sup>[219]</sup> Demonstrated devices include a microscale finger,<sup>[220]</sup> a

microscale inchworm,<sup>[221]</sup> a hand,<sup>[222–224]</sup> and “muscle cells” (Figure 8B,C).<sup>[90]</sup> Each of these uses the jets to increase the pressure in deformable chambers, thereby producing motion. A recent paper by Baoyun et al. gives a comprehensive comparison of different dielectric fluids for pumping,<sup>[225]</sup> and Table 3 includes fluid material properties and generated pressures.

### 3.3.3. Electrically Responsive Actuation Based on Surface Tension

In electrowetting, the wettability of liquids on solid surfaces changes under the application of electric fields. The surface tension and the resulting contact angle of fluids can be modified, allowing controlled wetting of an advancing liquid front or deformation and steering of individual droplets. Electrowetting is applied in particular approaches, including electrowetting on dielectric (EWOD), continuous electrowetting (CEW), and electrocapillary actuation (ECA).<sup>[229–231]</sup> Unlike in the previously mentioned electroactivated fluids, the electrowetting effect will function with a wide range of liquids. In fact, EWOD, where a fluid is placed on a nonconducting film over an electrode, will apply to almost any polar fluid.<sup>[230]</sup> Typical actuation voltages for electrowetting are on the order of  $\approx 1$  V and for EWOD  $\approx 100$  V, though the latter is dependent upon the thickness and type of dielectric surface used.<sup>[230,232]</sup>

Electrowetting is a popular method for manipulation of small liquid quantities at the microscale.<sup>[233]</sup> From applications including lab-on-a-chip and droplet sorting to miniature lenses, electrowetting has proved to be a valuable technique in microfluidics.<sup>[97,230,234–237]</sup> Controlled droplets, however, can also be used to manipulate objects, allowing the creation of effective soft actuators that can both locomote and achieve significant deformations. Their locomotion is not limited to planar, horizontal substrates; droplet motion across continuous surfaces with varied shapes was shown by Abdelgawad et al. using asymmetric electrowetting.<sup>[238]</sup> Speed can be high, with  $250 \text{ mm s}^{-1}$  motion shown by Cho et al.<sup>[239]</sup> Moon et al. has demonstrated a flexible millimeter-scale conveyor system where a team of four droplets transported a platform (Figure 9B.2).<sup>[240]</sup> By surrounding a droplet with a flexible film, controlled and repeatable origami-reminiscent folding has also been accomplished (Figure 9A).<sup>[241–243]</sup> Crane et al. presented work toward enhanced understanding of electrowetting forces and droplet behavior to assist in the design of object manipulators.<sup>[244]</sup>

Similarly, liquid-marble locomotion can be achieved with electrowetting approaches. Using asymmetric electrowetting with outrunning finger electrodes, liquid-marble deformation and rolling have been demonstrated.<sup>[245]</sup> Deformation of a liquid marble under a DC field can be significant allowing reversible translational displacements, and, under stronger fields, induce liquid-marble jetting.<sup>[246,247]</sup> Typical liquid marbles are composed of water coated with PVDF, poly(tetrafluoroethylene) (PTFE), or lycopodium powder.<sup>[69,245,247]</sup> With the creation of Janus-like liquid marbles, where half the marble is coated with a conductive carbon black and half with the dielectric PTFE, the marble can be oriented under an electric field and rolled (Figure 10A.1).<sup>[74]</sup> Composite liquid marbles (two connected marbles composed of immiscible fluids), have also been shown to move and climb one

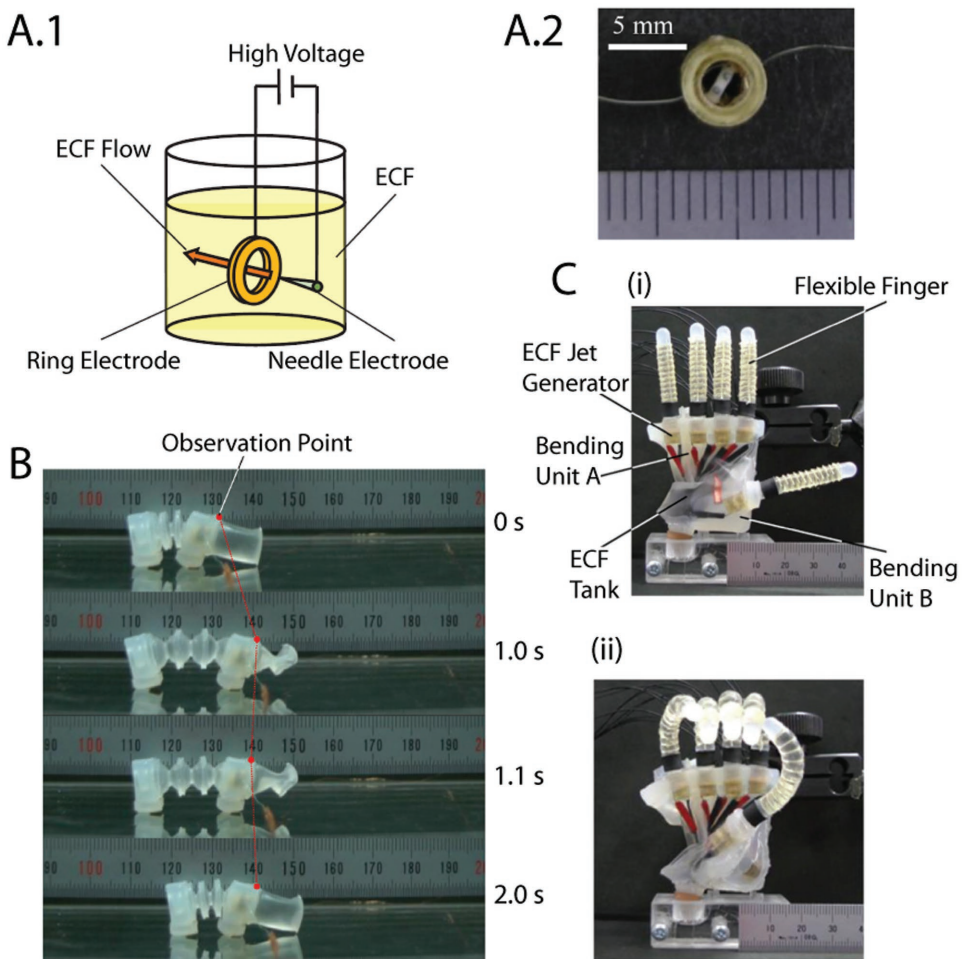


**Figure 8.** Dielectric fluid pumping, specifically ECF, in robotic systems A) ECF pump depicting a schematic diagram of ECF pump mechanism (A.1) and showing an implementation of needle and ring pump (A.2). B) Locomotion of an inchworm driven by an internal ECF pump. C) Miniature hand actuated with ECF pumps. The pumps are off in (i) and activated in (ii). A,B) Adapted with permission.<sup>[221]</sup> Copyright 2014, Elsevier. C) Adapted with permission.<sup>[222]</sup> Copyright 2012, Elsevier.

another due to their high dipole moments, which counteract the effect of gravity under an electric field (Figure 10A.2).<sup>[246]</sup> Under certain conditions, field-induced merging of liquid marbles is also possible.<sup>[248]</sup>

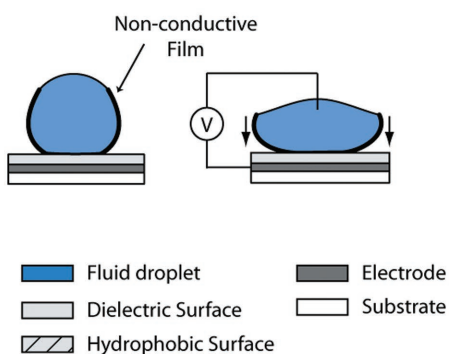
Liquid-metal electrowetting has the added advantage of being inherently conductive with the ability to transition between a liquid and a solid at near room temperature. When placed in an electric field submerged in an electrolyte, the surface

**Table 3.** Comparison of dielectric fluids for pumping.

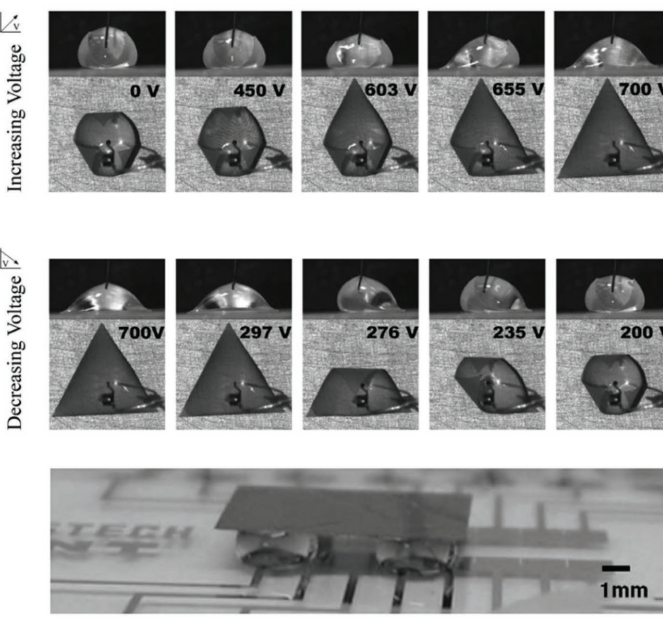
Fluid	Density [kg m <sup>-3</sup> ]	Viscosity [mPa s]	Dielectric constant	Conductivity [S m <sup>-1</sup> ]	Observed Performance
FF-101 <sub>EHA2</sub> <sup>[224]a)</sup>	1540	1.7	7.2	$2.2 \times 10^{-7}$	Electrode: 2 needle and ring, 0.2 mm gap; max. output: 33.6 kPa, 53.0 mL min <sup>-1</sup> @ 6.0 kV <sup>[222]</sup> Typical Power Consumption: 60 mW <sup>[226]</sup>
FF-1 <sub>EHA2</sub> <sup>[227]a)</sup>	1688	7.0	5.2	$4.5 \times 10^{-8}$	Electrode: 1 needle and ring, 0.2 mm gap; max. output: 13.5 kPa @ 8.0 kV <sup>[90]</sup>
Dibutyl decane-dioate (DBD) <sup>[224]</sup>	938	7.5	4.6	$6.8 \times 10^{-10}$	Electrode: 1 needle and ring; max. output: 10 kPa, 3 cm <sup>3</sup> min <sup>-1</sup> @ 6 kV <sup>[228]</sup>
Vertrel XF <sup>b,d)</sup>	1580	0.67	7–10	$1.0 \times 10^{-7}$ – $1.0 \times 10^{-9}$	Electrode: normal flat plates, gap 0.3175 mm; max. output: 13.7 kPa @ 21 MV m <sup>-1</sup> <sup>[225]</sup>
FR3 Envirotemp <sup>c,d)</sup>	920	33.0	3.2	$3.33 \times 10^{-12}$	Electrode: normal flat plates, gap 0.3175 mm; max. output: 3.45 kPa @ 15 MV m <sup>-1</sup> <sup>[225]</sup>

<sup>a)</sup>New Technology Management Co. Ltd., Japan; C5H<sub>2</sub>F<sub>10</sub>; <sup>b)</sup>Dupont; <sup>c)</sup>Cargill; <sup>d)</sup>Supplier data sheet.

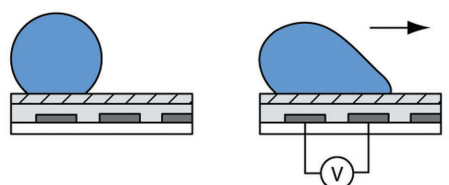
A.1



A.2



B.1



B.2



**Figure 9.** Fluid actuation with electric fields A) Symmetric EWOD for controllable membrane deformation depicting the general mechanism (A.1) and showing controlled, reversible capillary origami (A.2). B) Asymmetric EWOD where (B.1) shows a general mechanism schematic for inducing motion, and (B.2) depicts an EWOD-driven moveable droplet platform. A.2) Reproduced with permission.<sup>[241]</sup> Copyright 2010, The Royal Society of Chemistry. B.2) Reproduced with permission.<sup>[240]</sup> Copyright 2006, Elsevier.

properties of droplets can be manipulated using EWOD, CEW, and ECA.<sup>[229,231,250,251]</sup> With liquid gallium and gallium-based alloys, the removal and addition of its external oxide layer also serves to change the liquid's surface tension, allowing reversible flow in electrolyte-filled microchannels (Figure 9C).<sup>[252–254]</sup> This external oxide layer is hydrophobic, and, when oxidative electric potentials are applied, the creation of this thin layer induces capillary behavior, allowing flow outward. When reductive potentials are applied, the oxide layer is eliminated, and the liquid withdraws.<sup>[252]</sup> It is possible to control the flow of the liquid metal in these microchannels by strategic placement of the voltage source.<sup>[252]</sup>

Liquid metal can also be coated with micro- or nanoparticles, creating liquid-metal marbles. This has the added advantage of reducing droplet corrosivity, which can be an issue when working with liquid metals.<sup>[255]</sup> Using electrochemically induced actuation of a liquid metal, Galinstan, droplet coated with tungsten trioxide ( $\text{WO}_3$ ) nanoparticles in a basic electrolyte, Tang et al. demonstrated a significant droplet speed of 50 body lengths per second (100  $\text{mm s}^{-1}$  at 15  $\text{V}_{\text{DC}}$ ), which can be seen in Figure 10B.<sup>[249]</sup>

### 3.4. Electrically Responsive Paper

The piezoelectric properties of cellulose have been known for some time, however, it wasn't until the early 2000s that it was functionalized.<sup>[256,257]</sup> Termed electroactive papers, the first actuators were composed of metal-coated (silver, gold, aluminum) paper cantilevers 30 mm long, able to displace the tip 4.2 mm with a force of 12.7 mN at 0.23  $\text{V m}^{-1}$  and 7 Hz.<sup>[257–259]</sup>

The mechanism of cellulose actuation is attributed to a combination of ion migration and piezoelectric effects.<sup>[259]</sup> Ion transport is facilitated and increased with water absorption, leaving electroactive papers highly sensitive to humidity and temperature. Kim et al.<sup>[259]</sup> observed a displacement increase by as much as two orders of magnitude with an increase in humidity from 50% to 95%. Efforts to increase performance include enhancing the ion-migration effect by coatings with conducting polymer and ionic liquids,<sup>[260]</sup> and incorporating MWCNTs into the cellulose for an increase in mechanical strength and power output.<sup>[261]</sup> By carefully aligning the cellulose chains, the piezoelectric effect can also be increased, improving overall performance.<sup>[262]</sup>

### 3.5. Electrically Responsive Carbon Actuators

Several mechanisms for electrically actuating CNTs exist, including electrostatics and, more commonly, double-layer charge injection.<sup>[263,264]</sup> The latter is, in fact, an electrochemical reaction, where various ionic liquids have been inserted between the layers of a carbon structure. Under an applied electric field, atoms of the infused liquid will transfer electrons to the carbon, leaving the liquid positively charged, the carbon negatively charged, and the overall charge neutral. The result is an increase in the distance between the carbon layers and the length of the covalent bonds between them.<sup>[84,264]</sup> The total CNT structure can then be observed to expand and contract.

The majority of related papers demonstrate translational displacements or cantilever bending, but CNT torsional actuators have also been shown, with as much as 15 000° reversible rotations at 590 rev  $\text{min}^{-1}$  using twist-spun yarns.<sup>[265]</sup> Creating

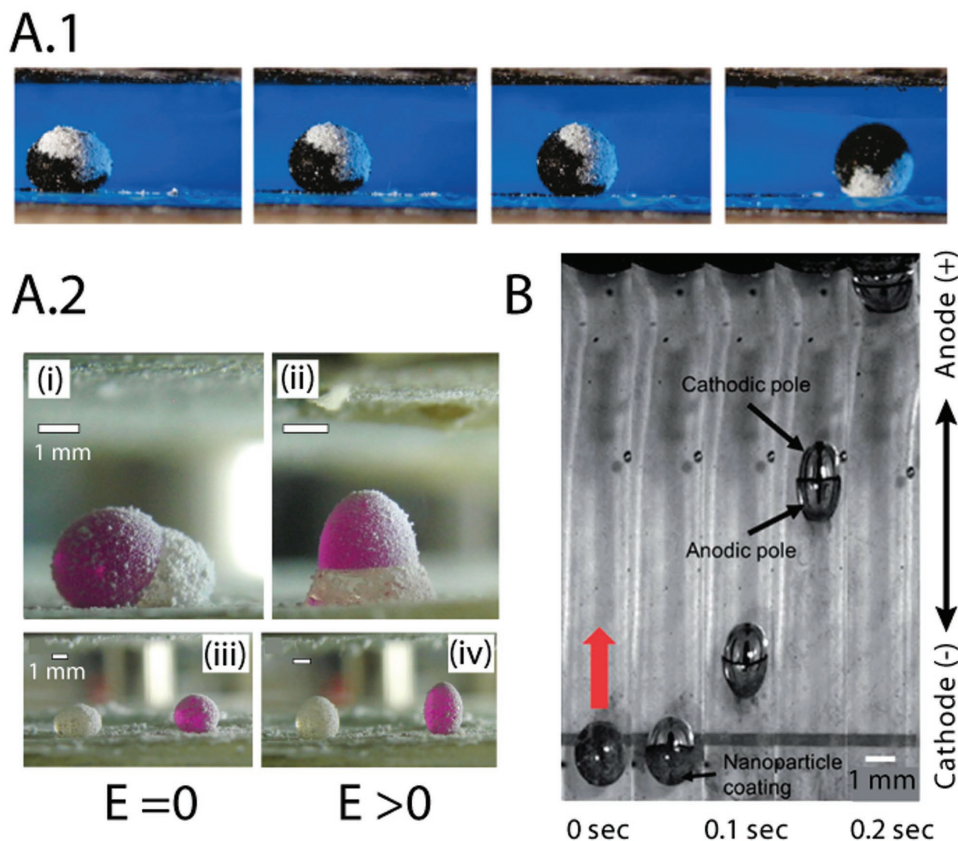


**Figure 10.** Motion of liquid marbles under an electric field. A.1) Rolling of Janus liquid marbles coated with carbon black and PTFE particles under increasing electric field (0 to  $6.7 \times 10^5 \text{ V m}^{-1}$ ) with electrode placed above and below. A.2-i,ii) Climbing composite liquid marbles composed of water (pink) and methylene iodide (white) coated with PTFE with no field (i) and a field of  $\approx 10^6 \text{ V m}^{-1}$ , iii,iv) deformation of individual marbles with initial zero-field state (iii) and a field of  $7 \times 10^5 \text{ V m}^{-1}$  (iv); electrode is placed above and below marbles. B) Electrochemically induced motion of liquid-metal liquid marble in electrolyte. A.1) Reproduced with permission.<sup>[74]</sup> Copyright 2011, American Chemical Society. A.2) Adapted with permission.<sup>[246]</sup> Copyright 2012, AIP Publishing. B) Adapted with permission.<sup>[249]</sup> Copyright 2013, The Royal Society of Chemistry.

a composite actuator with ionic gels avoids the typical issues involved with liquid electrolytes and tends to increase the actuator's producible strain.<sup>[189,191,266]</sup> At high cycled potentials, Spinks et al. demonstrated giant deformations (up to 300%) of CNT sheets immersed in an electrolyte.<sup>[85]</sup> As the applied electrical potential increases, the mechanism of double-layer charge injection is replaced by the evolution of gas bubbles, which push against the chambers in the CNT sheet, causing it to expand. Cycle life, however, is low, resulting in failure within a few hundred cycles. Further work has been done examining the effect of different sources of CNTs with different electrolytes on the work capacity and efficiency.<sup>[267]</sup>

There are many advantages in general to incorporating CNTs into soft actuators to improve their performance. Combinations with conducting polymers or ionic-polymer actuators may improve conductivity, modulus, and tensile strength.<sup>[98]</sup> Using CNTs for both composite electrodes and to anisotropically stiffen a cantilever actuator, Liu et al. produced an ionic-polymer actuator that demonstrated fast actuation times ( $>10\% \text{ strain s}^{-1}$ ) and strain  $> 8\%$ .<sup>[157]</sup> In the work of Aliev et al., thin CNT aerogel sheets with a thickness of  $\approx 20 \mu\text{m}$  have shown giant electrically activated elongation of 220% and elongation rates of  $3.7 \times 10^4\% \text{ s}^{-1}$ .<sup>[268]</sup>

#### 4. Magnetically Responsive Soft Actuators

Soft composites with magnetic fillers can be actuated in an external magnetic field. Typically this involves incorporation of magnetic particles or discrete magnets into a soft compound, creating an effective magnetization profile where both the magnetization direction and magnitude can vary.<sup>[269–273]</sup> When these actuators are subjected to an external magnetic field, the embedded magnetic particles or the attached permanent magnets try to align with the fields, generating torques, deformation, contraction, elongation, and bending. These forces can be created when the spatial gradients of the field interact with the magnetic particles or magnets. In small workspaces, the magnetic fields and their spatial gradients can be generated independently and the actuating magnetic torques and forces considered to be decoupled, effectively allowing two independent types of actuation for complex motions.<sup>[274]</sup> Different deformation patterns of these actuators can be designed by varying the actuating signals, the magnetization profiles, and the overall shape and stiffness of the materials.

As magnetic fields can penetrate through a wide range of materials, these magnetic actuators are ideal candidates for working in enclosed confined spaces and are especially

appealing for targeted drug delivery, microsurgery, microfluidics, and assembly within the body.<sup>[13,274–279]</sup> Another advantage is that their response is relatively fast compared to other modes of actuation, with demonstrations up to  $\approx 100$  Hz presented,<sup>[28]</sup> and they can also be controlled and assembled together in teams.<sup>[280–284]</sup> As a result, magnetic soft actuators have been successfully utilized for creating a variety of swimmers, crawling devices, and micropumps.<sup>[270,285–288]</sup> Due to the poor scaling of magnetic forces, however, external actuating magnetic coils tend to be large and have high power consumption. Workspaces where the applied magnetic field and gradients are of significant strength and can be well controlled tend to be small.

#### 4.1. Magnetically Responsive Polymers and Gels

There are generally two types of polymer-based magnetically responsive soft actuators. The first has a continuous magnetization profile and involves the incorporation of magnetic particles and/or ferrofluid into the entire sample. The second involves the attachment of individual magnets, creating a discrete magnetization profile, where only specific parts of the actuator will respond to an applied field. While the former tends to be more difficult to design and has lower magnetization magnitudes, they can be completely soft and have the potential for creating motions that are more complex. Such actuators have been realized across a wide range of soft polymers, such as poly(dimethylsiloxane) (PDMS), a silicon-based organic polymer,<sup>[28,288]</sup> Ecoflex,<sup>[270]</sup> rubbers,<sup>[289]</sup> and polyurethanes,<sup>[290]</sup> and also numerous types of gels.<sup>[291–294]</sup> A large variety of magnetic materials and ferrofluids have also been used, including a variety of superparamagnetic, paramagnetic, and ferromagnetic particles with length scales of nanometers to micrometers.<sup>[270,28,287]</sup>

Magnetic particles have been incorporated into soft polymers and gels in several different ways. The most widely used approach is to simply mix the particles into uncured material and encase them upon curing. Alternative approaches involve porous base materials absorbing magnetic-particle fluids, or precipitating particles onto nanofibril networks.<sup>[295,296]</sup> Once the particles have been embedded, if they have hard magnetic properties, the material can be magnetized by a large applied magnetic field. A typical process results in an actuator that has a continuous uniform magnetization, where each part of the actuator is magnetized at the same magnitude and in the same direction. The fabrication method is simple, and has been shown quite useful in a variety of implementations. For example, with a ferrogel (gel swollen with a fluid carrying magnetic particles), Zrinyi et al. has shown that it is possible to use the spatial gradients of the actuating fields to elongate the length of a uniformly magnetized gel.<sup>[297–299]</sup> The elongation of such ferrogels allows the actuators to create smooth motions that resemble soft pseudomuscular contraction, with reported strains of 60% under a load of 0.1 N with a corresponding stress of  $1.5 \text{ g cm}^{-2}$ .<sup>[300]</sup> Mitsumata et al. introduced soft actuators, termed two-phase magnetic gels, for improvement of the generated stress and strain, consisting of a thin layer of magnetic gel bonded to a thick layer of unmodified gel.<sup>[301]</sup> Piotr et al.

demonstrated millimeter-scale robots with uniform magnetization profiles that are able to generate a time-asymmetrical swimming gait with a maximum speed of  $0.3 \text{ mm s}^{-1}$  when subjected to a rotating magnetic field (Figure 11A.3).<sup>[28]</sup>

Long, flexible magnetic chains can also be created by binding individual micrometer-sized superparamagnetic particles together elastically. Dreyfus et al. was the first to demonstrate magnetic filaments used as an artificial flagella for cell propulsion.<sup>[304]</sup> Composed of colloidal magnetic particles connected with DNA, the flagella could be attached to a payload and used to control the object velocity. A number of oscillatory modes are possible when the filament is actuated with an external field, allowing various controlled locomotion patterns.<sup>[305]</sup>

Non-uniform continuous magnetization profiles were first introduced by Kim et al., with an example implementation shown in Figure 11A.1.<sup>[287]</sup> An external magnetic field was used to control the orientation of the magnetic particles in an uncured solution; next, UV light was used to polymerize areas in sequence to enable varying particle orientations along the material. This fabrication method, however, requires a curing method that is spatially controllable, limiting the possible range of materials. An alternative approach was proposed by Diller et al.<sup>[270]</sup> Here, the polymer was cured and then spatially deformed before magnetizing the embedded particles. The end result was an undulatory swimmer capable of propulsion, steering, and control in small groups (Figure 11A.2).<sup>[306]</sup> By combining thermally actuated hygromorphic materials and magnetic particles, Huang et al. was able to effectively change the magnetization profiles and the robot morphology on the fly.<sup>[285,307]</sup> Using temperature to alter the position and orientation of the internal magnetic particles, they demonstrated a microscale robot with varying gaits. Recent work by Lum et al. focused on the generalization of non-uniform continuous magnetization profile and applied field design in order to improve and increase the complexity of the produced shapes and motions.<sup>[273]</sup>

Discrete magnetization profiles can be fabricated by simply attaching permanent magnets to polymers and gels,<sup>[308–310]</sup> or by folding a material around them.<sup>[311]</sup> Although actuators with discrete magnetization profiles can generally achieve less-complex deformations, a variety of interesting soft actuators have been presented. With two attached permanent magnets, Crivaro et al. and Yim et al. created compliant bistable mechanisms that can be used for swimming<sup>[308]</sup> and drug delivery.<sup>[312,313]</sup> When excited by a relatively large external magnetic field, the devices switch between one metastable state and another, acting like a mechanical switch. Similarly, Qiu et al. developed a millimeter-scale swimmer composed of two rigid magnetic components connected via a central compliant hinge;<sup>[271,272]</sup> when subjected to a rotating magnetic field a clam-like motion propels the robot. At even smaller scales, Jang et al. developed a magnetically actuated multilink swimmer with a length of  $\approx 15 \mu\text{m}$  that was able to swim at up to  $0.93$  body lengths per second.<sup>[309]</sup>

#### 4.2. Magnetically Responsive Paper

Paper is also capable of absorbing fluids with magnetic particles. Ding et al. has tested a variety of papers and their uptake

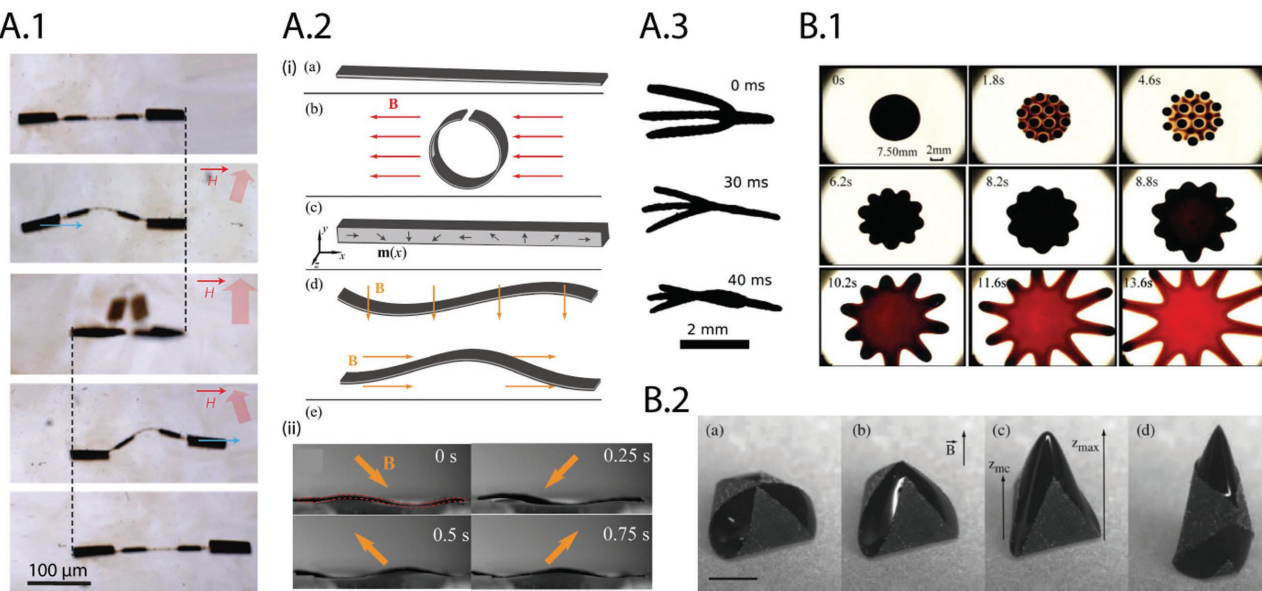


**Figure 11.** A,B) Magnetically responsive soft actuators based on polymers (A) and fluids (B). A.1) Microscale inchworm. A.2–i) Continuous-magnetization-profile fabrication method by Diller et al.<sup>[270]</sup> A direction-varying magnetization profile is created by folding the soft materials when it is magnetized. ii) Using this fabrication technique, a millimeter-scale undulating swimmer is created, shown actuated with a rotating magnetic field. A.3) A soft, millimeter-scale swimmer created by Piotr et al.<sup>[28]</sup> at several points in its gait. B.1) Shape change of a ferrofluid droplet over time with first a perpendicular field applied, then only radial. B.2) Magnetic capillary origami, subjected to an increasing field perpendicular to the surface (a–d). The scale bar is 2 mm. A.1) Reproduced with permission.<sup>[287]</sup> Copyright 2011, Macmillan Publishers Ltd. A.2) Reproduced with permission.<sup>[270]</sup> Copyright 2014, AIP Publishing. A.3) Adapted with permission.<sup>[28]</sup> Copyright 2009, IOP Publishing. B.1) Reproduced with permission.<sup>[302]</sup> Copyright 2010, The American Physical Society. B.2) Reproduced with permission.<sup>[303]</sup> Copyright 2011, The American Physical Society.

of an oil-based ferrofluid, reporting the cantilever deflection and force production when subjected to a magnetic field.<sup>[314]</sup> Inexpensive, commonly available paper was used and coated with Parylene to seal the ferrofluid and to improve the long-term robustness and stability. Depending on the material used, deflections of up to  $\approx 40^\circ$  and blocking forces of  $\approx 0.4$  N were achieved at 0.44 mT. In an alternative approach, Fragouli et al. demonstrated dry, waterproof magnetic cellulose sheets, which may prove to be an attractive option for future magnetically responsive paper actuators.<sup>[315]</sup>

#### 4.3. Magnetically Responsive Fluids

Magnetorheological fluids (MRFs) and ferrofluids are both liquid suspensions of magnetic particles. They differ primarily in their particle size, where ferrofluids commonly contain particles with diameters from 5 to 20 nm, and MRFs of one to tens of micrometers.<sup>[316,317]</sup> Accordingly, their properties and applications tend to be different.

When MRFs are exposed to a magnetic field, the magnetic particles within the fluid will form a gel of dipoles, aligning and forming columns along the direction of the field.<sup>[269,318]</sup> This, in turn, causes a significant increase in viscosity, and an effective transformation from liquid- to solid-like behavior. The viscosity of the MRF is dependent on several factors: the utilized fluid, the magnetic-field strength, and the concentration, size, and type of magnetic particles. The yield stress in an activated MRF tends to be around 100 kPa at a field strength of 0.8 T,

demonstrated by Genc et al.<sup>[319]</sup> Recent work has replaced magnetic particles with nanoscale wires to improve the yield stress at lower magnetic fields.<sup>[318]</sup> Predominant applications include active dampers or microvalves, but robotic demonstrations are still sparse.<sup>[269]</sup>

The small size of the magnetic particles in ferrofluids cause them to undergo Brownian motion, and can be viewed as being analogous to molecules of a paramagnetic gas.<sup>[316]</sup> As such, they are not subject to issues related to particle sedimentation that can occur in some MRFs with micrometer-sized particles. Under a magnetic field, complex spatial and time-varying patterns have been shown at the ferrofluid/air interface, which combine to balance the resultant magnetic force, gravity, and surface tension (Figure 11B.1).<sup>[316]</sup> With large, predictable, and repeatable deformations and locomotion, ferrofluid droplets represent an interesting actuator option for object manipulation and microassembly.<sup>[302,320,321]</sup> Similar to the capillary origami controlled by an electric field, magnetic capillary origami has been demonstrated with the use of a film suspended in a ferrofluid (Figure 11B.2).<sup>[303]</sup>

Liquid marbles can also be made responsive to magnetic fields, and are usually modified in one of two ways: by using hydrophobic or superhydrophobic magnetic nano- or micro-particle coatings,<sup>[322–324]</sup> or by using an internal liquid with suspended magnetic particles.<sup>[325,326]</sup> An interesting feature of magnetic particle coatings includes the ability to controllably “open” and “close” a liquid-marble surface,<sup>[323,324]</sup> allowing the potential for miniature chemical reactors or the ability to mix marble contents together.

## 5. Pressure-Driven Soft Actuators

Pressure-driven soft actuators fall under a category of structures known as compliant mechanisms. To generate effective actuation, compliant mechanisms have to spatially pattern their stiffness characteristics so that they can be stimulated by external pressure or forces to produce desired deformations. While a wide variety of compliant mechanisms exist, the studies pertaining to high-precision machines and microelectromechanical systems (MEMs) have been well discussed and reviewed,<sup>[327–332]</sup> with considerable focus toward the topological optimization of continuum structures.<sup>[333–343]</sup> Thus, here we will focus primarily on relatively new pressure-driven soft actuators that are employed for soft robotic applications. In particular, we will review elastic actuators based on the deformation of soft fluid-filled chambers, and briefly cover systems that utilize fluid interfaces and drag produced by pressurized flow. We end this section with a short overview of different methods to generate pressure differentials.

Although less popular than thermally and electrically driven nano- and microscale electromechanical systems,<sup>[344,345]</sup> miniature fluidic pressure-driven soft actuators are gaining traction. It has been shown that these soft actuators can produce admirable force, even at small scales. Scientists are pushing for easier manufacturing of small inflatable chambers, more accurate motions, higher force generation, and smaller devices to generate pressure differentials.<sup>[346,347]</sup> Reviews of miniature pneumatic and hydraulic actuators include the works of De Volder et al.<sup>[346]</sup> and Greef et al.<sup>[348]</sup>

### 5.1. Pressure-Driven Elastic Fluidic Actuators

Elastic fluidic actuators can be categorized into two main groups: membrane actuators and balloon actuators. Membrane actuators are systems composed of clamped, planar elastic sheets that are pressurized and expanded. Balloon actuators are composed of deformable or corrugated chambers, where motion is typically governed by heterogeneous chamber material or shape asymmetry.<sup>[349]</sup>

Historically, the most frequently used microfluidic actuators are membrane actuators. As early as the 1980s, arrays of thermopneumatic microscale pumps were used to peristaltically move fluid around in a channel.<sup>[350]</sup> This concept has later been extended to valves and pumps for microfluidic systems and lab-on-a-chip purposes,<sup>[351–355]</sup> as well as microoptics,<sup>[356]</sup> tactile/Braille displays,<sup>[357]</sup> and grippers.<sup>[358]</sup> However, an inherent shortcoming of membrane actuators is the restriction on deformation, resulting in a limited displacement per given footprint. By connecting these membranes to other mechanisms, however, researchers have expanded the range of motion. Ok et al. demonstrated a pneumatic-membrane microgripper with attached fingers capable of capturing motile microbes down to 400  $\mu\text{m}$ .<sup>[359,360]</sup> Membrane deformation has also been amplified with the use of structured membranes,<sup>[361,362]</sup> despite increased manufacturing complexity.

Balloon actuators have proven to be very versatile, with demonstrated soft actuators able to bend, twist, expand, and contract depending upon the design. Common at larger

scales,<sup>[4,363–365]</sup> there are also numerous examples at the milli- and microscale, where objects can be manipulated, and fluidic flow generated. Table 4 gives a comparison of small balloon actuator designs.

One of the most used materials for small-scale elastic fluidic actuators is PDMS, which is typically cast and bonded to create an internal void. The bending motion of such single-chambered cantilevers has been demonstrated in a number of cases, with Gorissen et al. showing 180° curling in a millimeter-scale cantilever,<sup>[379]</sup> Watanabe et al. achieving tool collapse for in-eye surgery,<sup>[378]</sup> and Konishi et al. creating a gripper for safe handling of delicate objects including fish eggs, cells, and hair.<sup>[376,377,380]</sup> The typical point of failure for these mechanisms is rupture along the bonding seam; however, several techniques to avoid this problem has been published. With a single-piece, high-aspect-ratio molding that avoids the bonding process, Benjamin et al. created a cylindrical cantilever with an eccentric cylindrical void.<sup>[349]</sup> Using a similar one-piece process, Gorissen et al. created an array of cantilevers ( $\varnothing$  1 mm  $\times$  8 mm) to achieve reversible fluid flow in a microchannel with a maximum velocity of 19  $\text{mm s}^{-1}$  (Figure 12A.2).<sup>[366]</sup> Paek et al. used a direct peeling-based soft-lithography technique to create spiraling tentacles ( $\varnothing \approx 150 \mu\text{m} \times 5\text{--}8 \text{ mm}$ ), able to deliver a grasping force of up to  $\approx 0.78 \text{ mN}$  at 5.5 kPa (Figure 12A.1).<sup>[32]</sup>

By adding a three-dimensional corrugated shape to a portion of the cantilever, the bending motion can be further modified and amplified. Using microstereolithography, a half-bellows three-finger microgripper was demonstrated gripping a 90  $\mu\text{m}$  bead.<sup>[371]</sup> More recently, with a corrugated mold, Wakimoto et al. demonstrated bidirectional cantilever motion with a single inflated chamber and air-line; under a positive pressure of 40 kPa, a maximum force of 2.2 mN was produced;<sup>[372,373]</sup> under a negative pressure of -16 kPa, a maximum of 0.6 mN was produced in reversed motion. Because of the relatively large possible deflections and compact size, this strategy is frequently used in active catheter design;<sup>[375,390]</sup> one of the smallest of which ( $\varnothing$  300  $\mu\text{m}$ ) was created using an embossing technique and was able to bend 180°.<sup>[374]</sup>

Another method of producing bending motion is to place balloon actuators at the joints between rigid links.<sup>[382,383]</sup> By adding balloon actuators in series, the overall deflection of the actuator can be amplified, allowing the creation of effective manipulators.<sup>[391,384]</sup> Choi et al. demonstrated fingers ( $\varnothing$  0.8 mm  $\times$  4 mm) with six actuated balloon joints that allowed full closure and grasping at 240 kPa (Figure 12A.3).<sup>[384]</sup>

The ability to generate compact twisting motion was relatively uncommon in elastic fluidic actuators until recently. Using PDMS soft-lithography techniques, a flat, layered cantilever with skewed, patterned internal chambers able to produce controlled twisting up to 6.5°  $\text{mm}^{-1}$  actuator length at 178 kPa was demonstrated (Figure 12B).<sup>[385]</sup> The use of negative pressure and chamber buckling has also allowed controlled contraction and twisting in molded silicone blocks;<sup>[392,386]</sup> up to 30° rotation at a pressure of -5 kPa has been shown. Although torque production is inherently limited by the maximum pressure differential between near vacuum and atmospheric pressure, the technique was used for both gripping, swimming, and inch-worm locomotion.

**Table 4.** Miniature pneumatic/hydraulic balloon actuator designs in the literature.

Actuator Design <sup>a)</sup>	Size ( $\varnothing \times l$ ) or ( $l \times w \times t$ )	Performance
Bending	( $\varnothing 1 \text{ mm} \times 10 \text{ mm}$ ) <sup>[349]</sup>	curvature $0.14 \text{ mm}^{-1}$ @ $0.1 \text{ MPa}$ <sup>[349]</sup>
	( $\varnothing 1 \text{ mm} \times 8 \text{ mm}$ ) <sup>[366]</sup>	$19 \text{ mm.s}^{-1}$ induced fluid flow <sup>[366]</sup>
	( $\varnothing 0.15 \text{ mm} \times 5\text{--}8 \text{ mm}$ ) <sup>[32]</sup>	spiraling, $\approx 0.78 \text{ mN}$ force @ $68 \text{ kPa}$ <sup>[32]</sup>
	( $\varnothing 5.6 \text{ mm} \times 23.4 \text{ mm}$ ) <sup>[220]</sup>	$7.2 \text{ mm}$ displacement, $0.9 \text{ mN}$ force @ $\approx 8 \text{ kPa}$ <sup>[220]</sup>
	( $\varnothing 1\text{--}20 \text{ mm}$ ) <sup>[367,368]</sup>	$\varnothing 12 \text{ mm}$ bends $100^\circ$ @ $0.4 \text{ MPa}$ <sup>[367,368]</sup>
	( $\varnothing 16 \text{ mm} \times 48 \text{ mm}$ ) <sup>[369]</sup>	bends $80^\circ$ @ $0.4 \text{ MPa}$ <sup>[369]</sup>
	Not specified <sup>[370]</sup>	$<1 \text{ N}$ <sup>[370]</sup>
	Not specified <sup>[371]</sup>	Not Specified <sup>[371]</sup>
	( $\varnothing 2 \text{ mm} \times 15 \text{ mm}$ ) <sup>[372,373]</sup>	( $16 \text{ mm}$ , $2.2 \text{ mN}$ at $40 \text{ kPa}$ ), ( $14 \text{ mm}$ , $0.6 \text{ mN}$ at $-16 \text{ kPa}$ ) <sup>[372,373]</sup>
	( $\varnothing 0.3 \text{ mm} \times 4 \text{ mm}$ ) <sup>[374]</sup>	$180^\circ$ bending <sup>[374]</sup>
Longitudinal View	( $\varnothing 3 \text{ mm} \times 40 \text{ mm}$ ) <sup>[375]</sup>	$\approx 90^\circ$ @ $70 \text{ kPa}$ <sup>[375]</sup>
	( $7 \text{ mm} \times 0.8 \text{ mm} \times 0.61 \text{ mm}$ ) <sup>[376,377]</sup>	bends $85^\circ$ @ $170 \text{ kPa}$ <sup>[376,377]</sup>
	( $3 \text{ mm} \times 3 \text{ mm} \times 0.10 \text{ mm}$ ) <sup>[378]</sup>	curling to $\approx 1 \text{ mm}$ width <sup>[378]</sup>
	( $11 \text{ mm} \times 2 \text{ mm} \times 0.23 \text{ mm}$ ) <sup>[379]</sup>	$7 \text{ mm}$ displacement @ $70 \text{ kPa}$ <sup>[379]</sup>
	( $0.56 \text{ mm} \times 0.90 \text{ mm} \times \approx 0.2 \text{ mm}$ ) <sup>[380]</sup>	gripper holding force $\approx 45 \mu\text{N}$ <sup>[380]</sup>
	( $6.60 \text{ mm} \times 4.95 \text{ mm} \times 1.50 \text{ mm}$ ) <sup>[381]</sup>	$10.5 \text{ mN}$ @ $12.5 \text{ kPa}$ <sup>[381]</sup>
	( $6 \text{ mm} \times 1 \text{ mm} \times 1 \text{ mm}$ ) <sup>[382]</sup>	$40^\circ$ bending, $20 \mu\text{N m}$ @ $1000 \text{ h Pa}$ <sup>[382]</sup>
	pressure cavity $10 \text{ mm} \times 10 \text{ mm}$ <sup>[383]</sup>	$\approx 4.5 \text{ mm}$ displacement, $50 \text{ mN}$ force @ $20 \text{ kPa}$ <sup>[383]</sup>
	( $4 \text{ mm} \times 0.80 \text{ mm} \times 0.12 \text{ mm}$ ) <sup>[384]</sup>	full closure and grasping @ $240 \text{ kPa}$ with six joints <sup>[384]</sup>
Torsion	Top View layer 1      layer 2	( $11 \text{ mm} \times 7 \text{ mm} \times 0.65 \text{ mm}$ ) <sup>[385]</sup> $70^\circ$ rotation @ $178 \text{ kPa}$ ( $6.5^\circ \text{ mm}^{-1}$ actuator length) <sup>[385]</sup>
	Longitudinal View	( $22 \text{ mm} \times 22 \text{ mm} \times 28 \text{ mm}$ ) <sup>[386]</sup> $30^\circ$ rotation @ $-5 \text{ kPa}$ <sup>[386]</sup>
Ext. and Contract.	Top View soft, low elastic modulus	( $\varnothing 0.8 \text{ mm}$ ) <sup>[387]</sup> $53 \mu\text{m}$ @ $138 \text{ kPa}$ <sup>[387]</sup>
	Longitudinal View stiff, higher elastic modulus	bellow corrugation $0.5 \text{ mm}$ <sup>[371]</sup> $175 \mu\text{m}$ @ $330 \text{ kPa}$ <sup>[371]</sup>
		( $\varnothing 1.5 \text{ mm} \times 22 \text{ mm}$ ) <sup>[388]</sup> $8 \text{ mm}$ , $6 \text{ N}$ @ $1 \text{ MPa}$ <sup>[388]</sup>
		( $\varnothing 5 \text{ mm} \times 10 \text{ mm}$ ) <sup>[389]</sup> $0.8 \text{ mm}$ , $0.17 \text{ N}$ @ $8 \text{ kPa}$ <sup>[389]</sup>

a) 

⊕ positive pressure applied

⊖ negative pressure applied

Pressure-driven linear actuators have been demonstrated using several main concepts. The first is microbellow actuators with symmetric corrugation, which extend upon pressurization.<sup>[371,387]</sup> Alternatively, contraction can be achieved, as in McKibben style actuators, where stiff fibers are added to the elastomer along the length of the cylindrical chamber. As the fibers inhibit further extension, upon pressurization, the chamber instead expands laterally resulting in a decrease in the overall actuator length.<sup>[393]</sup> DeVolder et al. demonstrated a miniaturized pneumatic version ( $\varnothing 1.5 \text{ mm} \times 22 \text{ mm}$ )

producing a force of  $6 \text{ N}$  and  $8 \text{ mm}$  stroke at  $1 \text{ MPa}$ .<sup>[388]</sup> Takemura et al. also demonstrated McKibben-style actuators using ECF pumps, the strongest ( $\varnothing 12.5 \text{ mm} \times 1.3 \text{ mm}$ ) generating  $1.56 \text{ mm}$  contraction and a force of  $0.32 \text{ N}$  at  $13.2 \text{ kPa}$  (Figure 12C).<sup>[90,389]</sup>

Although only demonstrated with chamber lengths on the order of tens of millimeters, pouch motors by Niyyama et al. present an interesting alternative fabrication method to lithography or molding.<sup>[394]</sup> Using layers of heat-stamped or heat-drawn thermoplastic films, actuators can be inexpensively mass produced.

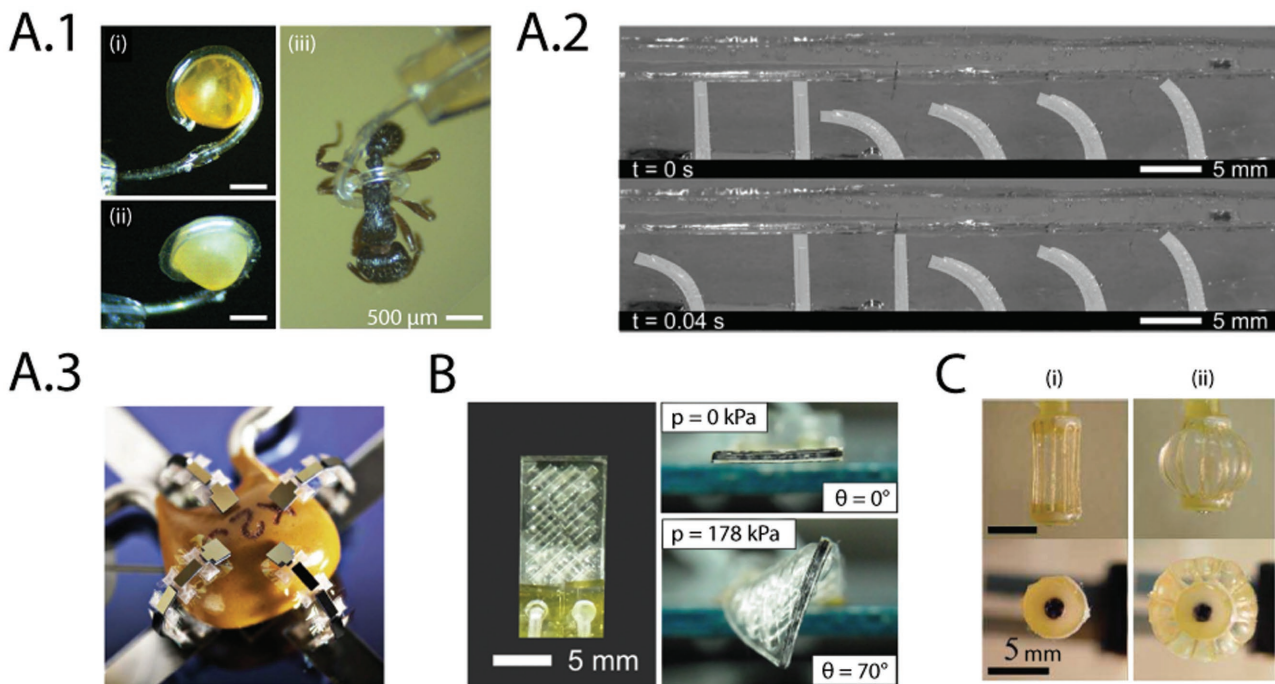


**Figure 12.** A) Pressure-driven bending actuators A.1) A microtentacle holding a fish (*Mallotus villosus*) egg (i,ii), and grasping an ant (iii). A.2) Flexing cantilever actuators forming cilia array for production of fluid flow in channel. A.3) Soft fingers holding a capacitor; each finger is actuated with inflatable chambers on joints. B) Twisting actuator in unpressurized and pressurized states. C) Contracting linear actuator, an artificial muscle, with an internal relative pressure of 0 (i) and 10 kPa (ii). A.1) Adapted with permission.<sup>[32]</sup> Copyright 2015, Macmillan Publishers Ltd. A.2) Reproduced with permission.<sup>[366]</sup> Copyright 2015, The Royal Society of Chemistry. A.3) Reproduced with permission.<sup>[384]</sup> Copyright 2009, IEEE. B) Reproduced with permission.<sup>[385]</sup> Copyright 2014, Elsevier. C) Adapted with permission.<sup>[389]</sup> Copyright 2005, IEEE.

As additional layers of more-rigid materials are added, they allow easy incorporation into printable robotic systems.<sup>[395]</sup> Both linear contraction (28% with 100 N at 40 kPa) and bending (80° with 0.2 N m at 20 kPa) has been demonstrated.<sup>[395]</sup> Finally, granular jamming deserves a quick mention. Based on sealed chambers filled with irregular particles, an applied vacuum results in chamber compression and particle interlocking. This allows controlled stiffness changes, and the concept has been used in grippers,<sup>[396]</sup> haptic surfaces,<sup>[397,398]</sup> rolling spheres,<sup>[399]</sup> and in conjunction with McKibben-style actuators.<sup>[400]</sup>

## 5.2. Pressure-Driven Fluids

With control over the internal volume of a fluid droplet or gas bubble, the surface or interfacial tension at the interface can be used directly to produce work. Casier et al. demonstrated 3 mm droplets that could tilt, raise, and lower a platform with 50 μm accuracy using a connected fluid pump.<sup>[401]</sup> Deflection of a cantilever in fluid was demonstrated by Lee et al. using a generated microscale bubble.<sup>[402]</sup>

Although it will not be discussed in depth here, fluid flow can also actuate objects using viscous forces.<sup>[388]</sup> Such fluid flow can be used to create near-frictionless interfaces for part levitation or manipulating objects in mass. Fluid jets, when generated on a moveable object, can also be used for propulsion.<sup>[403–405]</sup> For further reading, see the work by De Volder et al.<sup>[388]</sup> and Laurent et al.,<sup>[406]</sup> the latter of which is a thorough and recent review of pneumatic-manipulation surfaces. In addition, a

recent review by Sánchez et al.<sup>[407]</sup> covers chemical propulsion for miniature systems, including microjetting.

## 5.3. Generating Pressure Differentials

In many cases, the use of bulky off-board pumps, compressors, and valves is not feasible, and smaller pressure-generating devices must be used. Wehner et al. has reviewed a number of pneumatic energy sources for autonomous and wearable soft robots.<sup>[347]</sup> Battery powered microcompressors, compressed fluid cylinders, combustion, and monopropellant decomposition are viable options, depending upon the particular application and needed footprint. Battery-powered microcompressors are well suited for systems requiring lower pressures and flow rates, but currently are only commercially available down to ≈40 g. Compressed gas cylinders can supply higher pressures at higher rates, but are exhausted quickly and tend to be heavy. Combustion of materials, such as methane and butane, as well as monopropellant decomposition of hydrogen peroxide, can be used to drive smaller systems; however, the former tends to act excessively quickly, given the time constant of typical elastic systems, and the latter may require complicated designs.<sup>[347]</sup>

Another alternative is to utilize a temperature-induced material phase change. When transitioning between a solid and liquid or a liquid and vapor, an increase in occupied volume and corresponding pressure can occur. For example, heaters manufactured using the traditional micro electrical mechanical

systems (MEMS) technique allow the selected activation of any number of filled chambers. Bergstrom et al. introduced thermopneumatic actuation, where a pressure increase of 122 kPa could be maintained using methanol heated at 10 mW.<sup>[408]</sup> As an extension of this, Broek et al. has described explosive evaporation of ethanol to drive membrane actuators.<sup>[409]</sup> The solid–liquid phase change of paraffin is capable of producing pressures of 6.9–69 MPa,<sup>[410]</sup> with demonstrated microactuators in the work of Dowen et al.<sup>[410]</sup> and Carlen et al.<sup>[411]</sup> Furthermore, the pumping of ECFs, discussed earlier, requires high driving voltages, but has the advantage of creating high pressures (33.6 kPa) with small ( $\approx$ 5 mm diameter), simple pumps.<sup>[222]</sup>

Finally, to avoid the need for several compressors, multi-chambered fluid elastic actuators typically use valves such as solenoids, which are rigid, expensive, and large. Interesting work to address this problem involves a valve design similar to leaky check valves to allow control of pressures in a network of multiple connected chambers from a single input.<sup>[412]</sup> Although this valve requires more-accurate pressure control, is state dependent, and was implemented on a large scale, the concept may warrant further investigation on smaller scales.

## 6. Thermally Responsive Soft Actuators

Thermally triggered actuators include those activated by infrared (IR) or near-infrared (NIR) light, thermal radiation, or Joule heating. Joule heating, also known as resistive heating, works by stimulating conductive materials electrothermally. Thermal actuators can be remotely powered and heat can be applied globally or locally, e.g., via lasers. In addition, compared with solvent and UV stimuli, thermal triggers are typically safer and can be used around living cells, as long as the temperature remains between 4 and 37 °C.<sup>[413]</sup> However, actuators that are triggered by heat tend to be considerably less efficient and slower than their counterparts. Efforts to increase efficiency and response times include the use of thinner films, more-heat-absorbent material, and higher power.

### 6.1. Thermally Responsive Polymers, Gels, and Paper

Thermal actuators based on material expansion are widely used in traditional MEMS systems, in part due to the ease of Joule heating. As an example, hundreds of “stiff” actuators have been demonstrated based on polysilicon, because its resistivity allows heating at relatively low voltages.<sup>[414,415]</sup> Dependent upon the material’s coefficient of thermal expansion, heat will cause a volumetric change, inducing actuation. The same principles can be applied to soft materials, especially when light-absorbent and conductive carbon nanoparticles, CNTs, and graphene are incorporated. Although the actuation of CNTs themselves can be accomplished through the application of heat with the thermoelectric effect,<sup>[416]</sup> they are more frequently used in soft actuators as a composite component. By either distributing carbon throughout the material or adding it as a thin film on top, electro- and photothermal activation is possible while maintaining material flexibility.

Recent work includes a bilayer swimming robot (7 mm  $\times$  1 mm) made of PDMS and graphene, able to deflect its tail 1.5 mm due to uneven heating when an NIR laser was applied for 3.4 s.<sup>[417]</sup> Similarly, bilayers composed of PDMS and CNT bucky paper, as well as reduced graphene oxide (rGO), have also demonstrated large bending strains.<sup>[418,419]</sup> With the addition of uniformly aligned CNTs, Deng et al. were able to both improve heating and tune the bending direction in photothermal actuators.<sup>[420]</sup> Electrothermal actuation was shown by Li et al., with helical curling of up to  $\approx$ 630°, with 48 W power consumption, and finger deflections in a soft hand with bending of greater than 180° at 46 W over 12 s with a recovery time of 28 s.<sup>[418]</sup> Using thinner prestrained graphene and PDMS films, Hu et al. achieved faster bending of 84° to 563° in 3.6 s, with  $\approx$ 7 s recovery time.<sup>[419]</sup>

In a rather different approach, James et al. used PDMS, thermally expanding microspheres, and CNTs to create a dramatic nonreversible heat-induced transformation of >500% volume expansion, >80% density reduction, and >675% increase in elastic modulus.<sup>[421]</sup> The microspheres consisted of gas-tight acrylic polymer shells encapsulating a liquid hydrocarbon; when heated, the hydrocarbon vaporized causing a significant expansion of the surrounding shells.

In the following sections, we will go into more detail about alternative actuation mechanisms that are thermally triggered, but not based solely on thermal expansion. This includes hygromorphic materials, the phase transition of liquid-crystal materials, and SMPs.

#### 6.1.1. Thermally Responsive Hygromorphic Materials

Hygromorphic materials expand or contract when in contact with water or with changes in humidity. With certain gels and polymers, this water swelling is controllable with changes in temperature. These materials undergo a phase transition between a hydrophilic swollen form to a hydrophobic shrunken form at a critical temperature.<sup>[422,423]</sup> The ability to function immersed in fluid and the potential for low transition temperatures have led to extensive research in the use of these materials for cell encapsulation and biocompatible polymer alternatives for use internal to the human body. One of the most widely used materials is poly(N-isopropylacrylamide) (PNIPAM), which is suited for operation at room temperature and near living cells.<sup>[422]</sup> Bilayers of biodegradable hydrophobic polycaprolactone and PNIPAM have been demonstrated to encapsulate and release yeast cells in the work of Stoychev et al.<sup>[424]</sup> Gelatin has also been used as the active component, allowing complete biocompatible and biodegradable enclosure of cells in a rolling film.<sup>[413]</sup> Unfortunately, the transition of gelatin is irreversible, making the produced motion irreversible. A recent study by this same group resulted in a fully biodegradable and reversible gelatin and polycaprolactone film; the reversibility is accomplished with the melting and recrystallization of the polycaprolactone, which balances the stresses induced by the swollen gelatin.<sup>[425]</sup>

As with other thermally responsive materials, carbon and graphene have been employed to improve actuation speed. A bilayer composed of reduced graphene oxide (rGO) particles

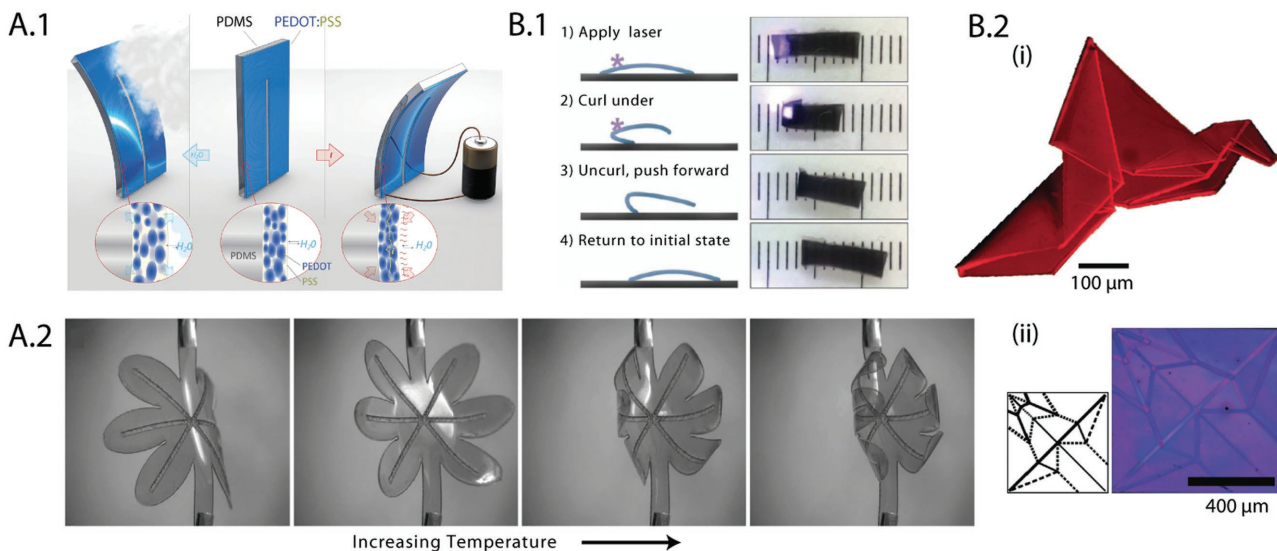


**Figure 13.** A,B) Thermally responsive hygromorphic actuators in air (A) and liquid (B). A.1) Hygromorphic actuator mechanism where water is absorbed from the surrounding air and released upon application of heat. A.2) Electrothermal hygromorphic flower actuator. B.1) Photothermally actuated hygromorphic crawler. B.2) Folded hygromorphic trilayer film (i) with initial sheet size of  $800 \times 800 \mu\text{m}$  (ii). The sheet unfolds when immersed in water at  $55^\circ\text{C}$  and refolds at  $22^\circ\text{C}$ . A.1) Reproduced with permission.<sup>[30]</sup> Copyright 2015, John Wiley & Sons Inc. A.2) Reproduced with permission.<sup>[426]</sup> Copyright 2015, John Wiley & Sons Inc. B.1) Reproduced with permission.<sup>[426]</sup> Copyright 2013, American Chemical Society. B.2) Reproduced with permission.<sup>[429]</sup> Copyright 2015, John Wiley & Sons Inc.

and elastin-like polypeptides allows actuation with an NIR laser, achieving  $>60^\circ$  bending in  $\approx 1$  s, recovering  $\approx 74\text{--}84\%$  within 10 s (**Figure 13B.1**).<sup>[426]</sup> Several studies have addressed how to further improve the photothermal efficiency in hygromorphic gels and films.<sup>[427,428]</sup> One of the most impressive demonstrations to date, in terms of achieved degree and complexity of bending and folding, was shown by Na et al. with a trilayer film.<sup>[429]</sup> With thin, rigid polymer layers bracketing a thermally responsive gel, Na et al. demonstrated a reversible, self-folding origami crane and Miura-ori composed out of a sheet ( $800 \mu\text{m} \times 800 \mu\text{m}$ ). The timescale of folding, however, was slow, requiring  $\approx 10$  min to swell and  $\approx 2$  min to deswell even when temperature was rapidly changed with immersion in appropriately heated or cooled water (**Figure 13B.2**).<sup>[429]</sup>

In 2009, Okuzaki et al. proposed a new class of EAPs based on the electrical conductivity and hygroscopic nature of conductive polymers.<sup>[430]</sup> These films, composed of polypyrrole, exhibit significant volume expansion in air, resulting from absorption and desorption of water vapor, and contract when an electric current is passed through them as a result of Joule heating. Recently, Taccolla et al. achieved bending through the use of a bilayer system composed of a humidity-responsive material backed by an inert material (**Figure 13A**).<sup>[30]</sup> This new type of actuator is multifunctional, with both intrinsic sensing and actuation capabilities. Speed and uniformity of bending were further improved with a combination of a stimuli-responsive hydrogel and fiber-like macroscopic graphene materials.<sup>[431]</sup> Activated with NIR light at 40% relative humidity, bending angles of up to  $60^\circ$  were achieved in 2 s, with recovery in 3 s.

Very recent work by Hamed et al. showed a similar implementation using paper.<sup>[432]</sup> Hamed created a conductive path in a sheet of paper that could contract due to a drop in moisture

content upon electrothermal actuation. This particular approach is promising because the produced actuation is nearly independent of relative humidity, and because the paper can be bent and creased without electrode failure. A  $50 \text{ mm} \times 10 \text{ mm}$  cantilever in 85% humidity was capable of  $3.53 \text{ mN}$  force and  $>30$  mm displacement at  $0.3 \text{ W cm}^{-2}$  with an activation and recovery time of 12–20 s.

#### 6.1.2. Thermally Responsive Liquid-Crystal Polymeric Materials

When exposed to a stimulus, typically heat, liquid-crystal materials can undergo phase transitions between a liquid-crystalline phase to an amorphous, isotropic phase. More generally, this corresponds to an ordered and a disordered mesogen arrangement. With good initial mesogen alignment, the phase transition can result in very large strain in this direction, as shown in Wermter et al. where  $>300\%$  was achieved.<sup>[433]</sup> A few examples found in the literature can be seen in **Figure 14**.

Considerable recent work has focused on this concept to make very complex shapes and motions, which would be otherwise difficult to achieve in most other actuators without complex control signals. Mesogens can be aligned using mechanical stretching and surface forces, as well as magnetic and electric fields,<sup>[52]</sup> after which the programming is completed by crosslinking the polymeric material. Ahn et al. used inhomogeneous and anisotropic material stretching to pattern the mesogen orientation;<sup>[437]</sup> others have demonstrated alignment using polarized light and photomasks, producing patterned, structured films (**Figure 14B**).<sup>[434,435]</sup> Using the latter approach, it is possible to align and crosslink individual groups of mesogens in arbitrarily complex patterns, with demonstrations that

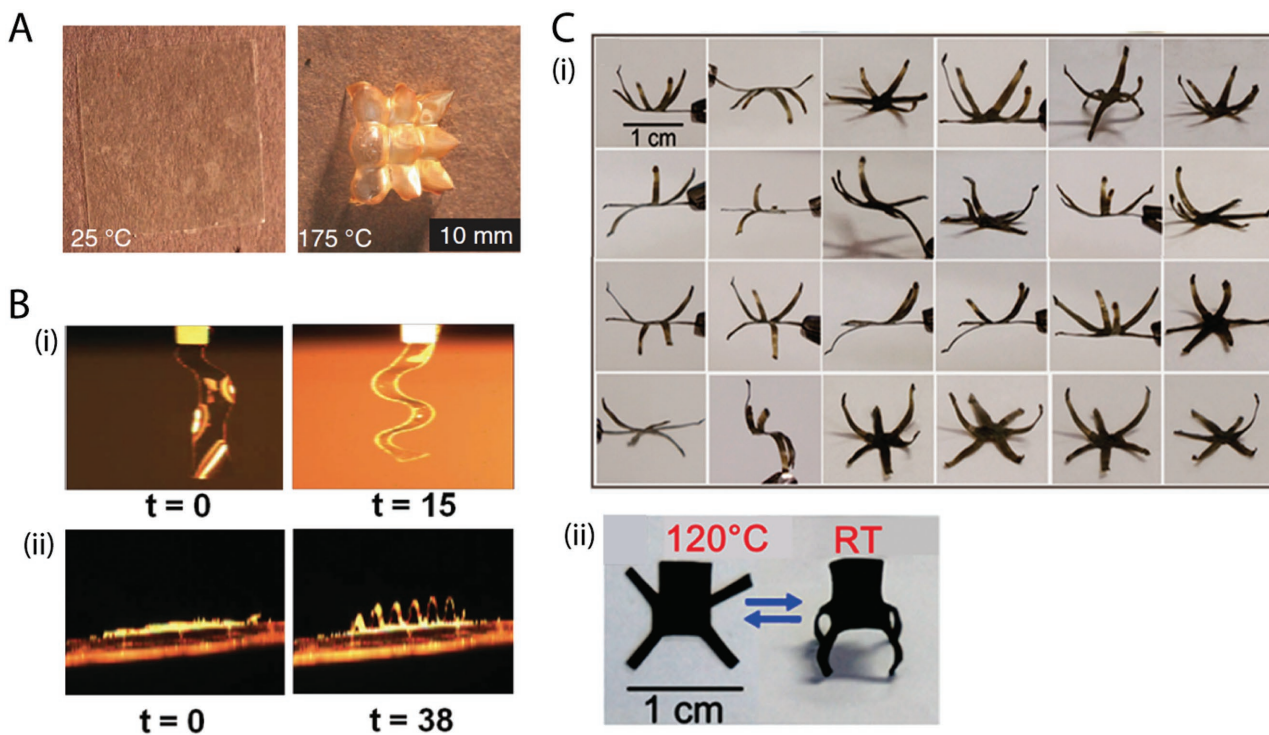


**Figure 14.** Thermally responsive liquid-crystal-based actuators A) LCE with mesogens aligned in groups or “voxels” using polarized light. B) IR actuation of two films with polarized-light mesogen alignment using lined photomasks. C) Reprogrammable LCE with training and actuation done with IR light: i) a single actuator film reprogrammed for actuation in more than 20 different shapes, and ii) reversible shape change of a miniature chair between room temperature and 120 °C. A) Reproduced with permission.<sup>[434]</sup> Copyright 2015, AAAS. B) Reproduced with permission.<sup>[435]</sup> Copyright 2014, John Wiley & Sons Inc. C) Reproduced with permission.<sup>[436]</sup> Copyright 2016, American Chemical Society.

include an initially flat heated sheet able to lift a load 147 times its own weight with a stroke of  $\approx 3000\%$ ; this impressive display was accomplished by Ware et al. with an LCE that had an actuated strain of  $\approx 55\%$  and specific and volumetric work capacities of  $2.6 \text{ J kg}^{-1}$  and  $3.6 \text{ kJ m}^{-3}$  respectively (Figure 14A).<sup>[434]</sup>

While the crosslinking, and therefore material programming, are typically permanent, recent work by Pei et al. has presented a technique in which LCE actuators can be retrained.<sup>[438]</sup> By using exchangeable covalent links whose topology can change with a change in temperature, LCEs can be heated, their mesogens realigned as desired, and then be actuated into a new shape.<sup>[438]</sup> With the incorporation of CNTs, this process can be accomplished photothermally, where both repeated programming and actuation are achieved with IR irradiation (Figure 14C).<sup>[436]</sup>

Microscale LCE actuators have not demonstrated the same motion complexity as their larger film counterparts, but the produced strain remains significant. LCE pillars smaller than  $100 \mu\text{m}$  have exhibited contractions of up to  $400\%$ ,<sup>[439,440]</sup> and have been incorporated into various smart, multifunctional surfaces and structures.<sup>[434–436,438,439–442]</sup> They are typically molded, but can also be manufactured using ink-jet-printing technology,<sup>[443]</sup> or produced in individual droplets in a continuous flow process.<sup>[444]</sup>

#### 6.1.3. Thermally Responsive Shape-Memory Polymers

Heat remains one of the most common stimuli used with SMPs, and includes SMP photothermal, electrothermal and

inductive heating with magnetic fields.<sup>[61]</sup> Conductive fillers, such as CNTs, carbon black, polypyrrole, and nickel powders, serve not only to increase thermal and electrical conductivity, but can also improve SMP mechanical strength and recovery stress.<sup>[445–451]</sup> Efforts to improve SMP properties have led to materials that can be strained up to 1000% before failure, with recovery up to 400% strain.<sup>[452]</sup> Work by Voit et al. has pushed this even further, with fully recoverable strains of over 800%, with a near-room-temperature glass transition of  $28^\circ\text{C}$ .<sup>[453]</sup> A recent comparison of SMP elastic-energy densities has shown values between  $0.01$  and  $2 \text{ MJ m}^{-3}$  for strains approaching 200%, with the best materials over  $1 \text{ MJ m}^{-3}$  for strains above 100%.<sup>[454]</sup>

Although traditional SMPs produce only a single irreversible deformation and limited force, their incorporation into a structure or film has allowed complex deployment and assembly tasks, as well as mechanism control. With a simple homogeneous SMP of pre-strained polystyrene (“Shrinky-Dinks”) printed with dark patterns, Liu et al. was able to achieve large bending and folding with local light absorption to assemble various shapes and enclosures.<sup>[455]</sup> Heat-activated SMP “Shrink Bags” of PVC incorporated into a trilayer film were used to create pop-up devices that, with the incorporation of basic electrical components and circuitry, bring fully printable robots closer to reality.<sup>[311,456,457]</sup> Using the ability to thermally tune the SMP stiffness, the motion of miniature flexure linkages can also be controlled<sup>[458]</sup> and be used to create effective bi-stable states in dielectric elastomer actuators.<sup>[459]</sup>

SMPs with multiple temporary shapes have also become possible using a broad transition-temperature range or a multiphase design. The latter is particularly difficult due to the need to design new composite polymeric materials, but the former is relatively straightforward, and can be accomplished with a range of SMP materials.<sup>[61]</sup> A broad thermal transition can be viewed as an infinite collection of sharp transition temperatures; by operating within this range, multiple shapes can be stored and recovered at adequately separated temperatures.<sup>[460]</sup> With this approach, up to quadruple and quintuple SMPs have been demonstrated.<sup>[58,460]</sup>

## 6.2. Thermally Responsive Fluids

Like the previously discussed electrowetting technique, surface-tension gradients and variable surface contact angles can be created with the application of heat through the thermocapillary effect. Droplets have been driven both in channels and on flat surfaces,<sup>[461,462]</sup> although the observed speeds generally compare unfavorably to their electrically driven counterparts, with  $\approx 0.7 \text{ mm s}^{-1}$  observed for a  $\approx 1.5 \text{ mm}$  radius water droplet and  $4 \text{ mm s}^{-1}$  for a  $26 \mu\text{m}$  droplet in work by Pratap et al.<sup>[463]</sup> and Hu et al.<sup>[464]</sup> A stationary liquid droplet was used as a deformable and actuatable mirror mount in the work of Dhull et al.,<sup>[465]</sup> where four surface microheaters induced a change in the droplet contact angle and therefore in the mirror tilting angle. Using small, embedded heaters, the applied voltage and current consumption can be kept low compared to their EWOD counterparts that can need upwards of 100 V.

With a uniformly heated and sawtooth structured surface, Linke et al. has demonstrated Leidenfrost droplet speeds as high as  $5 \text{ cm s}^{-1}$ .<sup>[466]</sup> A Leidenfrost droplet forms when a droplet is placed on a hot surface; the liquid boils and forms a vapor layer between the substrate and liquid, effectively levitating the droplet. With a ratchet-shaped surface, this vapor production can be used to propel the droplet forward.<sup>[466]</sup>

Finally, let us briefly return to liquid metals, such as gallium-based alloys, and their ability to transition between a liquid and solid near room temperature. While liquid metal can be directly actuated electrochemically or through electrowetting,<sup>[251,252]</sup> it also allows heat-based stiffness change.<sup>[117,467–469]</sup> For example, in a cantilever ( $3 \text{ mm} \times 5.7 \text{ mm} \times 0.24 \text{ mm}$ ) with microchannels filled with a low-melting-point alloy, Schubert et al. were able to demonstrate an elastic modulus change of greater than 25 times over  $<1 \text{ s}$  at  $<500 \text{ mW}$ .<sup>[468]</sup>

## 6.3. Thermally Responsive Metals

The shape-memory effect in metals, specifically the widely used nickel titanium (NiTi) shape-memory alloy (SMA), has become commonly used in soft robotic systems. We will not go into depth here due to our predominate focus on intrinsically soft materials, but direct interested readers to a recent review by Mohd et al.<sup>[470]</sup>

When the SMA is in the form of a coiled wire spring, both strain and force production can be significant; 50% contraction and an overall energy density of  $1226 \text{ J kg}^{-1}$  were demonstrated by Kim et al.<sup>[471]</sup> Their flexibility allows them to be easily incorporated into overall soft systems, such as the meshworm presented by Seok et al.,<sup>[2]</sup> as well miniature

printed and folded systems, such as a miniature flea-inspired jumper.<sup>[472]</sup> As a thin film, significant SMA bending can also be achieved, with both grippers and freestanding crawlers demonstrated.<sup>[473–475]</sup>

## 7. Photoresponsive Soft Actuators

Light-induced soft actuation is compelling because it can be remotely and accurately controlled, rapidly modulated, and easily focused on nano- and microscale areas.<sup>[476,477]</sup> Photochromic molecules play a major role in synthetic photoresponsive systems, capturing optical signals and translating these to useful property changes such as strain.<sup>[478]</sup> This is similar to light-driven mechanisms in nature, where, for example, the light-induced isomerization of retinal molecules triggers a number of chemical events, eventually leading to neural signals and the perception of light.<sup>[479]</sup> These molecules have found their use in microscale soft and flexible actuators composed of polymers, gels, fluids, and even photostrictive materials.

### 7.1. Photoresponsive Polymers

Light-responsive polymers are able to reversibly change their physical and/or chemical properties, including their shape, surface wettability, membrane potential and permeability, solubility, fluorescence, and transition and phase-separation temperatures upon irradiation.<sup>[476,479]</sup> Induced deformations of polymers include bending, contraction, and swelling motions. These deformations are typically reversible either by applying heat, by changing the wavelength of the light source, or by removing the light altogether. Several things influence the actuator response, including external factors such as the wavelength and intensity of the light and the irradiation time.<sup>[478]</sup> Increasing the light intensity or decreasing the thickness of the polymer films enhances the photochemical reactions in the bulk area of the film. Generally speaking, photochromic transitions are slower in a polymer matrix compared to a solution, but polymers have the obvious benefit of enabling dry air operation.<sup>[476]</sup>

To enable light-driven actuation, the polymers are filled with photosensitive functional groups or fillers; typically one of three groups: i) photoisomerizable molecules such as azobenzenes often found in photoresponsive LCEs and LCNs,<sup>[480]</sup> ii) triphenylmethane leuco derivates that undergo ionic dissociation<sup>[479]</sup> and need darkness to thermally reverse their reaction, or iii) photoreactive molecules such as cinnamates, which are often found in photoresponsive SMPs.<sup>[478]</sup> The two biggest classes of synthetic light-responsive polymers include liquid-crystal polymeric materials and SMPs, which are discussed in the following sections. Although we will treat them as distinct here, in very recent work, Kumar et al. have demonstrated a light-activated SMP effect in an LCN.<sup>[481]</sup> Furthermore, although most photoinduced actuation occurs by UV irradiation, there have been a few examples using NIR light on biological materials in aqueous solutions for intravenous drug-delivery applications.<sup>[482]</sup>

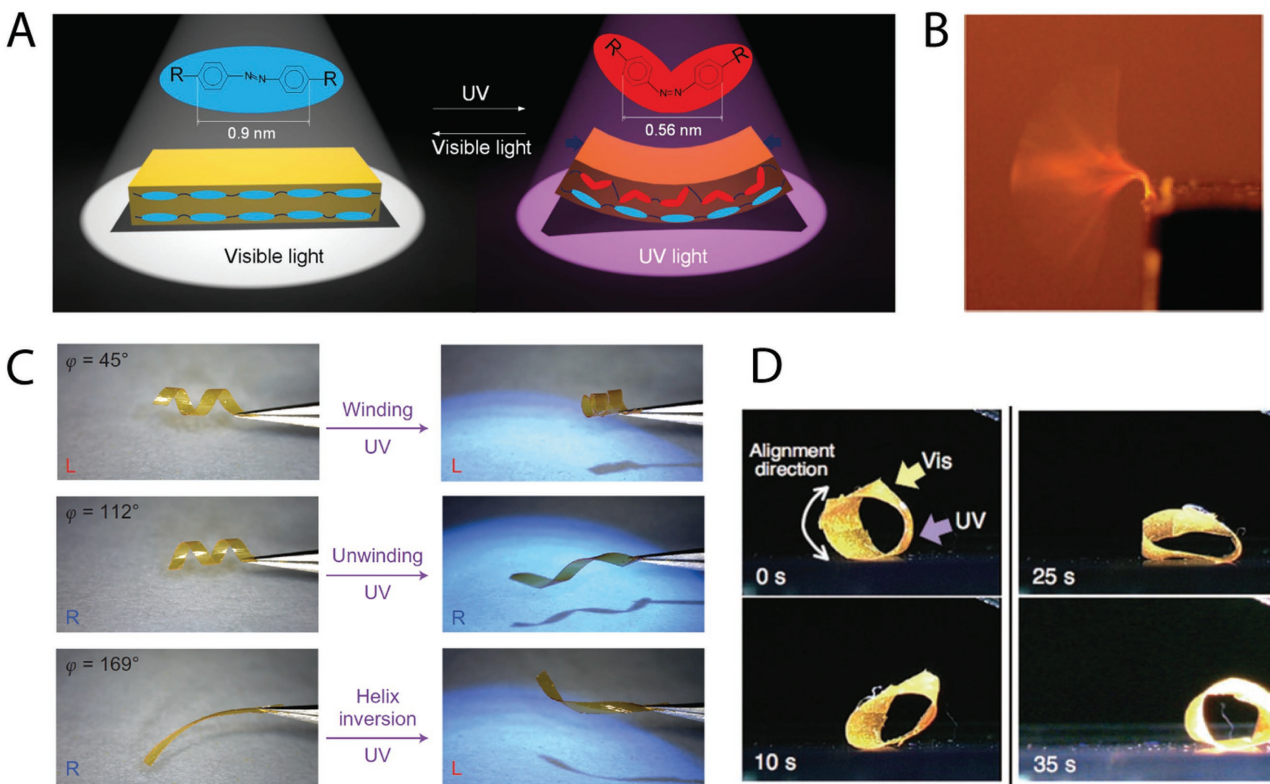


**Figure 15.** LC photoresponsive actuators based on azobenzene photoisomerization. A) Mechanism of operation. B) 28.4 Hz oscillation of an LCN cantilever with dimensions ( $5\text{ mm} \times 1\text{ mm} \times 0.05\text{ mm}$ ). C) Light-driven LCN “springs” with varying motion, dependent upon the initial shape and geometry. D) Rolling of an LCE film induced through the application of visible and UV light. Film is  $18\text{ mm} \times 3\text{ mm} \times 0.02\text{ mm}$  with a loop diameter of  $6\text{ mm}$ . A) Reproduced with permission.<sup>[485]</sup> Copyright 2015, Macmillan Publishers Ltd. B) Reproduced with permission.<sup>[486]</sup> Copyright 2008, The Royal Society of Chemistry. C) Reproduced with permission.<sup>[487]</sup> Copyright 2014, Macmillan Publishers Ltd. D) Reproduced with permission.<sup>[31]</sup> Copyright 2008, John Wiley & Sons Inc.

### 7.1.1. Photoresponsive Liquid-Crystal Polymeric Materials

Photoresponsive liquid-crystal polymeric materials are typically created using azobenzene fillers. When the azobenzenes are added to a material and irradiated, two types of effects can occur: cooperative motion at the nanoscale, where small portions of the molecules change their orientation, promoting others to do the same, effectively amplifying the signal,<sup>[476]</sup> or macroscopic motion at the microscale driven by pressure gradients and unequal isomerization patterns created by interfering light.<sup>[483]</sup> The basic mechanism of operation is depicted in Figure 15A. The former is now widely used in flat-panel displays and low-cost high-density optical-data-storage applications, which are robust, stable, have fast response times, and are inexpensive to produce.<sup>[476,483,484]</sup> The latter has found greater use generating large motion in microscale actuators (Figure 15B–D).

Most actuators demonstrated are in the shape of films.<sup>[488]</sup> In these polymer films light is predominantly absorbed in the surface layer (up to  $10\text{ }\mu\text{m}$ ).<sup>[489]</sup> Because of the strong absorption of UV light by the azobenzene chromophores, a substantial volume contraction occurs on the surface, consequently bending the films.<sup>[478]</sup> With linearly polarized light selective absorption can be achieved, allowing generation of precise motions aligned with the polarized light angle.<sup>[490–492]</sup>

As with thermally responsive liquid-crystal polymeric materials, mesogen alignment has been used to create photoresponsive actuators with greater motion complexity and stroke length.<sup>[487,493,494]</sup> By varying the initial actuator geometry cut from a chiral mesogen aligned film, Iamsaard et al. created actuators with expanding or contracting helical spring-like motions, reaching a steady state in minutes under UV light and relaxing in seconds under visible light (Figure 15C).<sup>[487]</sup> With an internal gradient in crosslink density, Oosten et al. was able to demonstrate bending reversibility of an LCN cantilever under a constant light source.<sup>[494]</sup>

Application-specific demonstrations include photocontrolled vesicle bursting for applications in drug delivery,<sup>[495]</sup> as well as LCE fish/flagellum-like films swimming in or on top of water at the micro- to centimeter scale.<sup>[485,496,497]</sup> Yamada et al. demonstrated a light-driven plastic motor and roller,<sup>[31]</sup> as well as a millimeter-scale flexible robotic arm.<sup>[488]</sup> Zeng et al. demonstrated a microscale walker able to speedily locomote on flat and structured surfaces.<sup>[498]</sup> Polymerized azobenzene compounds in LCNs have even been used to create activatable fingerprints to increase the gripping friction in robotic fingers.<sup>[499]</sup>

Liquid-crystal photoresponsive actuators have high processability, high corrosion resistance, low manufacturing costs, and, depending upon the desired motion complexity, can be

easy to manufacture. In general, however, their efficiency and speed are still far from optimal, and their thermal stability is poor.<sup>[489]</sup> As they do not rely upon the often lengthy heat-transfer times of their thermal counterparts, photoresponsive liquid-crystal polymeric materials do have the potential for higher speeds. White et al. demonstrated high-frequency ( $\approx 30$  Hz), large amplitude ( $>170^\circ$ ), and robust oscillations (little fatigue over 250 000 cycles) in photosensitive LCN cantilevers (Figure 15B).<sup>[486]</sup> Recent work by Zeng et al. shows the fastest response time of an LCE to date, at 1.8 kHz.<sup>[498]</sup> Future work includes targeting direct utilization of sunlight instead of high-power UV irradiation,<sup>[489]</sup> or use of other materials like diarylethene chromophores instead of azobenzenes for faster actuation speeds.

#### 7.1.2. Photoresponsive SMPs

Reversible light-induced stimulation of SMP films has been realized through the incorporation of cinnamic moieties, and must be differentiated from thermally induced SMPs.<sup>[500]</sup> Similar to the latter, photoresponsive SMPs are first stretched by an external force, then exposed to UV light to fix the elongated shape. After the external stress is released the film can stay in the elongated state for an extended period of time. Upon irradiation with a different wavelength, the original shape can be recovered.<sup>[501]</sup> Although this field is sparsely explored, these SMPs have been shown to work over a wide temperature range, be repeatedly deformable and temporarily fixed into predetermined complicated shapes, such as elongated films and tubes, arches, or spirals by UV irradiation of different wavelengths.<sup>[502]</sup> Because only the outer layer of the film reacts with the light source to become fixated, the opposite layer retains its elasticity, and has the potential to create curled shapes. If the shape programming is adjusted accordingly, the temporary shape can even be different in subsequent cycles.<sup>[478]</sup>

#### 7.2. Photoresponsive Gels

Photoreactive moieties can also be incorporated into gel networks to make them swell or shrink under irradiation. Macroscopically, the shrinking is referred to as a collapse of the gel causing the liquid to be expelled from the gel network.<sup>[503]</sup> Similarly, the three major principles of actuation include photoisomerization, photoionization, and photodimerization.<sup>[477]</sup> These gels have been applied to actuators, sensors, controllable membranes, and modulators for drug delivery. Photoresponsive gels are advantageous because of their potential to exhibit large deformations; however, big disadvantages include slow reaction times (minutes to hours) and the need to operate in liquids, often under potentially harmful UV light.<sup>[502]</sup>

The largest category of photoreactive gels is based on photoisomerization, commonly implemented via thermally sensitive PNIPAM hydrogel with azobenzene chromophores induced into the crosslinks.<sup>[476,477]</sup> These hydrogels exhibit contraction under UV or visible light;<sup>[504,505]</sup> the maximum collapse reported was 70% after 1 h.<sup>[477]</sup> Ikeda et al. showed bending of an LCE gel film in toluene and in air using different wavelengths over a

few minutes.<sup>[506]</sup> Sakai et al. introduced an alternative method, adding azobenzene chromophores as a sliding crosslinking unit, leading to gel expansion of 80–100% under UV light and contraction under visible light.<sup>[507]</sup> Another study reported superabsorbent hydrogels induced with azobenzenes causing the gel to completely liquefy under UV light.<sup>[508]</sup>

The second category involves photoionization, for example by incorporation of triphenylmethane leucocyanide groups into polyacrylamide hydrogels.<sup>[509,510]</sup> These non-ionic gels become ionic under UV irradiation, causing an inner osmotic pressure and consequent swelling. When left in darkness, the gels slowly return to their initial state. This gel dilation process can be repeated several times.<sup>[477]</sup>

The final category, includes photodimerization, meaning reversible photoisomerization of spirobenzopyran derivatives in hydrogel causing a collapse under UV light and swelling under visible light.<sup>[477]</sup> This phenomenon has been used to create microvalves, activatable by 18–30 s of UV light.<sup>[511]</sup> Furthermore, the asymmetric light intensity as the UV light passes through the gel has been used to create bending motions in gel rods and microconveyor belts.<sup>[512]</sup> A different strategy dependent on photodimerization was introduced by He et al. to gradually control the volume change in hydrogels using UV irradiation to reversibly change the crosslinking density.<sup>[513]</sup>

Photoresponsive gels typically show a combination of sensitivities to light, temperature, and pH values.<sup>[514]</sup> For example, the actuator presented by Al-Aribe et al. combines photo- and pH-sensitive gels in a bilayer structure to create microfluidic valves that contract by up to 28%.<sup>[515]</sup> Photothermally activated gel actuators were discussed in Section 6. Under every light condition, increased temperature typically causes a volume contraction; likewise, increased pH values typically diminish the swelling capability of the gel.<sup>[476]</sup>

#### 7.3. Photoresponsive Fluids

As with gels, most applications related to light-induced motion in fluids exist through photothermal effects. However, the following discussion describes a few research thrusts toward direct photoinduced motion of fluids.

Using assymetrical irradiation of UV and blue light, Ichimura et al. demonstrated the motion of an olive-oil droplet on a flat surface coated with a monolayer of azobenzene.<sup>[516]</sup> By shining light on the surface, azobenzenes are isomerized, creating a gradient in the surface free energy. The droplet first undergoes a decrease in diameter, increasing the contact angles of both the advancing and receding edges; eventually, the droplet starts moving at speeds  $\approx 35 \mu\text{m s}^{-1}$ .

Recently, researchers demonstrated the first photochemically induced actuation of a liquid-metal marble, composed of an alloy of gallium, indium, and tin, with a coating of nanoparticles made from  $\text{WO}_3$ .<sup>[517]</sup> When placed in hydrogen peroxide and illuminated by UV light, oxygen bubbles are created on the surface of the marble, resulting in accurate propulsion with an average speed of  $4.38 \text{ mm min}^{-1}$ . Performance characteristics given different hydrogen peroxide concentrations, light intensities, and marble sizes were examined.

#### 7.4. Photostrictive Thin Films

Although photostrictive materials have high elastic moduli, researchers have presented a few examples of flexible thin films. Photostriction in ferroelectric materials comes from the superposition of the photovoltaic effect, i.e., large voltage generation when irradiated with UV light, and the converse-piezoelectric effect, i.e., material contraction/expansion under the voltage applied.<sup>[518]</sup> Photostriction is largely dependent on the light penetration depth; therefore, the response time and magnitude of photostrictive actuators is improved by thinner films; recently, a response time in picoseconds has been reported.<sup>[519]</sup> A popular example of a photostrictive material is a lanthanum-modified lead zirconate titanate (PLZT) ceramic doped with WO<sub>3</sub>, because of its high piezoelectric coefficient and ease of fabrication.<sup>[520]</sup> This material has been used with polymer backings to produce photoresponsive films and micro-scale walking devices.<sup>[518]</sup> In 2004, Deshpande et al. discussed the option of using deflective diaphragms of photostrictive PLZT material for light-driven fluid dispenser units able to eject small amounts on the order of picoliters per second.<sup>[521]</sup>

### 8. Chemically Responsive Soft Actuators

Chemically responsive actuators are a rather broad category that can encompass a variety of mechanisms. Here, we take it to mean actuators that move upon application of a chemical stimulus in the form of a liquid or vapor, typically involving some chemical reaction, induced stress, and/or deformation. We also include capillary-force-based actuators that function on the introduction and evaporation of a fluid, commonly water.

The transformation of chemical energy into mechanical energy is called chemomechanical motion. Soft materials such as polymer networks and gels have the ability to selectively diffuse chemicals both in and out. The diffusion itself causes mechanical stress in the material and allows a variety of chemical reactions to occur internally. Reactions induced by stimuli such as acids, bases, organic solvents, or water vapor can modify polymer chains, alter their interactions, break bonds, or involve solution-based processes between the chains. This can alter the osmotic pressure or increase the chain affinity, and can eventually lead to material size and shape changes.<sup>[522]</sup> In an interesting robotic example of these reactions, Hore et al. demonstrated an elastomeric cylinder rolling uphill.<sup>[523]</sup> When organic solvent was added to the surface, it accumulated on the lower side of the cylinder, making it swell and thus pushing the cylinder upwards with enough force to carry 8–10 times its own weight.

While, in general, these types of actuators tend to be highly sensitive, response times are variable and depend upon the diffusion rate into the material.<sup>[522]</sup> In some cases, actuation rates can be on the order of minutes or hours. Correspondingly, this is a key research area with a number of recent publications. The rate of diffusion is classically increased by either increasing the actuator's porosity<sup>[524]</sup> or by employing surface treatments, such as oxygen plasma. Zhao et al., for example, were able to develop a porous polymer that was able to bend in complete circles in as little as ≈0.1 s;<sup>[525]</sup> they extended this work by coating other

materials, such as human hair and paper, to achieve further fast vapor-driven actuation (Figure 16A.1). Another method to improve the response time, reminiscent of the Venus flytrap, uses material snap-through instabilities to amplify motions; here, the instability was triggered in tens of milliseconds by the osmotic effect when hexane was introduced into an elastomer network.<sup>[526]</sup> A similar approach was used by Lee et al. to create a jumping microrobot with 12 ms response time and a release power of 34.2 mW g<sup>-1</sup> (Figure 16A.2).<sup>[29]</sup>

In the past decade chemically responsive SMPs have gained traction, especially toward the field of medical applications. Inside the body, where heating may be unfeasible, solvent-responsive SMPs can regain their original shape simply by immersing the sample in certain solvents at ambient temperatures.<sup>[176,529]</sup> Xiao et al. demonstrated multistage shape recovery using different solvents and temperature effects for eventual use in implantable medical devices.<sup>[530]</sup> Toward the same goal, Dong et al. presented redox and glucose-responsive SMPs.<sup>[531]</sup> Recent work on SMP hydrogels in ferric-ion solutions exhibits promising self-healing properties and materials that are capable of a change in elastic modulus from 2 to 70 kPa.<sup>[532]</sup> Unfortunately, many organic-solvent-driven SMPs suffer from very slow response times on the order of hours or days.

Liquid metals, such as eutectic-gallium-indium (EGaIn), can also fall into the category of soft chemically responsive actuators.<sup>[533]</sup> Droplets of EGaIn are surrounded by a layer of oxide that acts as an elastic membrane imparting soft properties for the liquid metal. Reminiscent of liquid marbles, Zhang et al. added aluminum flakes to the surface of an EGaIn droplet and achieved bubble propulsion when the droplet was immersed in a sodium hydroxide solution.<sup>[534]</sup> A significant advantage for these actuators is that the oxide layer is easily deformed, allowing the droplet to squeeze through narrow microchannels.

Finally, a notable type of chemically responsive actuator includes self-oscillating synthetic polymers and gels that undergo an effect called the Belousov–Zhabotinsky reaction,<sup>[535]</sup> very similar to oscillatory metabolic processes existing nature. By introducing reagents into the solvent, the reaction basically causes a “chemical wave” that result in periodic swelling and deswelling in the materials on the order of minutes (Figure 16B).<sup>[522,527]</sup> Recent demonstrations include enclosed substrates for biomimetic gel inchworms walking at a speed of 170 µm min<sup>-1</sup> and a ciliary motion array for mass transport.<sup>[536]</sup> The same group later published work on the easy fabrication of reproducible uniform microgels capable of self-assembly into millimeter-scale samples.<sup>[537]</sup> Large-oscillation amplitudes using the Belousov–Zhabotinsky reaction have been demonstrated by Maeda et al., where both period and amplitude were shown to be tunable through the actuator size and composition, as well as the temperature.<sup>[538]</sup> A great challenge still left in self-oscillating gels involves how to create time-asymmetrical responses relevant for more-complex motions.

#### 8.1. Water-Responsive Soft Actuators

Here, we discuss actuators that can create a volumetric change when actuated with water; the pervasiveness and general safety of water distinguishes them from other chemically responsive

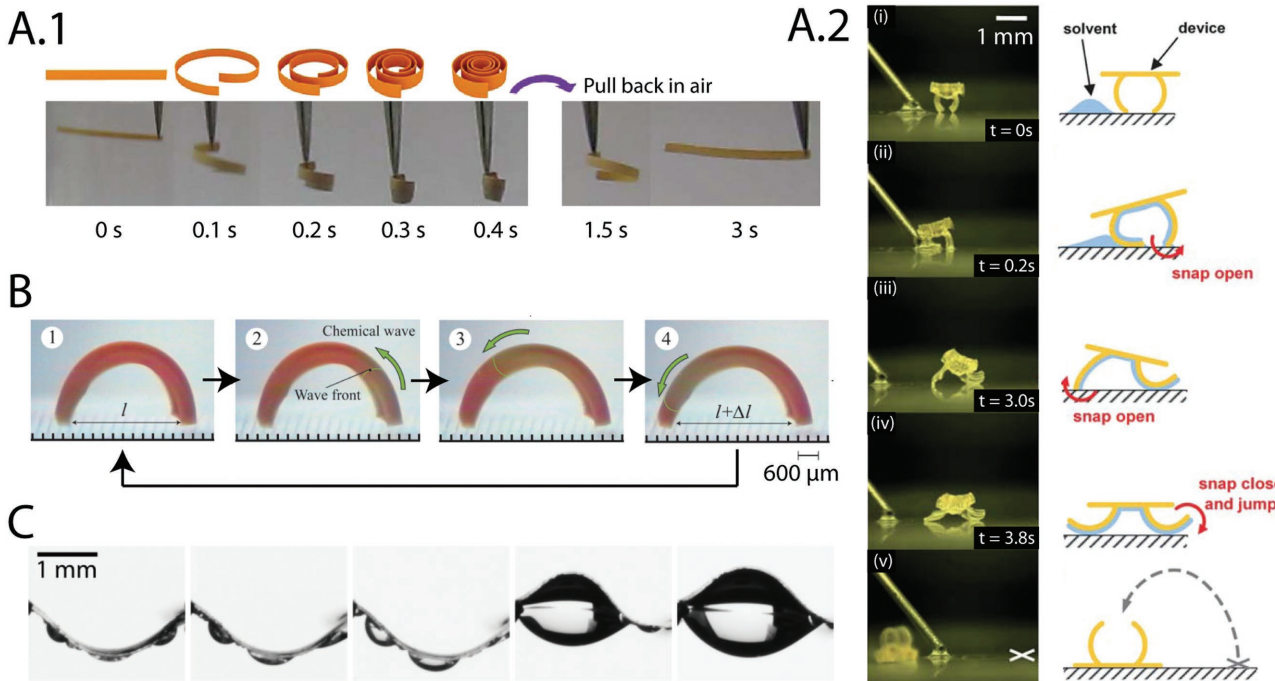


**Figure 16.** Chemical- and water-responsive actuators. A.1) Fast response of an actuator to acetone vapor. A.2) A microgel jumper induced with a liquid solvent. B) A self-walking gel driven by the oscillatory Belousov–Zhabotinsky (BZ) reaction. C) Snap-through of an elastic beam instability triggered by the surface tension of a condensation-formed water droplet. A.1) Adapted with permission.<sup>[525]</sup> Copyright 2014, Macmillan Publishers Ltd. A.2) Adapted with permission.<sup>[29]</sup> Copyright 2010, The Royal Society of Chemistry. B) Adapted with permission.<sup>[527]</sup> Copyright 2007, John Wiley & Sons Inc. C) Reproduced with permission.<sup>[528]</sup> Copyright 2014, The American Physical Society.

systems. Water is responsible for innumerable reactions in nature, proving that biocompatible actuation methods may work over broad size ranges, response times, and output power. Researchers have demonstrated water-responsive artificial systems using SMPs, LCPs, hydrogels, and paper, and have shown applications from simple benders to walkers, grippers, and artificial muscles.

Hydrogel sensitivity to changes in humidity has obvious applications in actuators.<sup>[188,539]</sup> As a great example of the power of water absorption/desorption on the nanoscale, Sidorenko et al. demonstrated fast (60 ms to 4 s) humidity-driven reversible switching of complex micropatterns in hydrogel nanostructures.<sup>[540]</sup> In addition to swelling, these hydrogels can also contract if their temperature is raised above a threshold known as the lower critical solution temperature and start to experience dehydration.<sup>[11]</sup> Actuators designed to respond to both temperature and humidity have been covered in Section 6.1.1.

More-traditional robotic demonstrations include that of Ma et al., where a millimeter-scale polymer-composite-film inchworm was developed. The water gradient-driven inchworm was able to generate contractile stress up to 27 MPa, lift objects 380 times its own weight, and transport cargo 10 times its own weight with second- to minute-long response times.<sup>[541]</sup> An earlier example by the same author showed a polyelectrolyte multilayer film walker (4.3 mm × 2.0 mm, weighing 0.3 mg) carrying loads up to 120 times its own weight under periodic alteration of the relative humidity between 11 and 40%.<sup>[542]</sup> The work by Taccolla et al., also mentioned in Section 6, used electrically controllable hygromorphic materials to move

hands, leaves, pedals, and bending actuators with changes in humidity.<sup>[30]</sup>

Humidity-responsive actuators based on liquid crystals were first reported in 2013 by Dai et al.,<sup>[543]</sup> and then again in 2014 by de Haan et al.<sup>[544]</sup> Whereas the former showed bending of bilayer structures, the latter managed to demonstrate both bending, folding, and curling with a single LCP sheet. Like humidity-responsive LCPs, humidity-responsive SMPs constitute a novel field where only a few examples exist.<sup>[545,546]</sup>

Much work is directed toward the creation of water-responsive materials that are completely biocompatible and biodegradable. Researchers have, for example, used humidity-responsive bacterial spores and natto cells as a material coating to achieve bending, contraction, and extending motions with high actuation forces, comparable to mammalian skeletal muscles, but with much higher strain capabilities.<sup>[547,548]</sup> Work by Su et al. showed a cellulose-acetate actuator using sodium chloride and osmotic effects to achieve up to 35.6 MPa in hydrostatic pressure.<sup>[549]</sup> In a recent example, Wu et al. developed biocompatible and biodegradable SMPs from cellulose nanocrystal composites for eventual use in minimally invasive surgery.<sup>[546]</sup>

## 8.2. pH-Responsive Soft Actuators

Researchers have proposed a range of actuators that experience swelling or shrinking depending on the level of pH in the surrounding fluid.<sup>[550]</sup> This is typically accomplished with the use of pH-responsive functional groups such as carboxyl

and pyridine, which undergo an ionization/deionization transition under certain pH ranges.<sup>[550]</sup> These types of chemically responsive actuators are considered to be especially useful for medical applications inside the body, where other stimuli such as heating and light, can be hard to apply; variations in physiological pH values exist naturally in the gastrointestinal tract, the vagina, and in blood vessels.<sup>[551]</sup>

Materials that are or can be made pH-responsive include organic polymers, hydrogels, LCEs, and SMPs. In an example of the former, Ye et al. demonstrated reversible rolling of rings, tubes, and helical tubes using biocompatible and biodegradable (150 nm × 20–100 μm) silk-on-silk sheets.<sup>[552]</sup> Hydrogels have been explored for their use as pH-responsive biocompatible cantilevers,<sup>[553]</sup> microgrippers,<sup>[554]</sup> smart microcapsules,<sup>[554]</sup> microscale lenses,<sup>[555]</sup> and valves for microfluidic systems.<sup>[556,557]</sup> Researchers have worked toward faster response times going from minutes to seconds by using new composites, geometries, or a combination of stimuli;<sup>[554,558]</sup> Gestos et al. demonstrated nano- and microscale hydrogel fibers achieving actuation strains of 20–100% with pH levels between 3 and 8 and response times down to 5–10 s.<sup>[558]</sup>

Although some materials that are insensitive to thermal stimuli have been fabricated, most still react to both temperature and pH.<sup>[554,555,557]</sup> As an example, LCE films devised by Haan et al. were capable of a nanoscale twisting motion when subjected to IR heating or changes in pH between 2.3 and 6.1.<sup>[435]</sup> Likewise, in SMPs, thermal sensitivity can be supplemented with pH sensitivity. Han et al. developed an SMP able to transition between the fixed and soft state in minutes with pH levels 7–11.5.<sup>[559]</sup> Song et al. demonstrated multi-stimuli-responsive SMP composites with the ability to store two or more shapes in a single shape-memory cycle; unfortunately, these changes happened over the course of hours.<sup>[524]</sup> Unlike these other actuators, Chen et al. demonstrated a highly pH-sensitive SMP with a functionality independent of heat.<sup>[551]</sup> Demonstrated pH-responsive SMPs in general, however, tend to be especially slow, and work is in progress to improve the response times from the scale of hours to minutes.<sup>[559–561]</sup>

### 8.3. Surface-Tension-Based Actuation

Controlled folding of flexible sheets with capillary forces, or capillary origami, has been discussed with respect to actuation by magnetic and electric fields. Although response times tend to be considerably slower, similar folding motions can also be accomplished with the introduction and later evaporation of liquid droplets.<sup>[562,563]</sup> This approach has long been used for accurate micropart assembly<sup>[564]</sup> and has been shown down to the nanoscale.<sup>[563,565,566]</sup>

Without the need for an accompanying electrode or coil system, there is more flexibility in the design of deformable elastic structures for capillary actuation. Ordered bundling of fibers is possible,<sup>[567,568]</sup> though once in contact, surfaces tend to self-bind due to van der Waals forces. Ruba et al. has demonstrated repeatable curling and uncurling of a millimeter-scale arm, with fibular ribs along one side, which are pulled closer together on the application of water.<sup>[569]</sup> Fargette et al. showed capillary-force triggering of snap-thorough instabilities in

elastic beams, with the resulting motion occurring in milliseconds (Figure 16C).<sup>[528]</sup> With liquid droplets at speed, dynamic capillary folding can also be accomplished. Here, the folding is dependent on both surface tension forces and inertia.<sup>[570]</sup> As long as the droplet does not need to be in motion, the production of condensation allows a way to introduce water droplets onto the designed structure in mass.

One particular limitation that exists in the interaction of flexible surfaces and droplets is the tendency for all surfaces, even hydrophobic, to wrap around the liquid. This phenomenon is the same as that which allows the particle coating of liquid marbles; the surface energy of the final wrapped state is lower than the initial unwrapped state. Gerald et al. recently explored the interaction of flexible superhydrophobic surfaces and liquid droplets, and were able to prevent this behavior.<sup>[571]</sup> Rough superhydrophobic surfaces do not allow water to penetrate into the surface structure, resulting in a nonadhesive reaction. With selective patterning of films, this could allow more-complex folding behavior and structures using capillary forces.

## 9. Perspective

We have given an extensive overview of soft-actuator methodologies on the nano- to centimeter scale, with a special focus on robotic implementations. This field includes a wealth of electrically responsive materials and, to a lesser but still significant extent, materials responsive to magnetic fields, pressure differentials, temperature, light, and chemicals. The materials consist not only of polymers and gels, but also fluids, paper, and carbon nanotubes. Each have their own advantages and disadvantages, summarized in Table 5, and a range of suitable applications.

The largest driving force behind the field of soft small-scale robotics is arguably biomedical applications for in-body diagnosis, treatment, and surgery, as well as precise manipulation of biological components such as embryos and cells.<sup>[348,579]</sup> Correspondingly, a great area of ongoing research involves biocompatible and biodegradable actuators that are able to operate under safe stimuli conditions. While the possible stimuli and their associated actuation mechanisms vary, many tend to be slow (e.g., those based on heat, ionic motion, and diffusion), which has led to additional effort to increase response times by modifying materials, with some notable examples including the works of White et al.,<sup>[486]</sup> Jiang et al.,<sup>[428]</sup> and Zhao et al.<sup>[525]</sup>

In almost all categories, we see a recent trend to exploit actuator nonlinearities to amplify the strain, force output, and response time for a given input. Examples include hyperelastic materials used with DEAs<sup>[112–114]</sup> and elastic fluidic actuators,<sup>[580]</sup> as well as mechanical instabilities introduced in capillary-driven actuators<sup>[528]</sup> and actuators responding to chemicals, solvents, and water.<sup>[29,526,541]</sup> This approach not only allows fast and large responses, but can also introduce reversible multistable states where continuous stimulus is no longer required.

As actuators shrink, more and more researchers depend on remotely applied stimuli, leaving control and sensing off board while working toward more complex material programming for added functionality. Liquid-crystal mesogen alignment and magnetic profile programming has already shown

**Table 5.** Summary of main soft actuator materials and actuation mechanisms.

Actuation Method	Mechanism	Material	Length scale	Advantages	Disadvantages <sup>a)</sup>	Motion, ex. Performance <sup>a)</sup>	References
Electric field	Motion of ions	Conductive polymers	nm–cm	Low voltage ( $\approx 1$ V), moderate strain and force production ( $\approx -10\%$ $\epsilon$ , work density $\approx 100 \text{ kJ m}^{-3}$ ), light weight, biocompatible	Requires submersion in or encapsulation of electrolyte, slow ( $>1$ s)	Bending • (cantilever $38 \times 10 \times 0.45 \text{ mm}$ ) $1.8\% \epsilon$ , $36 \text{ mN } F_b @ 3 \text{ V}$ • (cantilever $5 \times 0.8 \times 0.05 \text{ mm}$ ) $8\% \epsilon$ , $0.3 \text{ mN } F_b @ 4 \text{ V}$ in $\approx 5$ s	[40,92,138,157,572]
Ionic-polymer–metal composites (IPMCs)		$\mu\text{m}$ –cm	Low voltage ( $\approx 1$ – $5$ V), moderate strain and force production ( $\approx -3\%$ $\epsilon$ , work density $5.5 \text{ kJ m}^{-3}$ )	Generally slow ( $>1$ s), more durable in high humidity, high costs	Contr./exp. • (strip) $8\% \epsilon$ with $0.5 \text{ MPa}$ load @ $1.5\text{V}$ in $20$ s	Bending • (cantilever $40 \times 8 \text{ mm}$ ) $>2\% \epsilon$ , $3.6 \text{ mN } F_b @ 2 \text{ V}$	[153,573–575]
Carbon nanotubes (CNTs)		nm–mm	Low voltage ( $\approx 1$ – $5$ V), fast ( $<10$ ms), conductive, high power densities ( $>100 \text{ W kg}^{-1}$ )	Low strain ( $<1\%$ ), requires submersion in or encapsulation of electrolyte	Contr./exp. • (yarn $\varnothing 18 \times 120 \mu\text{m}$ ) $0.5\% \epsilon$ @ $2.5 \text{ V}$	Twisting • (yarn $\varnothing 12 \times 120 \mu\text{m}$ ) $15 \text{ }000^\circ$ rotation, $10 \text{ nN m} @ 5 \text{ V}$	[82,265,576]
Motion of ions and dipole orientation	Paper (cellulose)	$\mu\text{m}$ –cm	Inexpensive, low voltage ( $\approx 1$ – $5$ V), mass producible	Sensitive to RH%	Bending • (cantilever $30 \times 10 \times 0.03 \text{ mm}$ ) $4 \text{ mm}$ , $12 \text{ mN} @ 0.23 \text{ V m}^{-1}$		[259,260]
Dipole orientation	Liquid-crystal polymeric materials	nm–cm	Fast ( $<10$ ms), moderate strain ( $\approx 1$ – $30\%$ $\epsilon$ ), change in optical properties possible	High voltage ( $>1$ kV)	Contr./exp. • (gel sheet $t: 50 \mu\text{m}$ ) $32\%$ @ $20.8 \text{ MV m}^{-1}$ • (sheet $t: 75 \text{ nm}$ ) $4\%$ @ $1.5 \text{ MV m}^{-1}$		[20,54]
Electrorheological fluids (ERFs)	Electrorheological fluids	$\mu\text{m}$ –cm	Fast ( $<10$ ms), can stop and direct fluid flow	No direct actuation, possible sedimentation, high voltage ( $>1$ kV)	Liquid-to-solid transition • $>100 \text{ kPa YS} @ 5 \text{ MV m}^{-1}$		[200]
Electrostatic force	Dielectric elastomer actuators (DEAs)	$\mu\text{m}$ –cm	Large strains ( $>1000\%$ ), high energy density ( $>3 \text{ MJ m}^{-3}$ ), self-sensing, possibly fast ( $10 \text{ ms} \rightarrow 1 \text{ s}$ , speed material- and setup-dependent)	High voltage ( $\approx 1$ – $10$ kV), leakage currents, risk of electrical breakdown, prestrain required for greatest deformation	Contr./exp. • (sheet $100 \times 100 \times \approx 50 \mu\text{m}$ ) $37\% \epsilon$ @ $3.6 \text{ kV}$ in $\approx 50$ ms • (inflated sheet $\varnothing 45 \times 1 \text{ mm}$ ) $1692\%$ area $\epsilon$ @ $5.5 \text{ kV}$		[8,38,113,143]
CNT aerogel		$\mu\text{m}$ –cm	Fast ( $<10$ ms), high strain ( $>100\%$ ), work density $\approx 20 \text{ kJ m}^{-3}$ , operating temperatures $80$ – $1900 \text{ K}$	Low restoring force, high voltage ( $\approx 1$ – $10$ kV)	Contr./exp. • (sheet $l/w = 36$ , $t: \approx 20 \mu\text{m}$ ) $180\%$ width $\epsilon$ @ $5 \text{ kV}$ in $5 \text{ ms}$		[268]
Dielectric fluid (Electroconjugate fluid (ECF))		$\mu\text{m}$ –cm	Moderate generated pressures ( $>30 \text{ kPa}$ ), compact electrode pumps	High voltage ( $\approx 1$ – $10$ kV), potential eventual degradation, must be encapsulated, speed fluid and setup dependent ( $>1$ s)	Pressure generation (for bending) • $33.6 \text{ kPa} @ 6 \text{ kV}$ • (cantilever $\approx 6 \times 28 \text{ mm}$ ) $\approx 35^\circ$ bending @ $4.3 \text{ kV}$ in $1.5 \text{ s}$		[90,220,222]

Table 5. Continued.

Actuation Method	Mechanism	Material	Length scale	Advantages	Disadvantages <sup>a)</sup>	Motion, ex. Performance <sup>a)</sup>	References
(Surface-tension control with electrowetting)	Fluid droplets (on dielectric surfaces)	μm-mm	Applies to many fluids	Moderately high voltage ( $\approx$ 10–200 V, dependent on dielectric surface), possible leakage	Locomotion • (droplet) $\approx$ 2.5 mm s $^{-1}$ @ $\approx$ 100 V, load 180 mg • (droplet 55 μL) $\approx$ 250 μN @ 100 V • (droplet) 250 mm s $^{-1}$ @ 150 V AC	[239,240,244]	
Liquid marbles	Liquid marbles	μm-mm	Low friction, fully encapsulated, functionalizable liquid and coatings	High voltage ( $>500$ V)	Contr./exp. • (droplet 10 μL) $\approx$ 30% ε @ 0.7 MV m $^{-1}$	[246]	
Electrochemical (gallium, ECahn, etc.) (Surface-tension control with oxidation)	Liquid metal (gallium, ECahn, etc.)	μm-mm	Low voltage ( $\approx$ 1–20 V), conductive, stiffness change	Requires immersion in electrolyte	Locomotion • (droplet) 100 mm s $^{-1}$ @ 15 V • (liquid front) $\approx$ 4mm s $^{-1}$ @ 1 V	[252,249]	
(Gas evolution for pressure generation)	Carbon nanotubes	μm	Low voltage ( $\approx$ 1 V), conductive, high strain	Requires immersion in electrolyte, low cycle-life	Contr./exp. • (sheet t = 30 μm) 300% ε @ 1.5 V	[85]	
Magnetic Field	Various polymers or gels (with embedded magnetic particles)	μm-mm	Remote actuation, complex 2D shape-programming, fast ( $<10$ ms), high force/torques (can reach torque densities $>100$ N m m $^{-3}$ )	Scales down poorly	Locomotion • (swimmer l = $\approx$ 15 μm) 0.93 body lengths s $^{-1}$ • (swimmer l = 5.9 mm) 2.2 nm s $^{-1}$ @ 75 Hz, $10^3$ A m $^{-1}$	[270,28,309]	
Magnetic torque (field gradients)	Liquid marbles (with magnetic particles or using ferrofluid)	mm	Remote actuation, low friction, control of particle coating	Only simple deformation/motion	Locomotion • (droplet) 0.32 m s $^{-1}$ @ 0.02 T	[323]	
Magno-rheological fluid (MRF)	Magno-rheological fluid (MRF)	μm-mm	Remote actuation, fast change in viscosity ( $\approx$ 10 ms)	No direct actuation, possible sedimentation and leakage	Liquid-to-solid transition • >100 kPa YS @ 0.8 T	[319]	
Ferrofluids	Ferrofluids	μm-mm	Remote actuation, fast shape change & motion possible ( $<10$ ms to $>1$ s), large & complex deformation possible	Possible leakage	Contr./exp. • (droplet) aspect ratio change from 1 to 5 @ 0.078 T	[303,320,321]	
Pressure Differential	Elastomers (PDMS, silicones, poly-lactide, etc.)	μm-cm	High force densities ( $>1$ mN mm $^{-3}$ ), inexpensive	Pressure source required	Bending • (cantilever $\varnothing$ 0.15 $\times$ 5–8 mm) $\approx$ 0.78 mN force @ 68 kPa	[32,346]	

Table 5. Continued.

Actuation Method	Mechanism	Material	Length scale	Advantages	Disadvantages <sup>a)</sup>	Motion, ex. Performance <sup>a)</sup>	References
Heat	Thermal expansion	Various (paraffin wax, PDMS, etc.)	μm–cm	Remote actuation, simple, easy to manufacture	Slow ( $\approx 1$ s to 1 min)	Bending • (cantilever $20 \times 5 \times 0.12$ mm) $84^\circ$ to $563^\circ$ in 3.6 s @ $250 \text{ W cm}^{-2}$ , recovery $\approx 7$ s Locomotion • (loop $14 \times 34 \times 0.12$ mm) $1.6 \text{ cm s}^{-1}$	[419]
Phase change	Liquid-crystal polymeric materials (LCNs, LCEs)	μm–cm	Remote actuation, complex shape programming, high strain ( $>50$ – $400\%$ ε), work densities $\approx 3$ kJ m <sup>-3</sup>	Slow ( $>10$ s), added manufacturing complexity with mesogen alignment	Bending • (sheet $\approx 20 \times 20 \times 0.05$ mm) $\approx 55\%$ ε, eff. stroke $\approx 3000\%$ @ $125^\circ \text{ C}$ Contr./exp. • (sheet) $>300\%$ ε @ $\approx 90^\circ \text{ C}$	[433,434,439]	
Shape-memory polymers (SMPs)	μm–cm	Remote actuation, multiple shapes possible, high strain ( $>50$ – $800\%$ ε), tailorable trans. temp., tunable stiffness, high possible work density ( $<50$ kJ m <sup>-3</sup> – $2$ MJ m <sup>-3</sup> )	Slow ( $>10$ s), typically one-way motion, low force (typical recovery stresses $\approx 0.1$ – $10$ MPa)	Slow ( $>10$ s), typically one-way motion, low force (typical recovery stresses $\approx 0.1$ – $10$ MPa)	Contr./exp. • (sheet $20 \times 1 \times 1$ mm) 800% ε, $T_g = 28^\circ \text{ C}$ Bending • (sheet $17 \times 17$ mm), folded in $\approx 1$ min @ $65^\circ \text{ C}$	[31],453,454,577]	
Liquid metal (Gallium, EGaIn, etc.)	mm–cm	Remote actuation, low melting temperatures ( $=10$ – $40^\circ \text{ C}$ )	No (heat based) direct actuation, slow solidification without active cooling ( $>1$ min)	Slow ( $>1$ s), sensitive to RH% if in air	Liquid-to-solid transition • (cantilever $3 \times 5.7 \times 0.24$ mm) 1.5– $40$ MPa change in elastic modulus	[468]	
(Change in hydrophobicity)	Hgromorphic polymers (PNIPAM, Polypyrrole, etc.) Paper (cellulose)	μm–cm	Can have low transition temperature ( $\approx 30^\circ \text{ C}$ )	Slow ( $>1$ s), sensitive to RH%	Bending • (cantilever) $>60^\circ \approx 1$ s, recovery $\approx 10$ s	[426]	
Thermocapillary effect	Fluid droplets	μm–mm	Applies to many fluids	Slow (velocities $\approx 1$ mm s <sup>-1</sup> ), possible leakage	Bending • (cantilever $5 \times 1$ cm) 3 cm @ $80^\circ \text{ C}$ , $0.3 \text{ W cm}^{-2}$ Locomotion • (droplet) $\approx 0.7$ mm s <sup>-1</sup> , with $2.77^\circ \text{ C mm}^{-1}$ • (droplet 4 μL) $\approx 4$ mm s <sup>-1</sup> , with $0.3^\circ \text{ C mm}^{-1}$	[432],463,578]	
Light	Photoisomerization	Various polymers or gels (with azobenzene chromophores)	μm–mm	Remote actuation	Slow ( $\approx 10$ s to $>1$ h)	Bending • (rod $\oslash 0.36$ μm) 180° in 50 s	[512]
		Liquid-crystal polymeric materials (LCEs and LCNs with azobenzene chromophores)	μm–mm	Remote actuation, complex shapes possible, fast speeds possible ( $<1$ ms to $>10$ s)	Poor thermal stability	Contr./exp. • (sheet $60 \times 30 \times 10$ μm), 20% ε, 260 kPa stress in $\approx 5$ ms with green light Locomotion • (walker $60 \times 30 \times 10$ μm) $37 \mu\text{m s}^{-1}$ with green light	[498,486]

Table 5. Continued.

Actuation Method	Mechanism	Material	Length scale	Advantages	Disadvantages <sup>a)</sup>	Motion, ex. Performance <sup>a)</sup>	References
(Surface-tension based)	Fluid droplets (on photosensitizable surface)	μm	Remote actuation, applies to many fluids	Slow (velocities <1 mm s <sup>-1</sup> )	Locomotion • (droplet 2 μL) 35 μm s <sup>-1</sup> @ 100 mW cm <sup>-2</sup>	[51,6]	
Photodimerization	SMP (with photoreactive molecules such as cinnamates)	cm	Remote actuation, low temperature dependence	Very slow (>1 h), one-way motion	Bending • (film) ~50% ε with UV	[50,1]	
Photochemical gas evolution	Liquid marble	mm	Remote actuation	Slow (velocities <8 mm min <sup>-1</sup> )	Locomotion • (droplet Ø 1 mm) ≈8 mm min <sup>-1</sup> with UV	[51,7]	
Diffusion-based swelling (water, solvent, pH + added carboxyl/pyridine groups)	Various materials (Hygromorphic polymers, hydrogels, paper, etc.)	nm–cm	Fast response times possible ( $\approx$ 100 ms to 1 min, diffusion rate dependent), often biocompatible	Sensitive to the environment – undesired motion possible	Bending • (film 20 × 1 × 0.03 mm) $>720^\circ$ in 0.5 s	[52,5,54,2]	
(Phase change by hydrogen-bond dissolution)	Liquid-crystal polymeric materials (LCEs & LCNs)	μm–cm	Complex shapes possible	Slow response (>1 s), often temperature dependent	Locomotion • (insect 4.3 × 2 mm), load capacity up to 120 times actuator mass	[54,3]	
SMPs	μm–cm	Multiple temporary shapes demonstrated	Slow ( $\approx$ 10 s to >10 min), typically one-way motion, low force, often temperature dependent	Bending • (film 20 × 3 × 0.018 mm) $>360^\circ$	Bending • (film Ø 1.5 mm) recovery in water in $\approx$ 25 min	[53,0,54,5]	
(Belousov–Zhabotinsky Reaction)	Self-oscillating gels	μm–cm	Self-sustaining motion	Difficult-to-achieve complex deformations/motions, slow (oscillation frequencies <0.01 Hz)	Locomotion • (film 12 × 10 × 0.25 mm) single shape recovery in solvent in 18 s	[52,7,53,6]	
Surface-tension based	Various fluids (on deformable structures)	nm–nm	Complex motion possible, scales well	Long cycle time (>10 s, evaporation dependent), environment dependent	Bending • (arm t = 10, 30 μm) up to 300°, 67.67 mN m <sup>-1</sup>	[56,9]	
Liquid metal	μm–mm	Fast (velocities > 50 mm s <sup>-1</sup> )	Could not actively control direction or speed	Locomotion • (droplet) max 180 mm s <sup>-1</sup>	[53,3]		

<sup>a)</sup>Yield strength: RΗ%; Relative humidity percentage; ε: strain; F<sub>b</sub>: blocking force; Contr./exp.: Contraction and expansion. Note: Dimensions are given in (l × w × t) or (Ød × l) when available, where l, w, t, and d are length, width, thickness and diameter respectively. Length-scale ranges are rough estimations based on the feature size of the demonstrated systems.

impressive demonstrations, and will most certainly continue to develop.<sup>[270,434,581]</sup> The alternative has been sparsely explored, and we hope to see greater effort toward smaller drivers for on board applications. These could, for example, include smaller and softer means to increase pressure in elastic fluidic actuators<sup>[347,582]</sup> or smaller devices to create high-voltage, low-power converters for non-ionic electroactivated polymers. Sustained chemical reactions that derive power from their environment or carry fuel are another option that has only seen sparse demonstrations in robots with self-oscillating gels<sup>[527]</sup> or propelled liquid-metal marbles.<sup>[533]</sup>

Combining the self-sensing capabilities that exist in many of these materials has the potential to create robots that truly sense, respond, and interact with their environment. Additionally, work toward mass manufacturing has the potential to enable swarms of these inexpensive soft small-scale robots.<sup>[394,421]</sup>

Because of the huge breadth of stimuli, materials, and applications, actuator characterization is understandably far from standardized. However, to reach a wider audience, we encourage researchers to report on most or all of the following factors: strain and stress capabilities, amplitude and frequency of the driving signal, generated force, energy densities, actuator durability, and sensitivity to parasitic signals. The pioneering work on small-scale soft actuators presented in this review is ripe to revolutionize our concept of how to design and operate robots with greater contributions to society.

## Acknowledgements

L.H. and K.P. contributed equally to this work.

Received: July 1, 2016

Revised: October 5, 2016

Published online: December 29, 2016

- [1] M. T. Tolley, R. F. Shepherd, B. Mosadegh, K. C. Galloway, M. Wehner, M. Karpelson, R. J. Wood, G. M. Whitesides, *Soft Rob.* **2014**, *1*, 213.
- [2] S. Seok, C. D. Onal, K.-J. Cho, R. J. Wood, D. Rus, S. Kim, *IEEE ASME Trans. Mechatron.* **2013**, *18*, 1485.
- [3] C. Majidi, *Soft Rob.* **2014**, *1*, 5.
- [4] D. Rus, M. T. Tolley, *Nature* **2015**, *521*, 467.
- [5] T. Mirfakhrai, J. D. W. Madden, R. H. Baughman, *Mater. Today* **2007**, *10*, 30.
- [6] F. Rosso, G. Marino, A. Giordano, M. Barbarisi, D. Parmeggiani, A. Barbarisi, *J. Cell Physiol.* **2005**, *203*, 465.
- [7] D. Morales, E. Palleau, M. D. Dickey, O. D. Velev, *Soft Matter* **2014**, *10*, 1337.
- [8] S. Akbari, *Ph.D. Thesis*, École Polytechnique Fédérale de Lausanne, Switzerland, **2013**.
- [9] G. H. Kwon, J. Y. Park, J. Y. Kim, M. L. Frisk, D. J. Beebe, S.-H. Lee, *Small* **2008**, *4*, 2148.
- [10] T. Hirai, T. Ogiwara, K. Fujii, T. Ueki, K. Kinoshita, M. Takasaki, *Adv. Mater.* **2009**, *21*, 2886.
- [11] Z. Wei, Z. Jia, J. Athas, C. Wang, S. R. Raghavan, T. Li, Z. Nie, *Soft Matter* **2014**, *10*, 8157.
- [12] D. Chen, J. Yoon, D. Chandra, A. J. Crosby, R. C. Hayward, *J. Polym. Sci., Part B: Polym. Phys.* **2014**, *52*, 1441.
- [13] S. Fusco, H.-W. Huang, K. E. Peyer, C. Peters, M. Häberli, A. Ulbers, A. Spyrogianni, E. Pellicer, J. Sort, S. E. Pratsinis, B. J. Nelson, M. S. Sakar, S. Pané, *ACS Appl. Mater. Interfaces* **2015**, *7*, 6803.
- [14] K. K. Westbrook, H. J. Qi, *J. Intell. Mater. Syst. Struct.* **2008**, *19*, 597.
- [15] M. Amjadi, M. Turan, C. P. Clementson, M. Sitti, *ACS Appl. Mater. Interfaces* **2016**, *8*, 5618.
- [16] M. Amjadi, K.-U. Kyung, I. Park, M. Sitti, *Adv. Funct. Mater.* **2016**, *26*, 1678.
- [17] L. Lu, W. Chen, *Adv. Mater.* **2010**, *22*, 3745.
- [18] L. D. Chambers, J. Winfield, I. Ieropoulos, J. Rossiter, *Proc. SPIE* **2014**, *9056*, 90560B; DOI: 10.1117/12.2045104.
- [19] J. Kim, S. Choi, H. Lee, S. Kwon, *Adv. Mater.* **2013**, *25*, 1415.
- [20] Y. Fuchigami, T. Takigawa, K. Urayama, *ACS Macro Lett.* **2014**, *3*, 813.
- [21] M. Sitti, *Nature* **2009**, *458*, 7242.
- [22] E. Diller, M. Sitti, *Found. Trends Rob.* **2013**, *2*, 143.
- [23] M. Sitti, H. Ceylan, W. Hu, J. Giltinan, M. Turan, S. Yim, E. Diller, *Proc. IEEE* **2015**, *103*, 205.
- [24] M. Sitti, *IEEE Rob. Autom. Mag.* **2007**, *14*, 53.
- [25] R. W. Carlsen, M. Sitti, *Small* **2014**, *10*, 3831.
- [26] K. Shimizu, H. Fujita, E. Nagamori, *J. Biosci. Bioeng.* **2013**, *115*, 115.
- [27] J. H. Sung, M. B. Esch, J.-M. Prot, C. J. Long, A. Smith, J. J. Hickman, M. L. Shuler, *Lab Chip* **2013**, *13*, 1201.
- [28] P. Garstecki, P. Tierno, D. B. Weibel, F. Saguès, G. M. Whitesides, *J. Phys.: Condens. Matter* **2009**, *21*, 204110.
- [29] H. Lee, C. Xia, N. X. Fang, *Soft Matter* **2010**, *6*, 4342.
- [30] S. Taccola, F. Greco, E. Sinibaldi, A. Mondini, B. Mazzolai, V. Mattoli, *Adv. Mater.* **2015**, *27*, 1668.
- [31] M. Yamada, M. Kondo, J. Mamiya, Y. Yu, M. Kinoshita, C. J. Barrett, T. Ikeda, *Angew. Chem., Int. Ed.* **2008**, *47*, 4986.
- [32] J. Paek, I. Cho, J. Kim, *Sci. Rep.* **2015**, *5*, 10768.
- [33] J. L. Pons, E. Rocon, *Bol. Soc. Esp. Ceram. Vidrio* **2006**, *45*, 132.
- [34] S. Chakraborty, *Mechanics Over Micro and Nano Scales*, Springer-Verlag, New York, USA, **2011**.
- [35] S. Baglio, S. Castorina, N. Savalli, *Scaling Issues and Design of MEMS*, John Wiley & Sons Ltd. Chichester, UK, **2007**.
- [36] A. Ghosh, B. J. Corves, *Introduction to Micromechanisms and Micro-actuators*, Springer, India, **2015**.
- [37] H. Janocha, *Adaptronics and Smart Structures*, Springer-Verlag, Heidelberg, Germany, **1999**.
- [38] R. Pelrine, R. Kornbluh, Q. Pei, J. Joseph, *Science* **2000**, *287*, 836.
- [39] R. Pelrine, R. Kornbluh, J. Joseph, R. Heydt, Q. Pei, S. Chiba, *Mater. Sci. Eng. C* **2000**, *11*, 89.
- [40] J. D. W. Madden, N. A. Vandesteeg, P. A. Anquetil, P. G. A. Madden, A. Takshi, R. Z. Pytel, S. R. Lafontaine, P. A. Wieringa, I. W. Hunter, *IEEE J. Ocean Eng.* **2004**, *29*, 706.
- [41] P. Brochu, Q. Pei, *Macromol. Rapid Commun.* **2010**, *31*, 10.
- [42] P. Freni, E. M. Botta, L. Randazzo, P. Ariano, *Innovative Hand Exoskeleton Design for Extravehicular Activities in Space*, Springer International Publishing, **2014**.
- [43] K. Autumn, C. Majidi, R. E. Groff, A. Dittmore, R. Fearing, *J. Exp. Biol.* **2006**, *209*, 3558.
- [44] T. J. White, D. J. Broer, *Nat. Mater.* **2015**, *14*, 1087.
- [45] C. Liu, H. Qin, P. T. Mather, *J. Mater. Chem.* **2007**, *17*, 1543.
- [46] O. Okay, in *Hydrogel Sensors and Actuators*, (Ed.: G. Urban), Springer, Heidelberg, Germany, **2009**, p. 1.
- [47] T. S. Keller, Z. Mao, D. M. Spengler, *J. Orthop. Res.* **1990**, *8*, 592.
- [48] N. Guz, M. Dokukin, V. Kalaparthi, I. Sokolov, *Biophys. J.* **2014**, *107*, 564.
- [49] J. Hu, Y. Zhu, H. Huang, J. Lu, *Prog. Polym. Sci.* **2012**, *37*, 1720.
- [50] S.-K. Ahn, R. M. Kasi, S.-C. Kim, N. Sharma, Y. Zhou, *Soft Matter* **2008**, *4*, 1151.

- [51] T. H. Ware, J. S. Biggins, A. F. Shick, M. Warner, T. J. White, *Nat. Commun.* **2016**, *7*, 10781; DOI: 10.1038/ncomms10781.
- [52] C. Ohm, M. Brehmer, R. Zentel, *Adv. Mater.* **2010**, *22*, 3366.
- [53] M.-H. Li, P. Keller, *Philos. Trans. R. Soc. A* **2006**, *364*, 2763.
- [54] W. Lehmann, H. Skupin, C. Tolksdorf, E. Gebhard, R. Zentel, P. Krüger, M. Lösche, F. Kremer, *Nature* **2001**, *410*, 447.
- [55] P. T. Mather, X. F. Luo, I. A. Rousseau, *Annu. Rev. Mater. Res.* **2009**, *39*, 445.
- [56] G. McKnight, C. Henry, *Proc. SPIE* **2005**, *5761*, 119; DOI: 10.1117/12.601495.
- [57] S. Kim, M. Sitti, T. Xie, X. Xiao, *Soft Matter* **2009**, *5*, 3689.
- [58] J. Li, T. Liu, S. Xia, Y. Pan, Z. Zheng, X. Ding, Y. Peng, *J. Mater. Chem.* **2011**, *21*, 12213.
- [59] M. Behl, K. Kratz, J. Zottmann, U. Nöchel, A. Lendlein, *Adv. Mater.* **2013**, *25*, 4466.
- [60] M. Botho, T. Preisch, *J. Mater. Chem. A* **2013**, *1*, 14491.
- [61] M. D. Hager, S. Bode, C. Weber, U. S. Schubert, *Prog. Polym. Sci.* **2015**, *49*, 3.
- [62] Y. Liu, J. Genzer, M. D. Dickey, *Prog. Polym. Sci.* **2016**, *52*, 79.
- [63] A. A. Collyer, *Liquid Crystal Polymers: From Structures to Applications*, Springer, The Netherlands, **1992**.
- [64] D. Broer, G. P. Crawford, S. Zumer, *Cross-Linked Liquid Crystalline Systems: From Rigid Polymer Networks to Elastomers*, CRC Press, London, UK, **2011**.
- [65] H. Yang, G. Ye, X. Wang, P. Keller, *Soft Matter* **2011**, *7*, 815.
- [66] H. Meng, G. Li, *Polymer* **2013**, *54*, 2199.
- [67] L. Sun, W. M. Huang, Z. Ding, Y. Zhao, C. C. Wang, H. Purnawali, C. Tang, *Mater. Des.* **2012**, *33*, 577.
- [68] M. Behl, M. Y. Razzaq, A. Lendlein, *Adv. Mater.* **2010**, *22*, 3388.
- [69] P. Aussillous, D. Quéré, *Philos. Trans. R. Soc. A* **2006**, *364*, 973.
- [70] G. McHale, *Langmuir* **2009**, *25*, 7185.
- [71] G. McHale, M. I. Newton, *Soft Matter* **2015**, *11*, 2530.
- [72] S. Lach, S. M. Yoon, B. A. Grzybowski, *Chem. Soc. Rev.* **2016**, *45*, 4766.
- [73] C. H. Ooi, N.-T. Nguyen, *Microfluid. Nanofluid.* **2015**, *19*, 483.
- [74] E. Bormashenko, Y. Bormashenko, R. Pogreb, O. Gendelman, *Langmuir* **2011**, *27*, 7.
- [75] M. Alava, K. Niskanen, *Rep. Prog. Phys.* **2006**, *69*, 669.
- [76] J. T. Connelly, J. P. Rolland, G. M. Whitesides, *Anal. Chem.* **2015**, *87*, 7595.
- [77] Y. Zheng, Z. He, Y. Gao, J. Liu, *Sci. Rep.* **2013**, *3*, 1786; DOI: 10.1038/srep01786.
- [78] D. Tobijsk, R. Österbacka, *Adv. Mater.* **2011**, *23*, 1935.
- [79] C. D. Onal, M. T. Tolley, R. J. Wood, D. Rus, *IEEE ASME Trans. Mechatron.* **2015**, *20*, 2214.
- [80] M.-F. Yu, B. S. Files, S. Areppalli, R. S. Ruoff, *Phys. Rev. Lett.* **2000**, *84*, 5552.
- [81] M. Endo, H. Muramatsu, T. Hayashi, Y. A. Kim, M. Terrones, M. S. Dresselhaus, *Nature* **2005**, *433*, 476.
- [82] T. Mirfakhrai, J. Oh, M. Kozlov, E. C. W. Fok, M. Zhang, S. Fang, R. H. Baughman, J. D. W. Madden, *Smart Mater. Struct.* **2007**, *16*, S243.
- [83] R. H. Baughman, *Synth. Met.* **1996**, *78*, 339.
- [84] R. H. Baughman, C. Cui, A. A. Zakhidov, Z. Iqbal, J. N. Barisci, G. M. Spinks, G. G. Wallace, A. Mazzoldi, D. De Rossi, A. G. Rinzler, O. Jaschinski, S. Roth, M. Kertesz, *Science* **1999**, *284*, 1340.
- [85] G. M. Spinks, G. G. Wallace, L. S. Fifield, L. R. Dalton, A. Mazzoldi, D. De Rossi, I. I. Khayrullin, R. H. Baughman, *Adv. Mater.* **2002**, *14*, 1728.
- [86] C. Li, E. T. Thostenson, T.-W. Chou, *Compos. Sci. Technol.* **2008**, *68*, 1227.
- [87] M. Yamano, N. Ogawa, M. Hashimoto, M. Takasaki, T. Hirai, in *Proc. 2008 IEEE International Conference on Robotics and Biomimetics (ROBIO)*, IEEE, Piscataway, NJ, USA **2008**.
- [88] N. Ogawa, M. Hashimoto, M. Takasaki, T. Hirai, in *2009 IEEE/RSJ International Conference on Intelligent Robots and Systems*, IEEE, Piscataway, NJ, USA, **2009**; DOI: 10.1109/IROS.2009.5354417.
- [89] R. Pelrine, R. D. Kornbluh, Q. Pei, S. Stanford, S. Oh, J. Eckerle, R. J. Full, M. A. Rosenthal, K. Meijer, *Proc. SPIE* **2002**, *4695*, 126.
- [90] K. Takemura, F. Yajima, S. Yokota, K. Edamura, *Sens. Actuators, A* **2008**, *144*, 348.
- [91] J. Kwangmok, K. Ja Choon, N. Jae-do, L. Young Kwan, C. Hyouk Ryeol, *Bioinspiration Biomimetics* **2007**, *2*, S42.
- [92] I. Must, F. Kaasik, I. Pöldsalu, L. Mihkels, U. Johanson, A. Punning, A. Aabloo, *Adv. Eng. Mater.* **2015**, *17*, 84.
- [93] N. L. Q. Nhat, N. Truong Thinh, *Adv. Mater. Res.* **2015**, *1119*, 251.
- [94] E. W. H. Jager, O. Inganäs, I. Lundström, *Science* **2000**, *288*, 2335.
- [95] X. Niu, M. Zhang, J. Wu, W. Wen, P. Sheng, *Soft Matter* **2009**, *5*, 576.
- [96] R. V. Raghavan, J. Qin, L. Y. Yeo, J. R. Friend, K. Takemura, S. Yokota, K. Edamura, *Sens. Actuators, B* **2009**, *140*, 287.
- [97] V. Srinivasan, V. K. Pamula, R. B. Fair, *Lab Chip* **2004**, *4*, 310.
- [98] U. Kosidlo, M. Omastová, M. Micusík, G. Čiric-Marjanović, H. Randriamahazaka, T. Wallmersperger, A. Aabloo, I. Kolaric, T. Bauernhansl, *Smart Mater. Struct.* **2013**, *22*, 104022.
- [99] S. Rosset, M. Niklaus, P. Dubois, H. R. Shea, *Sens. Actuators, A* **2008**, *144*, 185.
- [100] J. Shintake, *Ph.D. Thesis*, École Polytechnique Fédérale de Lausanne, Switzerland, **2016**.
- [101] W. Hong, *J. Mech. Phys. Solids* **2011**, *59*, 637.
- [102] B. Kussmaul, S. Risse, G. Kofod, R. Waché, M. Wegener, D. N. McCarthy, H. Krüger, R. Gerhard, *Adv. Funct. Mater.* **2011**, *21*, 4589.
- [103] Q. M. Zhang, H. Li, M. Poh, F. Xia, Z. Y. Cheng, H. Xu, C. Huang, *Nature* **2002**, *419*, 284.
- [104] S. Rosset, H. Shea, *Appl. Phys. Mater. Sci. Process.* **2013**, *110*, 281.
- [105] C. Keplinger, J.-Y. Sun, C. C. Foo, P. Rothemund, G. M. Whitesides, Z. Suo, *Science* **2013**, *341*, 984.
- [106] M. Niklaus, S. Rosset, P. Dubois, H. Shea, *Procedia Chem.* **2009**, *1*, 702.
- [107] I. A. Anderson, T. A. Gisby, T. G. McKay, B. M. O'Brien, E. P. Calius, *J. Appl. Phys.* **2012**, *112*, 041101.
- [108] J. Shintake, S. Rosset, B. Schubert, D. Floreano, H. Shea, *Adv. Mater.* **2016**, *28*, 205.
- [109] S. Shian, D. R. Clarke, *Soft Matter* **2016**, *12*, 3137.
- [110] M. Pollador, A. T. Conn, B. Mazzolai, J. Rossiter, *Appl. Phys. Lett.* **2014**, *105*, 141903.
- [111] G. Kofod, W. Wirges, M. Paajanen, S. Bauer, *Appl. Phys. Lett.* **2007**, *90*, 081916.
- [112] H. Godaba, C. C. Foo, Z. Q. Zhang, B. C. Khoo, J. Zhu, *Appl. Phys. Lett.* **2014**, *105*, 112901.
- [113] C. Keplinger, T. Li, R. Baumgartner, Z. Suo, S. Bauer, *Soft Matter* **2012**, *8*, 285.
- [114] L. Hines, K. Petersen, M. Sitti, *Adv. Mater.* **2016**, *28*, 3690.
- [115] F. Carpi, G. Frediani, D. De Rossi, *IEEE ASME Trans. Mechatron.* **2010**, *15*, 308.
- [116] Z. Yu, W. Yuan, P. Brochu, B. Chen, Z. Liu, Q. Pei, *Appl. Phys. Lett.* **2009**, *95*, 192904.
- [117] J. Shintake, B. Schubert, S. Rosset, H. Shea, D. Floreano, in *2015 IEEE/RSJ International Conference on Intelligent Robots and Systems (IROS)*, IEEE, Piscataway, NJ, USA **2015**; DOI: 10.1109/IROS.2015.7353507.
- [118] Q. M. Zhang, V. Bharti, X. Zhao, *Science* **1998**, *280*, 2101.
- [119] C. Huang, R. Klein, F. Xia, H. Li, Q. M. Zhang, F. Bauer, Z. Y. Cheng, *IEEE Trans. Dielectr. Electr.* **2004**, *11*, 299.
- [120] C. Miehe, D. Rosato, *Int. J. Eng. Sci.* **2011**, *49*, 466.
- [121] M. E. Alf, A. Asatekin, M. C. Barr, S. H. Baxamusa, H. Chelawat, G. Ozaydin-Ince, C. D. Petruzzok, R. Sreenivasan, W. E. Tenhaeff,

- N. J. Trujillo, S. Vaddiraju, J. Xu, K. K. Gleason, *Adv. Mater.* **2010**, 22, 1993.
- [122] S. Park, T. R. Shrout, *J. Appl. Phys.* **1997**, 82, 1804.
- [123] Q. M. Zhang, V. Bharti, G. Kavarnos, in *Encyclopedia of Smart Materials*, (Ed.: M. M. Schwartz), John Wiley and Sons, Inc. **2002**.
- [124] B. Mohammadi, A. A. Yousefi, S. M. Bellah, *Polym. Test.* **2007**, 26, 42.
- [125] A. Ask, A. Menzel, M. Ristinmaa, *Mech. Mater.* **2012**, 50, 9.
- [126] F. M. Guillot, E. Balizer, *J. Appl. Polym. Sci.* **2003**, 89, 399.
- [127] A. W. Richards, G. M. Odegard, *J. Appl. Mech.* **2010**, 77, 014502.
- [128] I. Diaconu, D.-O. Dorohoi, C. Ciobanu, *Rom. J. Phys.* **2006**, 53, 91.
- [129] H. Xu, D. Shen, Q. Zhang, *Polymer* **2007**, 48, 2124.
- [130] F. Bauer, E. Fousson, Q. M. Zhang, *IEEE Trans. Dielectr. Electr. Insul.* **2006**, 13, 1149.
- [131] J. Su, Z. Ounaies, J. S. Harrison, in *MRS Proceedings*, Vol. 600 (Eds.: Q. M. Zhang, T. Furukawa, Y. Bar-Cohen, J. Scheinbeim), Cambridge University Press, New York, USA **2000**.
- [132] T. Okamoto, K. Urayama, T. Takigawa, *Soft Matter* **2011**, 7, 10585.
- [133] Y. Yu, T. Ikeda, *Angew. Chem., Int. Ed.* **2006**, 45, 5416.
- [134] K. Urayama, H. Kondo, Y. O. Arai, T. Takigawa, *Phys. Rev. E* **2005**, 71, 051713.
- [135] S. Hashimoto, Y. Yusuf, S. Krause, H. Finkelmann, P. E. Cladis, H. R. Brand, S. Kai, *Appl. Phys. Lett.* **2008**, 92, 181902.
- [136] L. Dai, *Intelligent Macromolecules for Smart Devices: From Materials Synthesis to Device Applications*, Springer, London, UK **2004**.
- [137] M. H. Harun, E. Saion, A. Kassim, N. Yahya, E. Mahmud, *Int. J. Adv. Sci. Arts* **2007**, 2, 63.
- [138] L. Bay, K. West, P. Sommer-Larsen, S. Skaarup, M. Benslimane, *Adv. Mater.* **2003**, 15, 310.
- [139] Y. Fang, *Ph.D. Thesis*, Michigan State University, East Lansing, MI, USA, **2009**.
- [140] K. Kaneko, M. Kaneko, Y. Min, A. G. MacDiarmid, *Synth. Met.* **1995**, 71, 2211.
- [141] E. Smela, O. Inganäs, I. Lundstrom, *J. Micromech. Microeng.* **1993**, 3, 203.
- [142] E. Smela, O. Inganäs, I. Lundstrom, *Science* **1995**, 268, 1735.
- [143] E. W. H. Jager, O. Inganäs, I. Lundström, *Adv. Mater.* **2001**, 13, 76.
- [144] A. Khalidi, A. Maziz, G. Alici, G. M. Spinks, E. W. H. Jager, *Proc. SPIE* **2015**, 9430, 94301R; DOI: 10.1117/12.2084140.
- [145] C. W. Hou, Z. J. Cai, *Adv. Mater. Res.* **2011**, 298, 40.
- [146] I. Must, V. Vunder, F. Kaasik, I. Pöldsalu, U. Johanson, A. Punning, A. Aabloo, *Sens. Actuators, B* **2014**, 202, 114.
- [147] I. Must, T. Kaasik, I. Baranova, U. Johanson, A. Punning, A. Aabloo, *Proc. SPIE* **2015**, 9430, 94300Q; DOI: 10.1117/12.2084252.
- [148] Y. Xia, G. M. Whitesides, *Annu. Rev. Mater. Sci.* **1998**, 28, 153.
- [149] B. J. Akle, M. D. Bennett, D. J. Leo, *Sens. Actuators, A* **2006**, 126, 173.
- [150] Y. B. Shahinpoor, Mohsen, *Soft Rob.* **2014**, 1, 5480.
- [151] W.-S. Chu, K.-T. Lee, S.-H. Song, M.-W. Han, J.-Y. Lee, H.-S. Kim, M.-S. Kim, Y.-J. Park, K.-J. Cho, S.-H. Ahn, *Int. J. Precis. Eng. Manuf.* **2012**, 13, 1281.
- [152] M. Farid, G. Zhao, T. L. Khuong, Z. Z. Sun, N. Ur Rehman, M. Rizwan, *J. Biomimetics, Biomater. Biomed. Eng.* **2014**, 20, 1.
- [153] I.-S. Park, K. Jung, D. Kim, S.-M. Kim, K. J. Kim, *MRS Bull.* **2008**, 33, 190.
- [154] B. Kim, D.-H. Kim, J. Jung, J.-O. Park, *Smart Mater. Struct.* **2005**, 14, 496.
- [155] V. Vunder, M. Itik, A. Punning, A. Aabloo, *Proc. SPIE* **2014**, 9056, 90561Y; DOI: 10.1117/12.2045001.
- [156] M. Shahinpoor, K. J. Kim, *Smart Mater. Struct.* **2001**, 10, 819.
- [157] S. Liu, Y. Liu, H. Cebeci, R. G. de Villoria, J.-H. Lin, B. L. Wardle, Q. M. Zhang, *Adv. Funct. Mater.* **2010**, 20, 3266.
- [158] G. Shuxiang, T. Fukuda, K. Asaka, *IEEE ASME Trans. Mechatron.* **2003**, 8, 136.
- [159] N. Kamamichi, M. Yamakita, K. Asaka, Z.-W. Luo, in *Proc. IEEE Int. Conf. on Robotics and Automation*, IEEE, Piscataway, NJ, USA, **2006**; DOI: 10.1109/ROBOT.2006.1641969.
- [160] X. Tan, D. Kim, N. Usher, D. Laboy, J. Jackson, A. Kapetanovic, J. Rapai, B. Sabadus, X. Zhou, in *2006 IEEE/RSJ Int. Conf. on Intelligent Robots and Systems*, IEEE, Piscataway, NJ, USA, **2006**; DOI: 10.1109/IROS.2006.282110.
- [161] K. Takagi, M. Yamamura, Z. W. Luo, M. Onishi, S. Hirano, K. Asaka, Y. Hayakawa, in *Proc. IEEE/RSJ Int. Conf. on Intelligent Robots and Systems*, IEEE, Piscataway, NJ, USA, **2006**; DOI: 10.1109/IROS.2006.282308.
- [162] X. Ye, Y. Su, S. Guo, L. Wang, in *2008 IEEE/ASME Int. Conf. on Advanced Intelligent Mechatronics*, IEEE, Piscataway, NJ, USA, **2008**; DOI: 10.1109/AIM.2008.4601629.
- [163] M. Aureli, V. Kopman, M. Porfiri, *IEEE ASME Trans. Mechatron.* **2010**, 15, 603.
- [164] Z. Chen, S. Shatara, X. Tan, *IEEE ASME Trans. Mechatron.* **2010**, 15, 448.
- [165] Z. Chen, T. I. Um, H. Bart-Smith, *Proc. SPIE* **2011**, 7976, 797637; DOI: 10.1117/12.880452.
- [166] S.-W. Yeom, I.-K. Oh, *Smart Mater. Struct.* **2009**, 18, 085002.
- [167] W. Zhang, S. Guo, K. Asaka, *Appl. Bionics Biomech.* **2006**, 3, 245.
- [168] S. Guo, L. Shi, K. Asaka, in *2008 IEEE Int. Conf. on Automation and Logistics*, IEEE, Piscataway, NJ, USA, **2008**; DOI: 10.1109/ICAL.2008.4636588.
- [169] J. Barramba, J. Silva, P. J. C. Branco, *Sens. Actuators, A* **2007**, 140, 232.
- [170] S. Tadokoro, S. Fuji, M. Fushimi, R. Kanno, T. Kimura, T. Takamori, K. Oguro, in *Proc. IEEE Int. Conf. on Robotics and Automation*, IEEE, Piscataway, NJ, USA, **1998**; DOI: 10.1109/ROBOT.1998.680640.
- [171] Y. Bar-Cohen, *Expert Rev. Med. Dev.* **2005**, 2, 731.
- [172] R. K. Cheedarala, J. Jeon, C. Kee, I. Oh, *Adv. Funct. Mater.* **2014**, 24, 6005.
- [173] J. Song, J. Jeon, I. Oh, K. C. Park, *Macromol. Rapid Commun.* **2011**, 32, 1583.
- [174] S. Imaizumi, Y. Ohtsuki, T. Yasuda, H. Kokubo, M. Watanabe, *ACS Appl. Mater. Interfaces* **2013**, 5, 6307.
- [175] G. Gerlach, K.-F. Arndt, *Hydrogel Sensors and Actuators: Engineering and Technology*, (Ed.: G. Urban), Springer, Heidelberg, Germany, **2009**.
- [176] E. Palley, D. Morales, M. D. Dickey, O. D. Velev, *Nat. Commun.* **2013**, 4, 2257; DOI: 10.1038/ncomms3257.
- [177] W. Hong, X. Zhao, Z. Suo, *J. Mech. Phys. Solids* **2010**, 58, 558.
- [178] T. Shiga, in *Neutron Spin Echo Spectroscopy Viscoelasticity Rheology*, Springer-Verlag, Heidelberg, Germany, **1997**.
- [179] H. J. Kwon, Y. Osada, J. P. Gong, *Polym. J.* **2006**, 38, 1211.
- [180] W. T. S. Huck, *Mater. Today* **2008**, 11, 24.
- [181] M. Shahinpoor, *J. Intell. Mater. Syst. Struct.* **1995**, 6, 307.
- [182] P. Chiarelli, D. De Rossi, *2012*, arXiv:1206.4879.
- [183] M. Uddin, M. Watanabe, H. Shirai, T. Hirai, *J. Polym. Sci., Part B: Polym. Phys.* **2003**, 41, 2119.
- [184] K. Kruusamäe, T. Sugino, K. Asaka, *Proc. SPIE* **2015**, 9430, 94300P; DOI: 10.1117/12.2083812.
- [185] Y. Osada, H. Okuzaki, H. Hori, *Nature* **1992**, 355, 242.
- [186] Z. L. Wu, M. Moshe, J. Greener, H. Therien-Aubin, Z. Nie, E. Sharon, E. Kumacheva, *Nat. Commun.* **2013**, 4, 1586.
- [187] D. Das, T. Kar, P. K. Das, *Soft Matter* **2012**, 8, 2348.
- [188] L. Ionov, *Mater. Today* **2014**, 17, 494.
- [189] T. Fukushima, K. Asaka, A. Kosaka, T. Aida, *Angew. Chem.* **2005**, 117, 2462.
- [190] I. Takeuchi, K. Asaka, K. Kiyohara, T. Sugino, N. Terasawa, K. Mukai, T. Fukushima, T. Aida, *Electrochim. Acta* **2009**, 54, 1762.
- [191] I. Takeuchi, K. Asaka, K. Kiyohara, T. Sugino, N. Terasawa, K. Mukai, S. Shiraishi, *Carbon* **2009**, 47, 1373.

- [192] R. Hanaoka, S. Takata, H. Fujita, T. Fukami, K. Sakurai, K. Isobe, T. Hino, *Int. J. Mod. Phys. B* **2002**, *16*, 2433.
- [193] L. Gao, X. Zhao, *J. Appl. Polym. Sci.* **2004**, *94*, 2517.
- [194] Y. Kakinuma, T. Aoyama, H. Anzai, K. Isobe, K. Tanaka, *Int. J. Mod. Phys. B* **2005**, *19*, 1339.
- [195] K. Koyanagi, Y. Kakinuma, H. Anzai, K. Sakurai, T. Yamaguchi, T. Oshima, N. Momose, T. Matsuno, in *2007 International Conference on Mechatronics and Automation*, IEEE, Piscataway, NJ, USA, **2007**; DOI: 10.1109/ICMA.2007.4304085.
- [196] H. Xia, M. Takasaki, T. Hirai, *Sens. Actuators, A* **2010**, *157*, 307.
- [197] M. Ali, T. Hirai, *J. Mater. Sci.* **2011**, *46*, 7681.
- [198] P. Sheng, W. Wen, *Annu. Rev. Fluid Mech.* **2012**, *44*, 143.
- [199] J. Wu, W. Wen, P. Sheng, *Soft Matter* **2012**, *8*, 11589.
- [200] W. Wen, X. Huang, S. Yang, K. Lu, P. Sheng, *Nat. Mater.* **2003**, *2*, 727.
- [201] W. Wen, X. Huang, P. Sheng, *Soft Matter* **2008**, *4*, 200.
- [202] T. Miyoshi, K. Yoshida, J. wan Kim, S. I. Eom, S. Yokota, *Sens. Actuators, A* **2016**, *245*, 68.
- [203] J. Yin, X. Zhao, *Nanoscale Res. Lett.* **2011**, *6*, 256.
- [204] Y. D. Liu, H. J. Choi, *Soft Matter* **2012**, *8*, 11961.
- [205] Y. Hong, W. Wen, *J. Intell. Mater. Syst. Struct.* **2016**, *27*, 866.
- [206] M. D. Volder, K. Yoshida, S. Yokota, D. Reynaerts, *J. Micromech. Microeng.* **2006**, *16*, 612.
- [207] A. Inoue, S. Maniwa, *J. Appl. Polym. Sci.* **1995**, *55*, 113.
- [208] K. Kaneko, T. Kawai, N. Nakamura, *ChemPhysChem* **2008**, *9*, 2457.
- [209] K. Kaneko, A. Mandai, B. Heinrich, B. Donnio, T. Hanasaki, *ChemPhysChem* **2010**, *11*, 3596.
- [210] J. L. Sproston, R. Stanway, presented at the 4th Int. Conf. on New Actuators, Bremen, Germany, June **1992**.
- [211] R. Stanway, J. L. Sproston, A. K. El-Wahed, *Smart Mater. Struct.* **1996**, *5*, 464.
- [212] X. Niu, W. Wen, Y.-K. Lee, *Appl. Phys. Lett.* **2005**, *87*, 243501.
- [213] L. Liu, X. Chen, X. Niu, W. Wen, P. Sheng, *Appl. Phys. Lett.* **2006**, *89*, 083505.
- [214] G. J. Monkman, *Presence: Teleoperators Virtual Environ.* **1992**, *1*, 219.
- [215] D. Klein, H. Freimuth, G. J. Monkman, S. Egersdörfer, A. Meier, H. Böse, M. Baumann, H. Ermert, O. T. Bruhns, *Mechatronics* **2005**, *15*, 883.
- [216] V. G. Chouvardas, A. N. Miliou, M. K. Hatalis, *Displays* **2008**, *29*, 185.
- [217] L. Liu, X. Niu, W. Wen, P. Sheng, *Appl. Phys. Lett.* **2006**, *88*, 3119.
- [218] J. Seyed-Yagoobi, *J. Electrost.* **2005**, *63*, 861.
- [219] K. Hosoda, K. Takemura, K. Fukagata, S. Yokota, K. Edamura, *Proc. SPIE* **2013**, *8923*, 89234Z; DOI: 10.1117/12.2033791.
- [220] R. Abe, K. Takemura, K. Edamura, S. Yokota, *Sens. Actuators, A* **2007**, *136*, 629.
- [221] S. Ueno, K. Takemura, S. Yokota, K. Edamura, *Sens. Actuators, A* **2014**, *216*, 36.
- [222] A. Yamaguchi, K. Takemura, S. Yokota, K. Edamura, *Sens. Actuators, A* **2012**, *174*, 181.
- [223] S. Ueno, K. Takemura, S. Yokota, K. Edamura, *Proc. SPIE* **2013**, *8923*, 89234U; DOI: 10.1117/12.2033778.
- [224] A. Yamaguchi, K. Takemura, S. Yokota, K. Edamura, in *Proc. IEEE Int. Conf. on Robotics and Automation*, IEEE, Piscataway, NJ, USA **2011**; DOI: 10.1109/ICRA.2011.5979691.
- [225] B. Ge, D. C. Ludois, in *2014 IEEE Energy Conversion Congress and Exposition (ECCE)*, IEEE, Piscataway, NJ, USA **2014**; DOI: 10.1109/ECCE.2014.6953590.
- [226] K. Takemura, S. Yokota, M. Suzuki, K. Edamura, H. Kumagai, T. Imamura, *Sens. Actuators, A* **2009**, *149*, 173.
- [227] K. Mori, H. Yamamoto, K. Takemura, S. Yokota, K. Edamura, *Sens. Actuators, A* **2011**, *167*, 84.
- [228] K. Takemura, S. Yokota, K. Edamura, *Sens. Actuators, A* **2007**, *133*, 493.
- [229] L. Junghoon, K. Chang-Jin, *J. Microelectromech. Syst.* **2000**, *9*, 171.
- [230] J. Lee, H. Moon, J. Fowler, T. Schoellhammer, C.-J. Kim, *Sens. Actuators, A* **2002**, *95*, 259.
- [231] R. C. Gough, A. M. Morishita, J. H. Dang, M. R. Moorefield, W. A. Shiroma, A. T. Ohta, *Micro Nano Syst. Lett.* **2015**, *3*, 1.
- [232] H. J. Verheijen, M. W. J. Prins, *Langmuir* **1999**, *15*, 6616.
- [233] F. Mugele, J.-C. Baret, *J. Phys.: Condens. Matter* **2005**, *17*, R705.
- [234] S. K. Cho, H. Moon, C.-J. Kim, *J. Microelectromech. Syst.* **2003**, *12*, 70.
- [235] M. G. Pollack, R. B. Fair, A. D. Shenderov, *Appl. Phys. Lett.* **2000**, *77*, 1725.
- [236] B. Berge, J. Peseux, *Eur. Phys. J. E: Soft Matter Biol. Phys.* **2000**, *3*, 159.
- [237] M. D. Dickey, *ACS Appl. Mater. Interfaces* **2014**, *6*, 18369.
- [238] M. Abdalgawad, S. L. S. Freire, H. Yang, A. R. Wheeler, *Lab Chip* **2008**, *8*, 672.
- [239] S. K. Cho, S.-K. Fan, H. Moon, C.-J. Kim, in *Technical Digest. MEMS 2002 IEEE International Conference. Fifteenth IEEE Int. Conf. on Micro Electro Mechanical Systems*, IEEE, Piscataway, NJ, USA, **2002**; DOI: 10.1109/MEMSYS.2002.984073.
- [240] I. Moon, J. Kim, *Sens. Actuators, A* **2006**, *130*, 537.
- [241] M. Pineirua, J. Bico, B. Roman, *Soft Matter* **2010**, *6*, 4491.
- [242] S. Manakasettharn, J. Ashley Taylor, T. N. Krupenkin, *Appl. Phys. Lett.* **2011**, *99*, 144102.
- [243] Z. Wang, F.-C. Wang, Y.-P. Zhao, *Proc. R. Soc. Edinburgh, Sect. A: Math. Phys. Sci.* **2012**, *468*, 2485.
- [244] N. B. Crane, P. Mishra, A. A. Volinsky, *Rev. Sci. Instrum.* **2010**, *81*, 043902.
- [245] M. I. Newton, D. L. Herbertson, S. J. Elliott, N. J. Shirtcliffe, G. McHale, *J. Phys. Appl. Phys.* **2007**, *40*, 20.
- [246] E. Bormashenko, R. Pogreb, R. Balter, O. Gendelman, D. Aurbach, *Appl. Phys. Lett.* **2012**, *100*, 151601.
- [247] E. Bormashenko, R. Pogreb, G. Whyman, A. Musin, *Colloid Polym. Sci.* **2013**, *291*, 1535.
- [248] Z. Liu, X. Fu, B. P. Binks, H. C. Shum, *Soft Matter* DOI: 10.1039/C6SM00883F.
- [249] S.-Y. Tang, V. Sivan, K. Khoshnareh, A. P. O'Mullane, X. Tang, B. Gol, N. Eshtiaghi, F. Lieder, P. Petersen, A. Mitchell, K. Kalantar-zadeh, *Nanoscale* **2013**, *5*, 5949.
- [250] P. Sen, C.-J. Kim, *J. Microelectromech. Syst.* **2009**, *18*, 990.
- [251] R. C. Gough, A. M. Morishita, J. H. Dang, W. Hu, W. A. Shiroma, A. T. Ohta, *IEEE Access* **2014**, *2*, 874.
- [252] M. R. Khan, C. B. Eaker, E. F. Bowden, M. D. Dickey, *Proc. Natl. Acad. Sci. USA* **2014**, *111*, 14047.
- [253] M. R. Khan, C. Trlica, M. D. Dickey, *Adv. Funct. Mater.* **2015**, *25*, 654.
- [254] R. C. Gough, J. H. Dang, M. R. Moorefield, G. B. Zhang, L. H. Hihara, W. A. Shiroma, A. T. Ohta, *ACS Appl. Mater. Interfaces* **2016**, *8*, 6.
- [255] V. Sivan, S.-Y. Tang, A. P. O'Mullane, P. Petersen, N. Eshtiaghi, K. Kalantar-zadeh, A. Mitchell, *Adv. Funct. Mater.* **2013**, *23*, 144.
- [256] V. A. Bazhenov, *Piezoelectric Properties of Wood*, Consultant's Bureau, New York, NY, USA, **1961**.
- [257] J. Kim, J.-Y. Kim, S. Choe, *Proc. SPIE* **2000**, *3987*, 203; DOI: 10.1117/12.387779.
- [258] J. Kim, Y. B. Seo, *Smart Mater. Struct.* **2002**, *11*, 355.
- [259] J. Kim, S. Yun, Z. Ounaies, *Macromolecules* **2006**, *39*, 4202.
- [260] J. Kim, S. Yun, S. K. Mahadeva, K. Yun, S. Y. Yang, M. Maniruzzaman, *Sensors* **2010**, *10*, 1473.
- [261] S. Yun, J. Kim, *Smart Mater. Struct.* **2007**, *16*, 1471.
- [262] G. Y. Yun, H. S. Kim, J. Kim, K. Kim, C. Yang, *Sens. Actuators, A* **2008**, *141*, 530.
- [263] P. Kim, C. M. Lieber, *Science* **1999**, *286*, 2148.
- [264] S. Roth, R. H. Baughman, *Curr. Appl. Phys.* **2002**, *2*, 311.

- [265] J. Foroughi, G. M. Spinks, G. G. Wallace, J. Oh, M. E. Kozlov, S. Fang, T. Mirfakhrai, J. D. W. Madden, M. K. Shin, S. J. Kim, R. H. Baughman, *Science* **2011**, *334*, 494.
- [266] K. Mukai, K. Asaka, K. Kiyohara, T. Sugino, I. Takeuchi, T. Fukushima, T. Aida, *Electrochim. Acta* **2008**, *53*, 5555.
- [267] B. Xi, P. G. Whitten, A. Gestos, V.-T. Truong, G. M. Spinks, G. G. Wallace, *Sens. Actuators, B* **2009**, *138*, 48.
- [268] A. E. Aliev, J. Oh, M. E. Kozlov, A. A. Kuznetsov, S. Fang, A. F. Fonseca, R. Ovalle, M. D. Lima, M. H. Haque, Y. N. Gartstein, M. Zhang, A. A. Zakhidov, R. H. Baughman, *Science* **2009**, *323*, 1575.
- [269] N.-T. Nguyen, *Microfluid. Nanofluid.* **2012**, *12*, 1.
- [270] E. Diller, J. Zhuang, G. Zhan Lum, M. R. Edwards, M. Sitti, *Appl. Phys. Lett.* **2014**, *104*, 174101.
- [271] T. Qiu, S. Palagi, P. Fischer, in *2015 37th Annual International Conference of the IEEE Engineering in Medicine and Biology Society (EMBC)*, IEEE, Piscataway, NJ, USA, **2015**; DOI: 10.1109/EMBC.2015.7319496.
- [272] T. Qiu, T.-C. Lee, A. G. Mark, K. I. Morozov, R. Münster, O. Mierka, S. Turek, A. M. Leshansky, P. Fischer, *Nat. Commun.* **2014**, *5*, 5119; DOI: 10.1038/ncomms6119.
- [273] G. Z. Lum, Z. Ye, X. Dong, H. Marvi, O. Erin, W. Hu, M. Sitti, *Proc. Natl. Acad. Sci. USA* **2016**, *113*, E6007.
- [274] E. Diller, J. Giltinan, G. Z. Lum, Z. Ye, M. Sitti, presented at *Robotics: Science and Systems*, Rome, Italy, July **2014**.
- [275] E. Diller, J. Giltinan, G. Z. Lum, Z. Ye, M. Sitti, *Int. J. Rob. Res.* **2016**, *35*, 114.
- [276] M. P. Kummer, J. J. Abbott, B. E. Kratochvil, R. Borer, A. Sengul, B. J. Nelson, *IEEE Trans. Robot.* **2010**, *26*, 1006.
- [277] S. Tasoglu, E. Diller, S. Guven, M. Sitti, U. Demirci, *Nat. Commun.* **2014**, *5*, 3124; DOI: 10.1038/ncomms4124.
- [278] E. Diller, S. Miyashita, M. Sitti, *RSC Adv.* **2012**, *2*, 3850.
- [279] E. Diller, C. Pawashe, S. Floyd, M. Sitti, *Int. J. Rob. Res.* **2011**, *30*, 1667.
- [280] S. Miyashita, E. Diller, M. Sitti, *Int. J. Rob. Res.* **2013**, *32*, 591.
- [281] E. Diller, J. Giltinan, M. Sitti, *Int. J. Rob. Res.* **2013**, *32*, 614.
- [282] E. Diller, S. Floyd, C. Pawashe, M. Sitti, *IEEE Trans. Rob.* **2012**, *28*, 172.
- [283] S. Floyd, E. Diller, C. Pawashe, M. Sitti, *Int. J. Rob. Res.* **2011**, *30*, 1553.
- [284] C. Pawashe, S. Floyd, M. Sitti, *Appl. Phys. Lett.* **2009**, *94*, 164108.
- [285] H.-W. Huang, M. S. Sakar, K. Riederer, N. Shamsudhin, A. Petruska, S. Pan, B. J. Nelson, in *2016 IEEE International Conference on Robotics and Automation (ICRA)*, IEEE, Piscataway, NJ, USA, **2016**; DOI: 10.1109/ICRA.2016.7487315.
- [286] Z. Ye, S. Régner, M. Sitti, *IEEE Trans. Rob.* **2014**, *30*, 3.
- [287] J. Kim, S. E. Chung, S.-E. Choi, H. Lee, J. Kim, S. Kwon, *Nat. Mater.* **2011**, *10*, 747.
- [288] M. Khoo, C. Liu, *Sens. Actuators, A* **2001**, *89*, 259.
- [289] L. V. Nikitin, D. G. Korolev, G. V. Stepanov, L. S. Mironova, *J. Magn. Magn. Mater.* **2006**, *300*, e234.
- [290] E. Diller, M. Sitti, *Adv. Funct. Mater.* **2014**, *24*, 4397.
- [291] L. Barsi, A. Büki, D. a. Z. M. Szabó, in *Gels: Progress in Colloid and Polymer Science*, (Eds.: F. Kremer, G. Lagaly, M. Zrinyi), Steinkopff, Darmstadt, Germany, **1996**.
- [292] J. Chatterjee, Y. Haik, C. J. Chen, *Biomagn. Res. Technol.* **2004**, *2*, DOI: 10.1186/1477-044X-2-2.
- [293] D. Collin, G. K. Auernhammer, O. Gavat, P. Martinoty, H. R. Brand, *Macromol. Rapid Commun.* **2003**, *24*, 737.
- [294] D. Szabó, G. Szeghy, M. Zrinyi, *Macromolecules* **1998**, *31*, 6541.
- [295] K. Kim, S. Young Ko, J.-O. Park, S. Park, *Proc. Inst. Mech. Eng., Part C* **2015**, DOI: 10.1177/0954406215616143.
- [296] R. T. Olsson, M. A. S. Azizi Samir, G. Salazar Alvarez, L. Belova, V. Strom, L. A. Berglund, O. Ikkala, J. Nogues, U. W. Gedde, *Nanotechnol.* **2010**, *5*, 584.
- [297] M. Zrinyi, L. Barsi, A. Büki, *J. Chem. Phys.* **1996**, *104*, 8750.
- [298] M. Zrinyi, D. Szabó, H.-G. Kilian, *Polym. Gels Networks* **1998**, *6*, 441.
- [299] M. Zrinyi, *Colloid Polym. Sci.* **2000**, *278*, 98.
- [300] M. Zrinyi, L. Barsi, A. Büki, *Polym. Gels Networks* **1997**, *5*, 415.
- [301] M. Tetsu, H. Yuki, N. Keisuke, *Jpn. J. Appl. Phys.* **2008**, *47*, 7257.
- [302] C.-Y. Chen, W. L. Wu, J. A. Miranda, *Phys. Rev. E* **2010**, *82*, 056321.
- [303] T. Jamin, C. Py, E. Falcon, *Phys. Rev. Lett.* **2011**, *107*, 204503.
- [304] R. Dreyfus, J. Baudry, M. L. Roper, M. Fermigier, H. A. Stone, J. Bibette, *Nature* **2005**, *437*, 862.
- [305] A. Cebers, K. Erglis, *Adv. Funct. Mater.* **2016**, *26*, 3783.
- [306] J. Zhang, P. Jain, E. Diller, in *2016 IEEE Int. Conf. on Robotics and Automation (ICRA)*, IEEE, Piscataway, NJ, USA, **2016**; DOI: 10.1109/ICRA.2016.7487339.
- [307] H.-W. Huang, M. S. Sakar, A. J. Petruska, S. Pane, B. J. Nelson, *Nat. Commun.* **2016**, *7*, 12263, DOI: 10.1038/ncomms12263.
- [308] A. Crivaro, R. Sheridan, M. Frecker, T. W. Simpson, P. Von Lockette, *J. Intell. Mater. Syst. Struct.* **2015**, *27*, 2049.
- [309] B. Jang, E. Gutman, N. Stucki, B. F. Seitz, P. D. Wendel-García, T. Newton, J. Pokki, O. Ergeneman, S. Panè, Y. Or, B. J. Nelson, *Nano Lett.* **2015**, *15*, 4829.
- [310] S. Yim, M. Sitti, *Int. J. Rob. Res.* **2014**, *33*, 1083.
- [311] S. Miyashita, S. Guitron, M. Ludersdorfer, C. R. Sung, D. Rus, in *2015 IEEE Int. Conf. on Robotics and Automation (ICRA)*, IEEE, Piscataway, NJ, USA, **2015**; DOI: 10.1109/ICRA.2015.7139386.
- [312] S. Yim, M. Sitti, *IEEE Trans. Rob.* **2012**, *28*, 1198.
- [313] S. Yim, M. Sitti, *IEEE Trans. Rob.* **2012**, *28*, 183.
- [314] Z. Ding, P. Wei, G. Chitnis, B. Ziaie, *J. Microelectromech. Syst.* **2011**, *20*, 59.
- [315] D. Fragouli, I. S. Bayer, R. Di Corato, R. Brescia, G. Bertoni, C. Innocenti, D. Gatteschi, T. Pellegrino, R. Cingolani, A. Athanassiou, *J. Mater. Chem.* **2012**, *22*, 1662.
- [316] I. Torres-Diaz, C. Rinaldi, *Soft Matter* **2014**, *10*, 8584.
- [317] J. de Vicente, D. J. Klingenberg, R. Hidalgo-Alvarez, *Soft Matter* **2011**, *7*, 3701.
- [318] R. C. Belli, D. T. Zimmerman, N. M. Wereley, in *Electrodeposited Nanowires and their Applications*, (Ed.: N. Lupu), InTech Publishers, Vienna, Austria, **2010**.
- [319] S. Genc, P. P. Phulé, *Smart Mater. Struct.* **2002**, *11*, 140.
- [320] J. V. I. Timonen, M. Latikka, L. Leibler, R. H. A. Ras, O. Ikkala, *Science* **2013**, *341*, 253.
- [321] A. Beyzavi, N.-T. Nguyen, *J. Micromech. Microeng.* **2009**, *20*, 015018.
- [322] Y. Hu, H. Jiang, J. Liu, Y. Li, X. Hou, C. Li, *RSC Adv.* **2014**, *4*, 3162.
- [323] Y. Zhao, J. Fang, H. Wang, X. Wang, T. Lin, *Adv. Mater.* **2010**, *22*, 707.
- [324] Y. Zhao, Z. Xu, M. Parhizkar, J. Fang, X. Wang, T. Lin, *Microfluid. Nanofluid.* **2012**, *13*, 555.
- [325] S. Zhang, Y. Zhang, Y. Wang, S. Liu, Y. Deng, *Phys. Chem. Chem. Phys.* **2012**, *14*, 5132.
- [326] N.-T. Nguyen, *Langmuir* **2013**, *29*, 13982.
- [327] L. L. Howell, *Compliant Mechanisms*, Wiley, New York, USA, **2001**.
- [328] S. T. Smith, *Flexures: Elements of Elastic Mechanisms*, CRC Press, Boca Raton, FL, USA, **2000**.
- [329] P. R. Ouyang, R. C. Tjiptoprodjo, W. J. Zhang, G. S. Yang, *Int. J. Adv. Manuf. Technol.* **2008**, *38*, 463.
- [330] J. B. Hopkins, M. L. Culpepper, *Precis. Eng.* **2010**, *34*, 259.
- [331] D. L. Blanding, *Exact Constraint: Machine Design Using Kinematic Principles*, ASME Press, New York, USA **1999**.
- [332] J. A. Gallego, J. Herder, *ASME Int. Des. Eng. Tech. Conf. Comput. Inf. Eng. Conf., Proc.* **2009**, *7*, 193; DOI: 10.1115/DETC2009-86845.
- [333] O. Sigmund, K. Maute, *Struct. Multidiscip. Optim.* **2013**, *48*, 1031.
- [334] M. P. Bendsoe, O. Sigmund, *Topology Optimization: Theory, Methods, and Applications*, Springer-Verlag, Heidelberg, Germany, **2003**.

- [335] X. Huang, Y.-M. Xie, *Struct. Multidiscip. Optim.* **2010**, *41*, 671.
- [336] M. Y. Wang, X. Wang, D. Guo, *Comp. Methods Appl. Mech. Eng.* **2003**, *192*, 227.
- [337] M. P. Bendsøe, N. Kikuchi, *Comp. Methods Appl. Mech. Eng.* **1988**, *71*, 197.
- [338] C. J. Kim, Y.-M. Moon, S. Kota, *J. Mech. Des.* **2008**, *130*, 022308.
- [339] Y. M. Xie, G. P. Steven, *Evolutionary Structural Optimization*, Springer-Verlag, London, UK **1997**.
- [340] M. Jin, X. Zhang, *Mech. Mach. Theory* **2016**, *95*, 42.
- [341] M. T. Pham, T. J. Teo, S. H. Yeo, *Precis. Eng.* **2017**, *47*, 131.
- [342] G. Z. Lum, T. J. Teo, S. H. Yeo, G. Yang, M. Sitti, *Precis. Eng.* **2015**, *42*, 195.
- [343] G. Z. Lum, T. J. Teo, G. Yang, S. H. Yeo, M. Sitti, *Precis. Eng.* **2015**, *39*, 125.
- [344] R. D. Kornbluh, R. Pelrine, H. Prahlad, R. Heydt, *Proc. SPIE* **2004**, *5344*, 13; DOI: 10.1117/12.538382.
- [345] N.-C. Tsai, C.-Y. Sue, *Sens. Actuators, A* **2007**, *134*, 555.
- [346] M. De Volder, D. Reynaerts, *J. Micromech. Microeng.* **2010**, *20*, 043001.
- [347] M. Wehner, M. T. Tolley, Y. Mengüç, Y.-L. Park, A. Mozeika, Y. Ding, C. Onal, R. F. Shepherd, G. M. Whitesides, R. J. Wood, *Soft Rob.* **2014**, *1*, 263.
- [348] A. De Greef, P. Lambert, A. Delchambre, *Precis. Eng.* **2009**, *33*, 311.
- [349] B. Gorissen, W. Vincentie, F. Al-Bender, D. Reynaerts, M. De Volder, *J. Micromech. Microeng.* **2013**, *23*, 045012.
- [350] F. C. M. van de Pol, D. G. J. Wonnink, M. Elwenspoek, J. H. J. Fluitman, *Sens. Actuators* **1989**, *17*, 139.
- [351] S. Haeberle, R. Zengerle, *Lab Chip* **2007**, *7*, 1094.
- [352] M. A. Unger, H.-P. Chou, T. Thorsen, A. Scherer, S. R. Quake, *Science* **2000**, *288*, 113.
- [353] J. Ok Chan, K. Satoshi, *J. Micromech. Microeng.* **2008**, *18*, 025022.
- [354] O. C. Jeong, S. Konishi, *Sens. Actuators, A* **2007**, *135*, 849.
- [355] Y.-N. Yang, S.-K. Hsiung, G.-B. Lee, *Microfluid. Nanofluid.* **2009**, *6*, 823.
- [356] N.-T. Nguyen, *Biomicrofluidics* **2010**, *4*, 031501.
- [357] M. Christopher, S. Yu, A. S. Craig, *J. Micromech. Microeng.* **2009**, *19*, 065015.
- [358] S. Song, M. Sitti, *Adv. Mater.* **2014**, *26*, 4901.
- [359] J. Ok, M. Chu, C.-J. Kim, in *Technical Digest. IEEE International MEMS 99 Conference. Twelfth IEEE Int. Conf. on Micro Electro Mechanical Systems*, IEEE, Piscataway, NJ, USA, **1999**; DOI: 10.1109/MEMSYS.1999.746872.
- [360] J. Ok, Y. W. Lu, C. J. C. Kim, *J. Microelectromech. Syst.* **2006**, *15*, 1499.
- [361] O. C. Jeong, S. S. Yang, *Sens. Actuators, A* **2000**, *83*, 249.
- [362] W. I. Jang, C. A. Choi, C. H. Jun, Y. T. Kim, M. Esashi, *Sens. Actuators, A* **2004**, *115*, 151.
- [363] R. V. Martinez, J. L. Branch, C. R. Fish, L. Jin, R. F. Shepherd, R. M. D. Nunes, Z. Suo, G. M. Whitesides, *Adv. Mater.* **2013**, *25*, 205.
- [364] R. F. Shepherd, F. Ilievski, W. Choi, S. A. Morin, A. A. Stokes, A. D. Mazzeo, X. Chen, M. Wang, G. M. Whitesides, *Proc. Natl. Acad. Sci. USA* **2011**, *108*, 20400.
- [365] B. Mosadegh, P. Polygerinos, C. Keplinger, S. Wennstedt, R. F. Shepherd, U. Gupta, J. Shim, K. Bertoldi, C. J. Walsh, G. M. Whitesides, *Adv. Funct. Mater.* **2014**, *24*, 2163.
- [366] B. Gorissen, M. de Volder, D. Reynaerts, *Lab Chip* **2015**, *15*, 4348.
- [367] K. Suzumori, S. Iikura, H. Tanaka, in *Proc. 1991 IEEE Int. Conf. on Robotics and Automation*, IEEE, Piscataway, NJ, USA, **1991**; DOI: 10.1109/ROBOT.1991.131850.
- [368] K. Suzumori, S. Iikura, H. Tanaka, *IEEE Contr. Syst.* **1992**, *12*, 21.
- [369] K. Suzumori, T. Maeda, H. Wantabe, T. Hisada, *IEEE/ASME Trans. Mech.* **1997**, *2*, 281.
- [370] M. Lazeroms, A. La Haye, W. Sjoerdsma, W. Schreurs, W. Jongkind, G. Honderd, C. Grimbergen, *Mechatronics* **1996**, *6*, 437.
- [371] H.-W. Kang, I. H. Lee, D.-W. Cho, *Microelectron. Eng.* **2006**, *83*, 1201.
- [372] S. Wakimoto, K. Ogura, K. Suzumori, Y. Nishioka, in *2009 IEEE Int. Conf. on Robotics and Automation*, IEEE, Piscataway, NJ, USA **2009**; DOI: 10.1109/ROBOT.2009.5152259.
- [373] S. Wakimoto, K. Suzumori, K. Ogura, *Adv. Rob.* **2011**, *25*, 1311.
- [374] M. Ikeuchi, K. Ikuta, in *2009 IEEE Int. Conf. on Robotics and Automation*, IEEE, Piscataway, NJ, USA **2009**; DOI: 10.1109/ROBOT.2009.5152869.
- [375] K. Ikuta, H. Ichikawa, K. Suzuki, in *Proc. 5th Int. Conf. on Medical Image Computing and Computer-Aided Intervention, Part I*, (Eds: T. Dohi, R. Kikinis), Springer, Heidelberg, Germany **2002**, p. 182.
- [376] S. Konishi, M. Nakata, O. C. Jeong, T. Sakakibara, S. Kusuda, M. Kuwayama, H. Tsutsumi, *presented at Int. Symposium on Robotics*, Tokyo, Japan, November **2005**.
- [377] S. Konishi, M. Nakata, O. C. Jeong, S. Kusuda, T. Sakakibara, M. Kuwayama, H. Tsutsumi, in *Proc. 2006 IEEE Int. Conf. on Robotics and Automation, 2006. ICRA 2006*, IEEE, Piscataway, NJ, USA **2006**; DOI: 10.1109/ROBOT.2006.1641846.
- [378] Y. Watanabe, M. Maeda, N. Yaji, R. Nakamura, H. Iseki, M. Yamato, T. Okano, S. Hori, S. Konishi, in *2007 IEEE 20th International Conference on Micro Electro Mechanical Systems (MEMS)*, IEEE, Piscataway, NJ, USA **2007**; DOI: 10.1109/MEMSYS.2007.4433083.
- [379] B. Gorissen, R. Donose, D. Reynaerts, M. De Volder, *Proc. Eng.* **2011**, *25*, 681.
- [380] S. Konishi, S. Shimomura, S. Tajima, Y. Tabata, *Microsyst. Nanoeng.* **2016**, *2*, 15048.
- [381] S. Bütfisch, V. Seidemann, S. Büttgenbach, *Sens. Actuators, A* **2002**, *97*–*98*, 638.
- [382] M. Schwörer, M. Kohl, W. Menz, in *Proc. Int. Conf. on New Actuators*, (Ed: H. Borgmann), Messe Bremen GmbH, Bremen, Germany, **1998**, p.103.
- [383] S. Konishi, F. Kawai, P. Cusin, *Sens. Actuators, A* **2001**, *89*, 28.
- [384] W. Choi, M. Akbarian, V. Rubtsov, C. J. Kim, *IEEE Trans. Ind. Electron.* **2009**, *56*, 1005.
- [385] B. Gorissen, T. Chishiro, S. Shimomura, D. Reynaerts, M. De Volder, S. Konishi, *Sens. Actuators, A* **2014**, *216*, 426.
- [386] D. Yang, B. Mosadegh, A. Ainla, B. Lee, F. Khashai, Z. Suo, K. Bertoldi, G. M. Whitesides, *Adv. Mater.* **2015**, *27*, 6323.
- [387] Y. Xing, Y.-C. Tai, C.-M. Ho, in *1997 Int. Conf. on Solid State Sensors and Actuators, 1997. TRANSDUCERS '97 Chicago*, IEEE, Piscataway, NJ, USA **1997**, DOI: 10.1109/SENSOR.1997.613577.
- [388] M. De Volder, A. J. M. Moers, D. Reynaerts, *Sens. Actuators, A* **2011**, *166*, 111.
- [389] K. Takemura, S. Yokota, K. Edamura, in *Proc. 2005 IEEE Int. Conf. on Robotics and Automation*, IEEE, Piscataway, NJ, USA, **2005**; DOI: 10.1109/ROBOT.2005.1570173.
- [390] Y. Haga, Y. Muyari, T. Mineta, T. Matsunaga, H. Akahori, M. Esashi, in *Proc. Eng. Med. Biol. Soc. Ann.*, IEEE, Piscataway, NJ, USA, **2005**, DOI: 10.1109/MMB.2005.1548439.
- [391] Y. Lu, C.-J. Kim, in *TRANSDUCERS, Solid-State Sensors, Actuators and Microsystems, 12th Int. Conf.*, **2003**, IEEE, Piscataway, NJ, USA, **2003**; DOI: 10.1109/SENSOR.2003.1215306.
- [392] J. Shim, C. Perdigou, E. R. Chen, K. Bertoldi, P. M. Reis, *Proc. Natl. Acad. Sci. USA* **2012**, *109*, 5978.
- [393] F. Daerden, D. Lefever, *Eur. J. Mech. Environ. Eng.* **2002**, *47*, 11.
- [394] R. Niijima, D. Rus, S. Kim, in *2014 IEEE International Conference on Robotics and Automation (ICRA)*, IEEE, Piscataway, NJ, USA **2014**; DOI: 10.1109/ICRA.2014.6907793.
- [395] R. Niijima, X. Sun, C. Sung, B. An, D. Rus, S. Kim, *Soft Rob.* **2015**, *2*, 59.

- [396] E. Brown, N. Rodenberg, J. Amend, A. Mozeika, E. Steltz, M. R. Zakin, H. Lipson, H. M. Jaeger, *Proc. Natl. Acad. Sci. USA* **2010**, *107*, 18809.
- [397] S. Follmer, D. Leithinger, A. Olwal, N. Cheng, H. Ishii, in *Proc. ACM Symposium on User Interface Software and Technology*, ACM, New York, USA **2012**, p.519.
- [398] A. Stanley, A. Okamura, *IEEE Trans. Visualization Comput. Graphics* **2016**, DOI: 10.1109/TVCG.2016.2525788.
- [399] E. Steltz, A. Mozeika, N. Rodenberg, E. Brown, H. M. Jaeger, in *2009 IEEE/RSJ Int. Conf. on Intelligent Robots and Systems*, IEEE, Piscataway, NJ, USA **2009**; DOI: 10.1109/IROS.2009.5354790.
- [400] E. Steltz, A. Mozeika, J. Rembisz, N. Corson, H. M. Jaeger, *Proc. SPIE* **2010**, 7642, 764225; DOI: 10.1117/12.853182.
- [401] R. Casier, C. Lenders, M. S. Lhernould, M. Gauthier, P. Lambert, *Sensors* **2013**, *13*, 5857.
- [402] H. J. Lee, Y. S. Chang, Y. P. Lee, K.-H. Jeong, H.-Y. Kim, *Sens. Actuators, A* **2007**, *136*, 717.
- [403] R. Yahiaoui, R. Zeggari, J. Malapert, J.-F. Manceau, *Mechatronics* **2012**, *22*, 515.
- [404] W. Gao, A. Uygun, J. Wang, *J. Am. Chem. Soc.* **2012**, *134*, 897.
- [405] E. Diller, Z. Ye, J. Giltinan, M. Sitti, in *Small-Scale Robotics: From Nano-to-Millimeter-Sized Robotic Systems and Applications*, (Eds: I. Paprotny, S. Bergbreiter), Springer, Heidelberg, Germany **2014**.
- [406] G. J. Laurent, H. Moon, *Intell. Serv. Rob.* **2015**, *8*, 151.
- [407] S. Sánchez, L. Soler, J. Katuri, *Angew. Chem., Int. Ed.* **2015**, *54*, 1414.
- [408] P. L. Bergstrom, J. Jin, L. Yu-Ning, M. Kaviani, K. D. Wise, *J. Microelectromech. Syst.* **1995**, *4*, 10.
- [409] D. M. van den Broek, M. Elwenspoek, *Sens. Actuators, A* **2008**, *145–146*, 387.
- [410] D. E. Dowen, *Proc. SPIE* **1997**, *3132*, 127; DOI: 10.1117/12.284075.
- [411] E. T. Carlen, C. H. Mastrangelo, *J. Microelectromech. Syst.* **2002**, *11*, 165.
- [412] N. Napp, B. Araki, M. T. Tolley, R. Nagpal, R. J. Wood, in *2014 IEEE Int. Conf. on Robotics and Automation (ICRA)*, IEEE, Piscataway, NJ, USA **2014**; DOI: 10.1109/ICRA.2014.6907041.
- [413] V. Stroganov, S. Zakharchenko, E. Sperling, A. K. Meyer, O. G. Schmidt, L. Ionov, *Adv. Funct. Mater.* **2014**, *24*, 4357.
- [414] J. H. Comtois, V. M. Bright, M. W. Phipps, *Proc. SPIE* **1995**, *2642*, 10; DOI: 10.1117/12.221154.
- [415] M. J. Sinclair, in *ITHERM 2000. The Seventh Intersociety Conference on Thermal and Thermomechanical Phenomena in Electronic Systems*, IEEE, Piscataway, NJ, USA **2000**; DOI: 10.1109/ITHERM.2000.866818.
- [416] Y. Zhang, S. Iijima, *Phys. Rev. Lett.* **1999**, *82*, 3472.
- [417] W. Jiang, D. Niu, H. Liu, C. Wang, T. Zhao, L. Yin, Y. Shi, B. Chen, Y. Ding, B. Lu, *Adv. Funct. Mater.* **2014**, *24*, 7598.
- [418] Q. Li, C. Liu, Y.-H. Lin, L. Liu, K. Jiang, S. Fan, *ACS Nano* **2015**, *9*, 409.
- [419] Y. Hu, G. Wu, T. Lan, J. Zhao, Y. Liu, W. Chen, *Adv. Mater.* **2015**, *27*, 7867.
- [420] J. Deng, J. Li, P. Chen, X. Fang, X. Sun, Y. Jiang, W. Weng, B. Wang, H. Peng, *J. Am. Chem. Soc.* **2016**, *138*, 225.
- [421] L. James, X. Peng, P. Balaji, *Nanotechnology* **2013**, *24*, 185703.
- [422] M. A. Ward, T. K. Georgiou, *Polymers* **2011**, *3*, 1215.
- [423] M. Lemanowicz, A. Gierczycki, W. Kuźnik, R. Sanczewicz, P. Imiela, *Miner. Eng.* **2014**, *69*, 170.
- [424] G. Stoychev, N. Puretskiy, L. Ionov, *Soft Matter* **2011**, *7*, 3277.
- [425] V. Stroganov, M. Al-Hussein, J.-U. Sommer, A. Janke, S. Zakharchenko, L. Ionov, *Nano Lett.* **2015**, *15*, 1786.
- [426] E. Wang, M. S. Desai, S.-W. Lee, *Nano Lett.* **2013**, *13*, 2826.
- [427] D. Kim, H. S. Lee, J. Yoon, *Sci. Rep.* **2016**, *6*, 20921; DOI: 10.1038/srep20921.
- [428] S. Jiang, F. Liu, A. Lerch, L. Ionov, S. Agarwal, *Adv. Mater.* **2015**, *27*, 4865.
- [429] J.-H. Na, A. A. Evans, J. Bae, M. C. Chiappelli, C. D. Santangelo, R. J. Lang, T. C. Hull, R. C. Hayward, *Adv. Mater.* **2015**, *27*, 79.
- [430] H. Okuzaki, H. Suzuki, T. Ito, *Synth. Met.* **2009**, *159*, 2233.
- [431] J. Mu, C. Hou, H. Wang, Y. Li, Q. Zhang, M. Zhu, *Sci. Adv.* **2015**, *1*, e1500533; DOI: 10.1126/sciadv.1500533.
- [432] M. M. Hamed, V. E. Campbell, P. Rothemund, F. Güder, D. C. Christodouleas, J. Bloch, G. M. Whitesides, *Adv. Funct. Mater.* **2016**, *26*, 2446.
- [433] H. Wermter, H. Finkelmann, *e-Polymers* **2001**, *1*, 111.
- [434] T. H. Ware, M. E. McConney, J. J. Wie, V. P. Tondiglia, T. J. White, *Science* **2015**, *347*, 982.
- [435] L. T. de Haan, V. Gimenez-Pinto, A. Konya, T.-S. Nguyen, J. M. N. Verjans, C. Sánchez-Somolinos, J. V. Selinger, R. L. B. Selinger, D. J. Broer, A. P. H. J. Schenning, *Adv. Funct. Mater.* **2014**, *24*, 1251.
- [436] Y. Yang, Z. Pei, Z. Li, Y. Wei, Y. Ji, *J. Am. Chem. Soc.* **2016**, *138*, 2118.
- [437] C. Ahn, X. Liang, S. Cai, *Extreme Mech. Lett.* **2015**, *5*, 30.
- [438] Z. Pei, Y. Yang, Q. Chen, E. M. Terentjev, Y. Wei, Y. Ji, *Nat. Mater.* **2014**, *13*, 36.
- [439] H. Yang, A. Buguin, J.-M. Taulemesse, K. Kaneko, S. Méry, A. Bergeret, P. Keller, *J. Am. Chem. Soc.* **2009**, *131*, 15000.
- [440] A. Buguin, M.-H. Li, P. Silberzan, B. Ladoux, P. Keller, *J. Am. Chem. Soc.* **2006**, *128*, 1088.
- [441] Z. L. Wu, A. Buguin, H. Yang, J. Taulemesse, N. Le Moigne, A. Bergeret, X. Wang, P. Keller, *Adv. Funct. Mater.* **2013**, *23*, 3070.
- [442] R. Wei, Y. He, X. Wang, P. Keller, *Macromol. Rapid Commun.* **2014**, *35*, 1571.
- [443] C. L. van Oosten, C. W. M. Bastiaansen, D. J. Broer, *Nat. Mater.* **2009**, *8*, 677.
- [444] C. Ohm, C. Serra, R. Zentel, *Adv. Mater.* **2009**, *21*, 4859.
- [445] H. H. Le, I. Kolesov, Z. Ali, M. Uthardt, O. Osazuwa, S. Ilisch, H.-J. Radusch, *J. Mater. Sci.* **2010**, *45*, 5851.
- [446] N. G. Sahoo, Y. C. Jung, H. J. Yoo, J. W. Cho, *Compos. Sci. Technol.* **2007**, *67*, 1920.
- [447] J. Leng, H. Lv, Y. Liu, S. Du, *J. Appl. Phys.* **2008**, *104*, 104917.
- [448] J. W. Cho, J. W. Kim, Y. C. Jung, N. S. Goo, *Macromol. Rapid Commun.* **2005**, *26*, 412.
- [449] J. S. Leng, X. Lan, Y. J. Liu, S. Y. Du, W. M. Huang, N. Liu, S. J. Phee, Q. Yuan, *Appl. Phys. Lett.* **2008**, *92*, 014104.
- [450] X. Luo, P. T. Mather, *Soft Matter* **2010**, *6*, 2146.
- [451] Y. J. Liu, H. B. Lv, X. Lan, J. S. Leng, S. Y. Du, *Compos. Sci. Technol.* **2009**, *69*, 2064.
- [452] A. Lendlein, R. Langer, *Science* **2002**, *296*, 1673.
- [453] W. Voit, T. Ware, R. R. Dasari, P. Smith, L. Danz, D. Simon, S. Barlow, S. R. Marder, K. Gall, *Adv. Funct. Mater.* **2010**, *20*, 162.
- [454] M. Anthamatten, S. Roddecha, J. Li, *Macromolecules* **2013**, *46*, 4230.
- [455] Y. Liu, J. K. Boyles, J. Genzer, M. D. Dickey, *Soft Matter* **2012**, *8*, 1764.
- [456] S. Miyashita, L. Meeker, M. T. Tolley, R. Wood, D. Rus, *Smart Mater. Struct.* **2014**, *23*, 094005.
- [457] S. Miyashita, C. D. Onal, D. Rus, in *2013 IEEE/RSJ International Conference on Intelligent Robots and Systems*, IEEE, Piscataway, NJ, USA **2013**; DOI: 10.1109/IROS.2013.6696938.
- [458] L. Hines, V. Arabagi, M. Sitti, *IEEE Trans. Rob.* **2012**, *28*, 987.
- [459] X. Niu, X. Yang, P. Brochu, H. Stoyanov, S. Yun, Z. Yu, Q. Pei, *Adv. Mater.* **2012**, *24*, 6513.
- [460] T. Xie, *Nature* **2010**, *464*, 267.
- [461] T. S. Sammarco, M. A. Burns, *AIChE J.* **1999**, *45*, 350.
- [462] A. A. Darhuber, J. P. Valentino, S. M. Troian, S. Wagner, *J. Microelectromech. Syst.* **2003**, *12*, 873.

- [463] V. Pratap, N. Moumen, R. S. Subramanian, *Langmuir* **2008**, *24*, 5185.
- [464] W. Hu, A. T. Ohta, *Microfluid. Nanofluid.* **2011**, *11*, 307.
- [465] R. K. Dhull, L. Fuller, P.-C. Kao, Y.-C. Liao, Y.-W. Lu, *Sens. Actuators, A* **2011**, *168*, 162.
- [466] H. Linke, B. J. Alemán, L. D. Melling, M. J. Taormina, M. J. Francis, C. C. Dow-Hygelund, V. Narayanan, R. P. Taylor, A. Stout, *Phys. Rev. Lett.* **2006**, *96*, 154502.
- [467] W. Wang, H. Rodrigue, S.-H. Ahn, *Composites, Part B* **2015**, *78*, 507.
- [468] B. E. Schubert, D. Floreano, *RSC Adv.* **2013**, *3*, 24671.
- [469] Z. Ye, G. Z. Lum, S. Song, S. Rich, M. Sitti, *Adv. Mater.* **2016**, *28*, 5088.
- [470] J. Mohd Jani, M. Leary, A. Subic, M. A. Gibson, *Mater. Des.* **2014**, *56*, 1078.
- [471] S. Kim, E. Hawkes, K. Cho, M. Jolda, J. Foley, R. Wood, in *2009 IEEE/RSJ International Conference on Intelligent Robots and Systems*, IEEE, Piscataway, NJ, USA, **2009**; DOI: 10.1109/IROS.2009.5354178.
- [472] M. Noh, S.-W. Kim, S. An, J.-S. Koh, K.-J. Cho, *IEEE Trans. Rob.* **2012**, *28*, 1007.
- [473] Y. Fu, H. Du, W. Huang, S. Zhang, M. Hu, *Sens. Actuators, A* **2004**, *112*, 395.
- [474] J. J. Gill, D. T. Chang, L. A. Momoda, G. P. Carman, *Sens. Actuators, A* **2001**, *93*, 148.
- [475] Y. Q. Fu, J. K. Luo, A. J. Flewitt, S. E. Ong, S. Zhang, H. J. Du, W. I. Milne, *Smart Mater. Struct.* **2007**, *16*, 2651.
- [476] F. Ercole, T. P. Davis, R. A. Evans, *Polym. Chem.* **2010**, *1*, 37.
- [477] J. Wei, Y. Yu, *Soft Matter* **2012**, *8*, 8050.
- [478] H. Y. Jiang, S. Kelch, A. Lendlein, *Adv. Mater.* **2006**, *18*, 1471.
- [479] M. Irie, in *New Polymer Materials*, Springer-Verlag, Heidelberg, Germany **1990**, p. 27.
- [480] P. Brown, C. P. Butts, J. Eastoe, *Soft Matter* **2013**, *9*, 2365.
- [481] K. Kumar, A. P. H. J. Schenning, D. J. Broer, D. Liu, *Soft Matter* **2016**, *12*, 3196.
- [482] Y. Zhao, *Macromolecules* **2012**, *45*, 3647.
- [483] A. Natansohn, P. Rochon, *Chem. Rev.* **2002**, *102*, 4139.
- [484] W. M. Gibbons, T. Kosa, P. Palfy-Muhoray, P. J. Shannon, S. T. Sun, *Nature* **1995**, *377*, 43.
- [485] C. Huang, J.-a. Lv, X. Tian, Y. Wang, Y. Yu, J. Liu, *Sci. Rep.* **2015**, *5*, DOI: 10.1038/srep17414.
- [486] T. J. White, N. V. Tabiryan, S. V. Serak, U. A. Hrozhyk, V. P. Tondiglia, H. Koerner, R. A. Vaia, T. J. Bunning, *Soft Matter* **2008**, *4*, 1796.
- [487] S. Iamsaard, S. J. Alhoff, B. Matt, T. Kudernac, J. J. L. M. Cornelissen, S. P. Fletcher, N. Katsonis, *Nat. Chem.* **2014**, *6*, 229.
- [488] M. Yamada, M. Kondo, R. Miyasato, Y. Naka, J.-i. Mamiya, M. Kinoshita, A. Shishido, Y. Yu, C. J. Barrett, T. Ikeda, *J. Mater. Chem.* **2008**, *19*, 60.
- [489] H. Yu, T. Ikeda, *Adv. Mater.* **2011**, *23*, 2149.
- [490] Y. Yu, M. Nakano, T. Ikeda, *Nature* **2003**, *425*, 145.
- [491] M. Li, P. Keller, B. Li, X. Wang, M. Brunet, *Adv. Mater.* **2003**, *15*, 569.
- [492] Y. Yu, M. Nakano, T. Ikeda, *Pure Appl. Chem.* **2004**, *76*, 1467.
- [493] K. D. Harris, R. Cuypers, P. Scheibe, C. L. van Oosten, C. W. M. Bastiaansen, J. Lub, D. J. Broer, *J. Mater. Chem.* **2005**, *15*, 5043.
- [494] C. L. van Oosten, D. Corbett, D. Davies, M. Warner, C. W. M. Bastiaansen, D. J. Broer, *Macromolecules* **2008**, *41*, 8592.
- [495] E. Mabrouk, D. Cuvelier, F. Brochard-Wyart, P. Nassoy, M.-H. Li, *Proc. Natl. Acad. Sci. USA* **2009**, *106*, 7294.
- [496] M. Carnacho-Lopez, H. Finkelmann, P. Palfy-Muhoray, M. Shelley, *Nat. Mater.* **2004**, *3*, 307.
- [497] S. Palagi, A. G. Mark, S. Y. Reigh, K. Melde, T. Qiu, H. Zeng, C. Parmeggiani, D. Martella, A. Sanchez-Castillo, N. Kapernaum, F. Giesselmann, D. S. Wiersma, E. Lauga, P. Fischer, *Nat. Mater.* **2016**, *15*, 647.
- [498] H. Zeng, P. Wasylczyk, C. Parmeggiani, D. Martella, M. Burresi, D. S. Wiersma, *Adv. Mater.* **2015**, *27*, 3883.
- [499] D. Liu, D. J. Broer, *Angew. Chem.* **2014**, *126*, 4630.
- [500] M. Behl, A. Lendlein, *Mater. Today* **2007**, *10*, 20.
- [501] A. Lendlein, H. Jiang, O. Jünger, R. Langer, *Nature* **2005**, *434*, 879.
- [502] Y. Yu, T. Ikeda, *Macromol. Chem. Phys.* **2005**, *206*, 1705.
- [503] S. Juodkazis, N. Mukai, R. Wakaki, A. Yamaguchi, S. Matsuo, H. Misawa, *Nature* **2000**, *408*, 178.
- [504] M. Irie, in *Responsive Gels: Volume Transitions II*, (Ed.: K. Dušek), Springer, Heidelberg, Germany **1993**.
- [505] M.-S. Kang, V. K. Gupta, *J. Phys. Chem. B* **2002**, *106*, 4127.
- [506] T. Ikeda, M. Nakano, Y. Yu, O. Tsutsumi, A. Kanazawa, *Adv. Mater.* **2003**, *15*, 201.
- [507] T. Sakai, H. Murayama, S. Nagano, Y. Takeoka, M. Kidowaki, K. Ito, T. Seki, *Adv. Mater.* **2007**, *19*, 2023.
- [508] T. K. Mudiyanselage, D. C. Neckers, *Soft Matter* **2008**, *4*, 768.
- [509] M. Irie, D. Kunwatchakun, *Macromolecules* **1986**, *19*, 2476.
- [510] A. Mamada, T. Tanaka, D. Kungwatchakun, M. Irie, *Macromolecules* **1990**, *23*, 1517.
- [511] S. Sugiura, K. Sumaru, K. Ohi, K. Hiroki, T. Takagi, T. Kanamori, *Sens. Actuators, A* **2007**, *140*, 176.
- [512] T. Satoh, K. Sumaru, T. Takagi, T. Kanamori, *Soft Matter* **2011**, *7*, 8030.
- [513] J. He, X. Tong, Y. Zhao, *Macromolecules* **2009**, *42*, 4845.
- [514] N. M. Sangeetha, U. Maitra, *Chem. Soc. Rev.* **2005**, *34*, 821.
- [515] K. Al-Arabe, G. K. Knopf, A. S. Bassi, *Proc. SPIE* **2006**, *6343*, 63432R; DOI: 10.1117/12.707765.
- [516] K. Ichimura, S.-K. Oh, M. Nakagawa, *Science* **2000**, *288*, 1624.
- [517] X. Tang, S.-Y. Tang, V. Sivan, W. Zhang, A. Mitchell, K. Kalantar-zadeh, K. Khoshmanesh, *Appl. Phys. Lett.* **2013**, *103*, 174104.
- [518] K. Uchino, in *IEEE Symp. on Ultrasonics*, IEEE, Piscataway, NJ, USA, **1990**; DOI: 10.1109/ULTSYM.1990.171457.
- [519] B. Kundys, *Appl. Phys. Rev.* **2015**, *2*, 011301.
- [520] F. Kurokawa, Y. Oochi, A. Sadana, Y. Tsujiura, H. Hida, I. Kanno, in *2015 Transducers - 2015 18th Int. Conf. on Solid-State Sensors, Actuators and Microsystems (TRANSDUCERS)*, IEEE, Piscataway, NJ, USA, **2015**; DOI: 10.1109/TRANSDUCERS.2015.7181087.
- [521] M. Deshpande, L. Saggere, *Proc. SPIE* **2004**, *5389*, 286; DOI: 10.1117/12.540231.
- [522] A. Grinthal, J. Aizenberg, *Chem. Soc. Rev.* **2013**, *42*, 7072.
- [523] D. Hore, A. Majumder, S. Mondal, A. Roy, A. Ghatak, *Soft Matter* **2012**, *8*, 5038.
- [524] H. Song, H. Lin, M. Antonietti, J. Yuan, *Adv. Mater. Interfaces* **2016**, *3*, 500743.
- [525] Q. Zhao, J. W. C. Dunlop, X. Qiu, F. Huang, Z. Zhang, J. Heyda, J. Dzubiella, M. Antonietti, J. Yuan, *Nat. Commun.* **2014**, *5*, 4293, DOI: 10.1038/ncomms5293.
- [526] D. P. Holmes, A. J. Crosby, *Adv. Mater.* **2007**, *19*, 3589.
- [527] S. Maeda, Y. Hara, T. Sakai, R. Yoshida, S. Hashimoto, *Adv. Mater.* **2007**, *19*, 3480.
- [528] A. Fargette, S. Neukirch, A. Antkowiak, *Phys. Rev. Lett.* **2014**, *112*, 137802.
- [529] H. Du, J. Zhang, *Soft Matter* **2010**, *6*, 3370.
- [530] R. Xiao, J. Guo, D. L. Safranski, T. D. Nguyen, *Soft Matter* **2015**, *11*, 3977.
- [531] Z.-Q. Dong, Y. Cao, Q.-J. Yuan, Y.-F. Wang, J.-H. Li, B.-J. Li, S. Zhang, *Macromol. Rapid Commun.* **2013**, *34*, 867.
- [532] A. Yasin, H. Li, Z. Lu, S. u. Rehman, M. Siddiq, H. Yang, *Soft Matter* **2014**, *10*, 972.
- [533] M. Mohammed, R. Sundaresan, M. D. Dickey, *ACS Appl. Mater. Interfaces* **2015**, *7*, 23163.

- [534] J. Zhang, Y. Yao, L. Sheng, J. Liu, *Adv. Mater.* **2015**, *27*, 2648.
- [535] R. Yoshida, T. Takahashi, T. Yamaguchi, H. Ichijo, *Adv. Mater.* **1997**, *9*, 175.
- [536] R. Yoshida, *Adv. Mater.* **2010**, *22*, 3463.
- [537] D. Suzuki, T. Kobayashi, R. Yoshida, T. Hirai, *Soft Matter* **2012**, *8*, 11447.
- [538] S. Maeda, Y. Hara, R. Yoshida, S. Hashimoto, *Macromol. Rapid Commun.* **2008**, *29*, 401.
- [539] L. Ionov, *Adv. Funct. Mater.* **2013**, *23*, 4555.
- [540] A. Sidorenko, T. Krupenkin, A. Taylor, P. Fratzl, J. Aizenberg, *Science* **2007**, *315*, 487.
- [541] M. Ma, L. Guo, D. G. Anderson, R. Langer, *Science* **2013**, *339*, 186.
- [542] Y. Ma, Y. Zhang, B. Wu, W. Sun, Z. Li, J. Sun, *Angew. Chem., Int. Ed.* **2011**, *50*, 6254.
- [543] M. Dai, O. T. Picot, J. M. N. Verjans, L. T. de Haan, A. P. H. J. Schenning, T. Peijs, C. W. M. Bastiaansen, *ACS Appl. Mater. Interfaces* **2013**, *5*, 4945.
- [544] L. T. de Haan, J. M. N. Verjans, D. J. Broer, C. W. M. Bastiaansen, A. P. H. J. Schenning, *J. Am. Chem. Soc.* **2014**, *136*, 10585.
- [545] W. M. Huang, B. Yang, L. An, C. Li, Y. S. Chan, *Appl. Phys. Lett.* **2005**, *86*, 114105.
- [546] T. Wu, M. Frydrych, K. O'Kelly, B. Chen, *Biomacromolecules* **2014**, *15*, 2663.
- [547] X. Chen, D. Goodnight, Z. Gao, A. H. Cavusoglu, N. Sabharwal, M. DeLay, A. Driks, O. Sahin, *Nat. Commun.* **2015**, *6*, 7346; DOI: 10.1038/ncomms8346.
- [548] L. Yao, J. Ou, C.-Y. Cheng, H. Steiner, W. Wang, G. Wang, H. Ishii, in *Proc. ACM Human Factors in Computing Systems*, ACM, New York, **2015**, p. 1.
- [549] Y.-C. Su, L. Lin, A. P. Pisano, *J. Microelectromech. Syst.* **2002**, *11*, 736.
- [550] J.-K. Chen, C.-J. Chang, *Materials* **2014**, *7*, 805.
- [551] H. Chen, Y. Li, Y. Liu, T. Gong, L. Wang, S. Zhou, *Polym. Chem.* **2014**, *5*, 5168.
- [552] C. Ye, S. V. Nikolov, R. Calabrese, A. Dindar, A. Alexeev, B. Kippelen, D. L. Kaplan, V. V. Tsukruk, *Angew. Chem., Int. Ed.* **2015**, *54*, 8490.
- [553] B. P. Lee, S. Korst, *Adv. Mater.* **2014**, *26*, 3415.
- [554] C. Yoon, R. Xiao, J. Park, J. Cha, T. D. Nguyen, D. H. Gracias, *Smart Mater. Struct.* **2014**, *23*, 094008.
- [555] L. Dong, A. K. Agarwal, D. J. Beebe, H. Jiang, *Nature* **2006**, *442*, 551.
- [556] P. Ji Young, O. Hyun Jik, K. Duck Joong, B. Ju Yeoul, L. Sang Hoon, *J. Micromech. Microeng.* **2006**, *16*, 656.
- [557] D. Kimab, D. J. Beebe, *Lab Chip* **2007**, *7*, 193.
- [558] A. Gestos, P. G. Whitten, G. G. Wallace, G. M. Spinks, *Soft Matter* **2012**, *8*, 8082.
- [559] X.-J. Han, Z.-Q. Dong, M.-M. Fan, Y. Liu, J.-H. Li, Y.-F. Wang, Q.-J. Yuan, B.-J. Li, S. Zhang, *Macromol. Rapid Commun.* **2012**, *33*, 1055.
- [560] Y. Zhang, X. Jiang, R. Wu, W. Wang, *J. Appl. Polym. Sci.* **2016**, *133*, DOI: 10.1002/app.43534.
- [561] H. Meng, J. Zheng, X. Wen, Z. Cai, J. Zhang, T. Chen, *Macromol. Rapid Commun.* **2015**, *36*, 533.
- [562] C. Py, P. Reverdy, L. Doppler, J. Bico, B. Roman, C. N. Baroud, *Phys. Rev. Lett.* **2007**, *98*, 156103.
- [563] B. Roman, J. Bico, *J. Phys.: Condens. Matter* **2010**, *22*, 493101.
- [564] R. R. A. Syms, E. M. Yeatman, V. M. Bright, G. M. Whitesides, *J. Microelectromech. Syst.* **2003**, *12*, 387.
- [565] J. Cho, M. D. Keung, N. Verellen, L. Lagae, V. V. Moshchalkov, P. Van Dorpe, D. H. Gracias, *Small* **2011**, *7*, 1943.
- [566] M. Mastrangeli, *Adv. Mater.* **2015**, *27*, 4254.
- [567] J. Bico, B. Roman, L. Moulin, A. Boudaoud, *Nature* **2004**, *432*, 690.
- [568] B. Pokroy, S. H. Kang, L. Mahadevan, J. Aizenberg, *Science* **2009**, *323*, 237.
- [569] T. B. Ruba, D. S. Joseph, M. M. Michel, *J. Micromech. Microeng.* **2006**, *16*, 2375.
- [570] A. Antkowiak, B. Audoly, C. Josserand, S. Neukirch, M. Rivetti, *Proc. Natl. Acad. Sci. USA* **2011**, *108*, 10400.
- [571] N. R. Geraldi, F. F. Ouali, R. H. Morris, G. McHale, M. I. Newton, *Appl. Phys. Lett.* **2013**, *102*, 214104.
- [572] G. M. Spinks, V.-T. Truong, *Sens. Actuators, A* **2005**, *119*, 455.
- [573] V. Palmre, D. Pugal, K. J. Kim, K. K. Leang, K. Asaka, A. Aabloo, *Sci. Rep.* **2014**, *4*, 6176.
- [574] S. Mohsen, J. K. Kwang, *Smart Mater. Struct.* **2005**, *14*, 197.
- [575] P. Viljar, B. Daniel, M. Uno, T. Janno, V. Olga, P. Andres, J. Urmast, K. Maarja, A. Alvo, *Smart Mater. Struct.* **2009**, *18*, 095028.
- [576] J. D. W. Madden, J. N. Barisci, P. A. Anquetil, G. M. Spinks, G. G. Wallace, R. H. Baughman, I. W. Hunter, *Adv. Mater.* **2006**, *18*, 870.
- [577] Q. Meng, J. Hu, *Composites, Part A* **2009**, *40*, 1661.
- [578] E. Yakhshi-Tafti, H. J. Cho, R. Kumar, *Appl. Phys. Lett.* **2010**, *96*, 264101.
- [579] E. Cabane, X. Zhang, K. Langowska, C. G. Palivan, W. Meier, *Biointerfaces* **2012**, *7*, 9.
- [580] J. T. B. Overvelde, T. Kloek, J. J. A. D'haen, K. Bertoldi, *Proc. Natl. Acad. Sci. USA* **2015**, *112*, 10863.
- [581] M. Rogóz, H. Zeng, C. Xuan, D. S. Wiersma, P. Wasylczyk, *Adv. Opt. Mater.* **2016**, *4*, DOI:10.1002/adom.201600503.
- [582] M. Wehner, R. L. Truby, D. J. Fitzgerald, B. Mosadegh, G. M. Whitesides, J. A. Lewis, R. J. Wood, *Nature* **2016**, *536*, 451.